The regulation of endocannabinoids after neuronal damage and the neuroprotective impact of GPR55 in organotypic hippocampal slice cultures

Dissertation

for

attaining the PhD degree of Natural Sciences

submitted to the Faculty of Biochemistry, Chemistry and Pharmacy
of the Johann Wolfgang Goethe University
in Frankfurt am Main

by

Sonja Kallendrusch
(from Filderstadt)

Frankfurt am Main 2013

Accepted by the Faculty of Biochemistry, Chemistry and Pharmacy
Johann Wolfgang Goethe-University

Dekan: Prof. Dr. Thomas Prisner

Supervised by

Prof. Dr. Jochen Klein

Prof. Dr. Faramarz Dehghani

Ganz gleich, wie beschwerlich das Gestern war, stets kann man im Heute von Neuem beginnen.

(Buddhistische Weisheit)

Declaration

I hereby declare that this thesis is my own original work and that I have fully acknowledged by name all of those individuals and organisations that have contributed to the research for this thesis. Due acknowledgement has been made in the text to all other material used.

Date, …….. Signature

Table of contents……..……

Table of Figures

Table of Tables

Acknowledgement

I would like to sincerely thank Faramarz Dehghani for providing me the opportunity and giving me the great support to master this work. I am very thankful for the amazing support from Marco Koch and Ingo Bechmann. All the persons in the office, laboratories and in life, especially my mother, my friend, Felicitas and Jule, I would like to express my deep gratitude for giving me hope and joy.

Abbreviations

% (m/V)	mass volume percent
% (V/V)	volume percent
°C	degree Celsius
Δ9-THC	Δ9-Tetrahydrocannabinol
2-AG	2-Arachidonoylglycerol
AEA	anandamide (N-Arachidonoylethanolamide)
AM-251	cannabinoid-receptor 1-antagonist / GPR55 agonist
AM -281	cannabinoid-receptor-antagonist
BSA	bovine serum albumine
cAMP	cyclic Adenosinmonophosphat
CB	cannabinoid
CB_x	cannabinoid-receptor type x
cDNA	reverse transcribed mRNA (complementary DNA)
DAG(L)	diacylglycerol(-lipase)
(d)GTP	(desoxy-) Guanosintriphosphat
DMSO	dimethylsulfoxid
DNA	desoxyribonucleic acid
dNTP	desoxynucleosidtriphosphat
(d)TTP	(desoxy-) Thymidintriphosphat
EC50	concentration of an agonist provoking 50 % of the maximal effect
eCB	endocannabinoid
eCBS	endocannabinoid system
ECL	enhanced chemiluminescence
EDTA	ethylenediaminetetraacetic acid
f	femto- (10^{-15})
FAAH	fatty acid amide hydrolase
g	gram
GABA	gamma-aminobutyric acid
GAPDH	glycerinaldehyd-3-phosphat-dehydrogenase
GDP	guanosin-5‘-diphosphat
Glu	glutamate
GPR	„orphan” G-protein-coupled receptor
G-Protein	guaninnucleotid-binding protein
HRP	horseradish peroxidase
h	hour
Hz	Hertz
IC50	concentration of an inhibitor provoking a 50 % downregulation
Ki	dissociation constant
m	meter m milli- (10^{-3})
M	molar (mol/l)
MAG(L)	monoacylglycerol(-Lipase)
MAP	mitogen-activated protein
Min	minute
mRNA	messenger RNA
µ	mikro-($10^{-6)}$

n	nano- (10^{-9})
NAAA	N-Acylethanolamide acid amidase
NADA	N-Arachidonoyldopamin
NAPE	N-Arachidonoyl-phosphatidylethanolamide
OHSC	organotypic hippocampal slice culture
OEA	N-Oleoylethanolamide
p	pico- (10-12)
PAGE	polyacrylamid-gel electrophorese
PCR	polymerase chain reaction
PEA	N-Palmitoylethanolamide
PGE_2	prostaglandine E_2
pH	potentia Hydrogenii
PKA	proteinkinase A
PPARalpha	peroxisom proliferatior activated receptor alpha
PVDF	polyvinylidenfluorid
RNA	ribonucleic acid
RNase	ribonuclease
rt	real time
SEM	standard error of the mean
TE	tris-EDTA-Puffer
TBS T	tris buffered saline with Tween
Tris	tris-(hydroxymethyl)-aminomethan
UV	ultraviolet

Summary

Endocannabinoids (eCB) are signaling lipids and became known for their importance in the central nervous system as well as in immune defense. Beneficial effects of eCB are shown in processes of excitotoxic lesion, secondary damage and neuronal plasticity throughout the last years. Two canabinoid receptors, type 1 (CB_1) and type 2 (CB_2) as the respective endogenous ligands belong to the endocannabinoid system (eCBS). In 1990, the CB_1 could be cloned and was localised mainly on neurons. Shortly thereafter in 1993, the CB_2 was characterised and found primarily on cells belonging to the immune system. N-arachidonoylethanolamide (AEA), often called anandamide, and 2-arachidonoylglycerol (2-AG) are the best characterised eCB. N-palmitylethanolamide (PEA) and N-oleoylethanolamide (OEA) have no or only low affinity to CB_1 but enhance the affinity of AEA significantly. This group is therefore often summarized as N-ethanolamides (NEA). ECB are derivates of arachidonic acid and are stored in membranes where they become hydrolysed on demand by specific enzymes. Traumatic brain injury altered the levels of eCB in the blood in vivo and when applied in vitro after neuronal damage, eCB could reduce the damaging burden. Further studies demonstrated that eCB are potent to down-regulate pro-inflammatory cytokines and most important to decrease neuronal excitation.

In the present study, the intrinsic regulation of the endocannabinoid system after neuronal damage over time was investigated in rat Organotypic Hippocampal Slice Cultures (OHSC). Temporal and spatial dynamics of eCB levels were analysed after transection of the perforant pathway (PPT) in originating neurons (enthorhinal cortex, EC), areas of deafferentiation/anterograde axonal degeneration (dentate gyrus, DG) and of the synaptically linked cornu ammonis region 1 (CA1) as well as after excitotoxic lesion in the respective regions.

A strong increase of all eCB was observed only in the denervation zone of the DG 24 hours post PPT. In excitotoxic lesioned OHSC all eCB were elevated, in the investigated regions up to 72 hours post lesion (hpl). The responsible enzyme for biosynthesis of the NEA, NAPE-PLD protein, was increased during the early timepoints of measurement (1-6 hpl). The responsible catabolizing enzyme, FAAH, and the CB_1 receptor were up-regulated at a later timepoint, 48 hpl, explaining the eCB levels. In the present model, the inhibition of the enzyme responsible for 2-AG hydrolysis (MAGL) was neuroprotective as previously shown

and a re-distribution within neurons and astrocytes during neuronal damage could be observed. In primary cell cultures microglia expressed the regulating enzymes of 2-AG and the enzyme responsible for NEA down-regulation, FAAH. Astrocytes expressed mainly the catalyzing enzymes, indicating the role for eCB break-down. All these findings together demonstrate the great capacity of the eCBS to control inflammatory processes and consequently neuronal cell death.

All effects of the known eCB could not be clarified by CB_1/CB_2 deficient mice. Several G-protein coupled receptors (GPR) are recently in discussion whether they might and should belong to the endocannabinoid system. The GPR55, the not yet cloned abnormal cannabidiol receptor and further GPRs are candidates as potential endocannabinoid receptors. Recently GPR55 has been discussed as a putative cannabinoid receptor type 3 (CB_3). Quantitative PCR revealed that *Gpr55* is present in primary microglia and the brain, but the exact regional and cellular distribution and the physiological/pathological effects downstream of GPR55 activation in the CNS still remain open. Therefore, the excitotoxic rat OHSC model, previously used to investigate the neuroprotective potency of eCB, was now used to investigate the neuroprotective potency of GPR55. Activation of GPR55 protected dentate gyrus granule cells *in vitro* after excitotoxic lesion, induced by NMDA. In parallel, GPR55 activation was able to reduce the number of microglia in the dentate gyrus. These neuroprotective effects vanished however in microglia depleted OHSCs as well as in OHSC transfected with *Gpr55* siRNA, indicating a strong involvement of microglia in GPR55 mediated neuroprotection.

In summary, the present study found a strong time-dependent and anterograde mechanism of action of eCB after long-range projection damage and provided further evidence for the neuroprotective properties of eCB. The potential cannabinoid receptor 3 (GPR55) mediates neuronal protection on behalf of microglia.

Zusammenfassung

Endocannabinoide (eCB) sind lipophile Signalstoffe und für Ihre Wirkung im zentralen Nervensystem und Immunsystem bekannt. Dem intrinsischem Cannabinoid System werden die Cannabinoid Rezeptoren des Typs 1 (CB_1) und 2 (CB_2), sowie die dazugehörigen endogenen Liganden zugeordnet. Der CB_1 Rezeptor wurde 1990 kloniert und hauptsächlich auf Neuronen lokalisiert. Dieser Rezeptor ist nachweisbar für die psychotrope Wirkung des Phytocannabinoid THC verantwortlich. Ein weiterer G-Protein gekoppelter Rezeptor, CB_2, welcher auf Immunzellen vorkommt, wurde 1993 aufgeklärt. Jedoch könnten in Kürze noch nicht klonierte Rezeptoren dem eCB System (eCBS) zugeordnet werden, da diese potentiellen Rezeptoren durch eCB aktivierbar sind. CB_1 und CB_2 defiziente Mäuse konnten in pharmakologischen Studien die Wirkung der unterschiedlichen eCB nicht vollständig klären. Der G-Protein gekoppelte Rezeptor GPR55, als auch der sogenannte, noch nicht klonierte, abnormale Cannabidiol Rezeptor sind Kandidaten für das eCBS.

N-Arachidonylethanolamin (AEA) und 2-Arachidonylglycerin (2-AG) sind Derivate der Arachidonsäure und die am Besten untersuchten Substanzen der eCB. AEA wird oft mit N-Palmitylethanolamin (PEA) und N-Oleoylethanolamin (OEA) zur Gruppe der N-Ethanolamine (NEA) zusammengefasst. Die Wirkung der eCB ist an den CB Rezeptoren unterschiedlich, so ist 2-AG ein Vollagonist an beiden CB Rezeptoren, AEA ein Vollagonist am CB_1 Rezeptor und ein Partialagonist am CB_2 Rezeptor. PEA und OEA stellen eine Besonderheit dar, da beide nicht an den CB Rezeptoren binden, jedoch die Bindung von AEA am CB_1 Rezeptor erhöhen.

Die Wirkung der eCB wird enzymatisch reguliert, da eCB mit ihrem stark lipophilen Charakter nicht in sekretorischen Vesikeln sondern aktivitätsabhängig aus Lipiden der Zellmembran synthetisiert werden. Die Gruppe der NEA wird aus dem Vorläufermolekül N-arachidonylphosphatidylethanolamin vom Enzym N-acylphosphatidylethanolamin Phospholipase D (NAPE-PLD) synthetisiert. Der Abbau von NEA wird von zwei Enzymen (Fettsäureaminhydrolase (FAAH) und N-Acylethanolamidsäure Amidase (NAAA)) intrazellulär übernommen. Der genaue Transportmechanismus von eCB ist noch unbekannt, neben der passiven Diffusion werden Membrantransporter diskutiert.
Die Synthese von 2-AG wird mit der Phospholipase C und Inositol Phospholipiden oder Phosphatidylcholin initiiert und durch Diacylglycerinlipase (DAGL) vervollständigt.

Monoacylglycerinlipase (MAGL) ist das 2-AG deaktivierende Enzym, welches 2-AG zu Arachidonsäure und Glycerin abbaut.

Nach traumatischen Schädigungen steigen eCB Mengen im Gewebe sowie im Blut deutlich an. Es konnte weiter auch eine Neuroprotektion von exogen applizierten eCB nach neuronaler Schädigung in vitro gezeigt werden. Die Reduktion der neuronalen Schädigung erfolgt durch die Einschränkung der Erregbarkeit von Neuronen, da die glutamaterge Transmission durch verminderten Kalziumeinstrom eingeschränkt wird. Es erfolgt jedoch auch eine verminderte Freisetzung von proinflammatorischen Zytokinen, wie z.B. TNF-alpha.

In der vorliegenden Arbeit wurden zwei Fragestellungen bearbeitet. Die erste Fragestellung sollte die Regulation von eCB nach unterschiedlicher neuronaler Schädigung am Modellsystem der organotypischen hippokampalen Schnittkultur (OHSC) untersuchen: zum Einen nach exzitotoxischer Läsion durch Applikation von *N*-Methyl-*D*-Aspartat (NMDA) und zum Anderen in retrograd und anterograd geschädigten Arealen nach axonaler Transektion. Die weitere Fragestellung der vorliegenden Arbeit, war der Einfluss des potentiellen CB Rezeptors GPR55 auf neuronale exzitotoxische Schädigung im Modell der OHSC.

Für beide Fragestellungen wurden OHSC von 8 Tage alten Ratten präpariert und kultiviert. Für die exzitotoxische Läsion wurden OHSC mit Hilfe von 50 µM NMDA geschädigt und nach unterschiedlichen Zeitpunkten fixiert. Die exzitotoxische Läsion bewirkt eine massive neuronale Erregung und somit neuronales Sterben sowie eine Aktivierung der Gliazellen in der gesamten hippocampalen Region. Die axonale Transektion der perforanten Projektion verursacht eine lokal begrenzte Schädigung, welche im Entorhinalen Cortex (EC) eine retrograde Schädigung und im Gyrus Dentatus (DG) sowie in der Cornu Ammonis Region 1 (CA1) eine anterograde Schädigung zur Folge hat.

Die beschriebenen Regionen wurden nach exzitotoxischer Läsion und nach axonaler Transektion auf ihre eCB Menge nach 0, 1, 6, 12, 24, 48 und 72 Stunden sowie 72 Stunden nach Applikation des MAGL Inhibitors JZL184 mit Hilfe von Flüssigchromatografie und Massenspektrometrie untersucht. Die regulierenden Enzyme und die Rezeptoren CB_1 und PPARalpha konnten mittels Immunhistochemischen Methoden und semiquantitativer Echtzeit polimerase-Kettenreaktion (rtPCR) dargestellt werden. OHSC wurden mittels *Magl* siRNA und dem MAGL Inhibitor JZL184 wie im Folgenden beschrieben auf ihre Neuroprotektivität untersucht. Zur Bestimmung der neuronalen Schädigung nach MAGL Reduktion und GPR55 Aktivierung wurde die Anzahl der toten Körnerzellen und der

Mikroglia des DG quantifiziert und mit der unbehandelten NMDA Kontrolle verglichen. Propidiumiodid (PI) diente als Marker für degenerierte Neurone und FITC-konjugiertes *Griffonia simplicifolia* Isolektin B4 (IB_4) wurde als Mikrogliamarker verwendet. Dargestellt und analysiert wurden die OHSC mit einem konfokalen Laserscanning Mikroskop.
Zur Überprüfung der GPR55 vermittelten Neuroprotektion wurden Versuche mit *Gpr55* siRNA transfizierten OHSC und Mikroglia depletierten OHSC durchgeführt. Versuche mit verschiedenen synthetischen Agonisten/Antagonisten (WIN, AM281) des CB_1 Rezeptors wurden durchgeführt um mögliche Interaktionen zu identifizieren. Die Wirkung des verwendeten GPR55 Liganden L-alpha Lysophosphatidylinositol (LPI) wurde weiterführend mit Hilfe von Migrationsversuchen mit Mikroglia untersucht.

Das Modell der OHSC konnte erfolgreich zur Bestimmung der eCB Regulation nach neuronaler Schädigung genutzt werden, da die eCB Mengen der beschriebenen Areale bestimmt und auf ihren Aktingehalt normiert werden konnten. Nach exzitotoxischer Schädigung konnte im EC ein Anstieg von NEA nach 24 Stunden beobachtet werden. Im DG waren NEA über den gesamten gemessenen Zeitraum erhöht, 2-AG war nach 24 Stunden und 72 Stunden signifikant erhöht. In der CA1 Region waren alle eCB 24 und 72 Stunden nach Läsion hochreguliert. Im Schädigungsmodell der axonalen Transektion wurde allein im anterograd gelegenen DG eine Erhöhung der eCB nach 24 Stunden festgestellt. Die enzymatische Regulation von NEA zeigte einen Anstieg des synthetisierenden Enzym NAPE-PLD nach einer und sechs Stunden post Läsion. Das abbauende Enzym FAAH war nach 48 Stunden hochreguliert. Das 2-AG synthetisierende Enzym DAGL war 24 Stunden post Läsion im DG in Western Blot Analysen herunter reguliert, zeigte jedoch in rtPCR Analysen eine Hochregulation 24 Stunden post Läsion. Das 2-AG katalysierende Enzym MAGL war keinen Veränderungen in Western Blot und rtPCR Analysen unterworfen. Der CB_1 Rezeptor zeigte eine marginale Erhöhung 6 Stunden nach axonaler Schädigung im EC und 48 Stunden nach Läsion in der CA1 Region. Die Auswertung der immunhistochemischen Färbungen im DG ergab für NAPE-PLD eine neuronale und Mikroglia positive Lokalisierung. FAAH und NAAA konnten auch neuronal exprimiert dargestellt werden. In primären Zellkulturen wurden unterschiedliche Exprimierungsmuster zu den OHSC sichtbar. Hier wurden NAPE-PLD, FAAH und NAAA schwach in Gliazellen exprimiert als auch neuronal. In OHSC war DAGL neuronal lokalisiert. Nach neuronaler Schädigung, axonal oder exzitotoxisch, zeigten auch Astrozyten DAGL Expressionen. Das 2-AG katalysierende Enzym MAGL konnte unter Kontrollbedingungen zunächst in Neuronen und Astrozyten mit Hilfe von immunhistochemischen Färbungen sichtbar gemacht werden, jedoch nicht nach neuronaler

Schädigung im DG. Anders stellte sich die Expression in primären Zellkulturen dar, hier zeigten sich Mikroglia und Astrozyten DAGL positiv. MAGL wurde in Mikroglia exprimiert und stellte sich nur nach Schädigung der Zellkulturen mit LPS auch in Astrozyten dar. Die beiden Rezeptoren CB_1 und PPARα waren in Neuronen exprimiert, PPARα konnte auch in Mikroglia gezeigt werden.

Die neuroprotektive Eigenschaft von endogenem 2-AG konnte mit Hilfe des MAGL Inhibitors JZL184 dargestellt werden. Nach Gabe von JZL184 war in allen untersuchten Arealen der OHSC eine erhöhte Menge an 2-AG zu messen. Im Vergleich zu NMDA geschädigten OHSC welche keine JZL184 oder *MAGL* siRNA Behandlung bekamen, war die Anzahl der PI positiven Neurone in der Körnerzellschicht des DG signifikant gesunken. Unbeschädigte OHSC wiesen kaum PI positive Neurone und nur wenige ramifizierte IB_4 positive Mikrogliazellen auf.

Nach Applikation des GPR55 Liganden LPI für 72 Stunden, konnte keine Veränderung in OHSC festgestellt werden. OHSC wurden mit NMDA für 4 Stunden geschädigt und wiesen 72 Stunden darauf ein hohes Maß an PI positiven Neuronen und vielen amöboiden IB_4 positiven Mikrogliazellen auf. Die Anzahl der PI positiven Neuronen und IB_4 positiven Mikroglia reduzierte sich signifikant bei NMDA Schädigung und Applikation von LPI (0.1-10 µM). Präapplikation von LPI (1 µM) vor der Schädigung mit NMDA und zeitliche Veränderungen von LPI Applikation, führten zu keiner Reduktion der PI positiven Neurone oder IB_4 positiven Mikrogliazellen. Der CB_1 Agonist WIN55 212-2 und CB1 Antagonist AM281 konnten die Wirkung von LPI auf IB_4 positive Mikroglia aufheben, jedoch hatte AM281 keinen Einfluss auf die Reduktion der PI positiven Neurone. Die GPR55 vermittelte Neuroprotektion konnte mit *GPR55* siRNA transfizierten OHSC und Mikroglia depletierten OHSC aufgehoben werden. Desweiteren konnte eine chemoattraktive Wirkung von LPI auf Mikroglia festgestellt werden.

Die erste Fragestellung beschäftigte sich mit der Regulation der eCB. Diese sind nach neuronaler Schädigung zeitlich und anterograd gerichtet reguliert und weisen auf ein endogenes neuroprotektives System. Dies könnte weiterführend auch auf einen Einfluss der eCB auf dendritische Reorganisation nach Wegfall des empfangenden Signals deuten. Die bisher bekannten Enzyme konnten die Regulation von NEA erklären, jedoch scheint das katalysierende Enzym NAAA nach neuronaler Schädigung nicht involviert zu sein. Für das 2-AG synthetisierende Enzym DAGL ist ein Abfall des Proteins mit einer gleichzeitigen Erhöhung des Transkripts beobachtet worden. Die Wirkung von eCB ist zeitlich und räumlich

begrenzt, daher könnte diese Resultate auf eine Ubiquitin gesteuerte Regulation hinweisen. Die Expression von DAGL nach neuronaler Schädigung in Astrozyten bezeugt eine hohe Flexibilität der eCB Regulation und das Zusammenspiel unterschiedlicher Zellpopulationen im ZNS. Die eindeutig neuroprotektive Wirkung von eCB nach neuronaler Schädigung, verbunden mit der hier gezeigten Regulation, ermöglicht nun die spezifische Manipulation des eCBS um potentielle Therapien im Bereich der traumatischen Schädigung und Wirbelsäulenverletzungen zu testen.

Die zweite Fragestellung mit Bezug auf die Rolle des GPR55 Rezeptors nach neuronaler Schädigung konnte mit Hilfe des GPR55 Liganden LPI studiert werden. Die Applikation von LPI bewirkte eine Neuroprotektion und führte zu einer verminderten Mikroglia Anzahl in OHSC nach exzitotoxischer Schädigung. Dieser neuroprotektive Effekt von LPI wurde durch ein Ausschalten von GPR55 oder nach Entfernung der immunkompetenten Mikroglia aufgehoben. Dies hebt die prominente Rolle der Mikrogliazellen in der Protektion von Neuronen durch GPR55 hervor. Auch die hier gezeigte chemoattraktive Wirkung von LPI auf Mikrogliazellen weist auf eine wichtige Signalfunktion von LPI selbst.

Zusammenfassend untermauert die vorliegende Arbeit teilweise bekannte Befunde und zeigt interessante neue Erkenntnisse der neuroprotektiven Wirkung des eCBS. Die Daten bieten eine Ausgangsbasis für spezifische Modulationen des eCBS mit exogenen Cannabinoiden für mögliche Therapien bei traumatischen neuronalen Schädigungen.

1. General Introduction

Stroke, spinal cord injury (SCI) and traumatic brain injury (TBI) are common health threatening incidences in our society. Severe physical and mental impairments of the patient and high costs for our health system are often the result of central nervous tissue damage (Blight 1985; Signoretti, Vagnozzi et al. 2010). The endocannaboid system (eCBS) is induced in various brain disorders and is involved in both, neuronal protection as well as secondary damage. The result however, is dependent on cannabinoid derivate and receptor subtype. To understand the eCBS in the healthy organism and during pathologic variances, as well as to manipulate the eCBS pharmacologically, it is important to obtain knowledge of its intrinsic regulation.

In the present chapter the endocannabinoid system in the field of neurobiology will be presented, explaining the aim and relevance of the present dissertation. The second chapter describes the used material and methods followed by the third chapter describing the results of the present dissertation. Finally, the results will be discussed in chapter four.

1.1 The endocannabinoid system

Background and discovery

Cannabis sativa (cannabis) was one of the first plants cultivated and used by mankind. The world oldest pharmacopoeia, the chinese pen-ts'ao ching containing medical knowledge reaching back until 2700 years BC, reported for the first time medicinal cannabis indication (Read, 1936). At that time, cannabis was used for rheumatic pain, intestinal constipation,

female disorders and further diseases. The cannabis plant was also regarded as a holy plant in asian shamanism, hinduism and buddhism, not only due to its beneficial health effects, but also to facilitate meditation (Köfalvi, Attila, 2012)[e-book].

In 1839 the first publication on cannabis in the western world was written by Wiliam B. O'Saughnessy, an irish physician 'On the preparations of the Indian hemp, or gunjah' starting with:'… the narcotic effects of Hemp are popularly known in the south of Africa, South America, Turkey, Egypt, Middle East, Asia, India and the adjacent territories of the Malays, Burmese and Siamese … ', further:'… extensively employed for a multitude of affections … ' (Frankhauser 2002). The broad affections of the Indian hemp were hardly known in the European area at this time. After the publication of O'Saughnessy many investigations started with the hope to find new remedies. After several years however, the Indian hemp was almost forgotten and even got forbidden by law due to its mental effects. New pharmacological possibilities and therapeutics were available and the plant cannabis lost its importance in the popular medical use.

The interest in the possible medical force of *cannabis sativa* still continued. In 1990 the first endogenous cannabis receptor was identified on behalf of the main psychoactive ingredient of cannabis, Δ^9-tetrahydrocannabinol (Δ^9-THC). The molecular characterisation of the neuronal cannabinoid receptor type 1 (CB_1) released a new and enormous interest in the field of cannabis, publications were 3-times enhanced compared to the years before (Köfalvi, 2008). After CB_1 the characterisation of the cannabinoid receptor type 2 (CB_2) followed and their endogenous ligand `anandamide` was detected, now more than 20 years ago. A new endogenous signaling system was discovered. The endocannabinoid system is involved in important cognitive, sensory, motor and metabolic functions of our organism. Accordingly, the pharmacological research focuses on unraveling the various endogenous ligands and its receptors.

For about 80 years now, the use of cannabis is forbidden and regarded as illicit drug. However, cannabis is regaining its character as a medicinal plant. At the moment it is used legally in just a few countries but research with its developing possibilities will unravel its properties, which might be applied in favor of our physical and mental health.

1.2 Cannabinoid receptors

The CB_1 receptor found in 1990 by Matsuda et al. showed that psychotropic cannabinoids can inhibit adenylate cyclase by acting through the G-i/o proteins (Munro, Thomas et al. 1993). It was also Munro et al, who shortly thereafter discovered the second cannabinoid receptor ($CB_{2)}$ (Munro, Thomas et al. 1993). The similarity of the CB_1 and CB_2 was leading to the conclusion that cannabinoids act on the superfamily of G-protein coupled receptors (GPR). CB_1 consists of seven alpha helical transmembrane domains with a 68% amino acid homology within the transmembrane domains and with a 44% overall homology to CB_2 (Lutz 2002). Three more GPRs, GPR55, GPR18 and GPR119 are intensively discussed as cannabinoid receptors due to the activating ability of endocannabinoids at these receptors. Other receptors are also in discussion, e.g. the abn-CBD receptor or the TRPV channels (Begg, Pacher et al. 2005; Brown 2007; Pertwee, Howlett et al. 2010; McHugh, Page et al. 2012)

CB_1 is the most abundant GPR in the brain, found mainly at the central and peripheral nerve terminals where it inhibits transmitter release (Pertwee 1997; Howlett 1998). The highest CB_1 concentration was found on perisynaptic axons of GABA and glutamatergic neurons in the hippocampus, basal ganglia, the cerebellum and the cortex (Herkenham, Lynn et al. 1991; Katona, Sperlagh et al. 1999; Morozov and Freund 2003; Katona, Urban et al. 2006). The expression pattern of CB_1 on astrocytes and microglia is discussed controversially in literature but there is evidence showing CB_1 on rat microglia (Bouaboula, Poinot-Chazel et al. 1995;

Salio, Doly et al. 2002; Facchinetti, Del Giudice et al. 2003; Walter, Franklin et al. 2003; Stella 2004; Ramirez, Blazquez et al. 2005) and also on astrocytes (Navarrete and Araque 2008). To a lesser extent CB_1 is present in adipose tissue, liver, muscle, adrenal gland and the gastro intestinal tract (Pagotto, Marsicano et al. 2006).

CB_2 is predominantly (10-100 -fold higher than CB_1) expressed in the immune system and modulates cytokine production and immune cell migration (Munro, Thomas et al. 1993; Galiegue, Mary et al. 1995; Kurihara, Tohyama et al. 2006). Expression of CB_2 has been confirmed in many immune cells like neutrophils, macrophages, T cells and B cells, as well as in the endothelium of blood vessels and different tissues like spleen and thymus (Galiegue, Mary et al. 1995; Pertwee 1997; Kishimoto, Gokoh et al. 2003; Maestroni 2004; Howlett 2005). Osteoblast and osteoclast are also CB_2 positive (Bab and Zimmer 2008). In the central nervous system CB_2 is found on microglia and to a minor extent in neurons but not on astrocytes (Carlisle, Marciano-Cabral et al. 2002; Walter, Franklin et al. 2003; Carrier, Kearn et al. 2004; Nunez, Benito et al. 2004; Maresz, Pryce et al. 2007; Brusco, Tagliaferro et al. 2008; Dittel 2008). On neurons, CB_2 is found in regions including the cerebellum (Ashton, Friberg et al. 2006), brainstem (Van Sickle, Duncan et al. 2005), thalamus, striatum, cortex, amygdala and hippocampus (Gong, Onaivi et al. 2006), as well as in the spinal cord (Beltramo, Bernardini et al. 2006). However, protein content measured by Western blot analysis or PCR makes it difficult to conclusively determine the cell type expressing CB_2 receptors (Van Sickle, Duncan et al. 2005; Ashton, Friberg et al. 2006; Beltramo, Bernardini et al. 2006; Cabral, Raborn et al. 2008).

Several not yet cloned receptors might belong to the eCBS and still need to be characterised e.g. the orphan G protein coupled receptor GPR55 (Matsuda, Lolait et al. 1990; Mackie 2006; Mackie and Stella 2006; Petitet, Donlan et al. 2006; Harkany, Guzman et al. 2007; Pertwee 2010; Pertwee, Howlett et al. 2010). GPR55 is recently discussed whether it should become

the cannabinoid receptor type 3 (CB_3). Pharmacological enterprises claimed GPR55 in 2004, ((Ryberg, Larsson et al. 2007), Class A Orphans: GPR55. Last modified on 30/11/2011, accessed on 06/07/2012 IUPHAR database) however, Oka et al. refuted the claim having evidence that the endogenous L-alpha-lysophosphatidyl inositol (LPI) is a GPR55 ligand (Oka, Nakajima et al. 2007). LPI does not belong to the eCB but to the group of lysophospholipids hydrolysed by the phospholipase A (PLA) from phosphatidylinositol and is localised in plasma membranes. It was first shown by Falasca et al. that LPI possesses mitogenic abilities (Falasca and Corda 1994). However, LPI has no direct cannabinoid receptor affinities and offers therefore the possibility to investigate the patho-physiological role of GPR55 without simultaneous CB_1 or CB_2 activation. The expression pattern of GPR55 is contradictory. Johns et al. stated that GPR55 is mainly expressed in adipose tissue and in brain (Johns, Behm et al. 2007), whereas Ryberg et al. did not find GPR55 in adipose tissues (Ryberg, Larsson et al. 2007). GPR55 expression was also found in adrenal glands, parts of the gastrointestinal tract, the CNS and on endothelial cells (Lauckner, Jensen et al. 2008; Waldeck-Weiermair, Zoratti et al. 2008; Obara, Ueno et al. 2011; Romero-Zerbo, Rafacho et al. 2011). First GPR55 was thought to be the missing abnormal cannabidiol (abn-CBD) receptor due to the presence of GPR55 on blood vessels (Jarai, Wagner et al. 1999). This hypothesis was rejected by Johns et al. (2007), showing that GPR55 KO mice had no changed basal blood pressure and heart rate compared with wild-type mice. Abn-CBD also did not mediate the vascular changes via GPR55 in the mesenteric artery (Johns, Behm et al. 2007).

1.3 Cannabinoid receptor ligands

Cannabinoids are differentiated into three groups: First the bioactive substances of the cannabis plant, second the endocannabinoids and finally the synthetic cannabinoids. Although the present study investigates the intrinsic temporal dynamics of the eCBS the most known

plant derived cannabinoid and the best characterised aminoalkylindole is described shortly to clarify the differences to the group of endocannabinoids.

Plant-derived cannabinoids

The best known phytocannabinoid is Δ^9-THC but there exist about 65 more plant-derived active cannabinoids (Di Marzo et al. 2004). Δ^9-THC binds to both cannabinoid receptors with low affinity and is a partial agonist (Pertwee 1997; Howlett 2002). Further plant-derived cannabinoids are tricyclic dibenzopyran derivatives (Klein 2005).

Aminoalkylindoles

WIN55212-2 is a synthetic CB_1 agonist, coincidently found by the company Sterling-Winthrop. The chemical structure is different from the structure of natural cannabinoids, belonging to the pravidoline derivates. However, in vivo WIN55212-2 is a very potent CB_1 agonist showing high similarity to Δ^9-THC effects (Jarbe, Li et al. 2010).

Endocannabinoids

After the cannabinoid receptors were identified, two endogenous ligands were discovered, belonging to the group of eicosanoids. The endocannabinoids (eCB) have a polyunsaturated fatty acid chain with a C20 body and a polar head chain linked with an ester- or ether-binding. The present knowledge states that eCB act in the CNS as neurotransmitter integrated in the cell membrane and become released on demand (Pertwee 2008). Well characterised eCB like N-arachidonoylethanolamine (anandamide) or 2-arachidonoylglycerol (2-AG) are partial or full agonists at CB_1 and CB_2, described later on (Devane, Hanus et al. 1992; Sugiura, Kondo et al. 1995). However, some structurally-related fatty acids like N-palmitoylethanolamine (PEA) and N-oleoylethanolamine (OEA), which contain palmitic

(PA) and oleic (OA) fatty acids respectively are structural moieties (Pacher, Batkai et al. 2006). The family of N-acylethanolamides (NEA) are usually considered, on the basis of their structure and mode of action as eCB analogues, as they do not bind with high affinity to CB receptors but e.g. can potentiate anandamide responses by enhancing the binding capacity of anandamide to CB_1 (Pacher, Batkai et al. 2006; Pertwee 2010). Anandamide has higher affinities to CB_1 than to CB_2 (K_i(CB_1 vs. CB_2)= 89 vs. 371 nM, reviewed by (Hohmann 2002)), acting on both receptors as a partial agonist (Hillard 2000; Pertwee and Ross 2002). Furthermore, anandamide has also been shown to be an agonist at the pro-nociceptive transient vanilloid ($TRPV_1$) receptor (Zygmunt, Petersson et al. 1999; Smart, Gunthorpe et al. 2000). Interestingly, the CB_1 receptor has an extracellular binding site (Shire, Calandra et al. 1996) whereas the $TRPV_1$ agonist binds intracellular (Jung, Hwang et al. 1999). This suggests that anandamide might regulate anti- and pro-nociceptive effects depending on the activation sites. The uptake of NEA, especially of anandamide into the cell, is still in discussion. A broad array of anandamide transporters are suggested as well as the permeability of cell membranes to anandamide, which is not clarified yet and was recently summarized by Fowler in 2012 (Fowler 2012). However, recently the assumption of bidirectional trafficking of eCB is strengthened by evidence that shows indirectly a membrane target for eCB with an arachidonoyl chain in U937 cells (Chicca, Marazzi et al. 2012).

Anandamide was shown to be generated by neurons in the brain (Di Marzo, Fontana et al. 1994; Giuffrida, Parsons et al. 1999) and DRGs (van der Stelt, Trevisani et al. 2005) as well as in macrophages, microglia, astrocytes (Varga, Wagner et al. 1998; Walter, Franklin et al. 2002; Carrier, Kearn et al. 2004) and in the vascular endothelium (Hillard 2000; Liu, Gao et al. 2000).

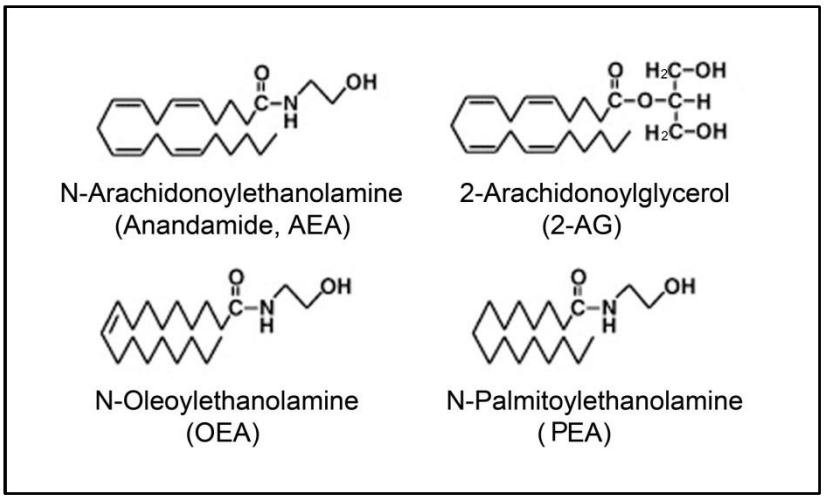

Figure 1.1 Endocannabinoids

The two main endocannabinoids are N-arachidonoylethanolamine (anandamide, AEA) and 2-arachidonoylglycerol (2-AG). Belonging to the group of N-acylethanolamines, like anandamide, N-oleoylethanolamine (OEA) and N-palmitoylethanolamine (PEA) are members of the endocannabinoid family. Adapted and modified from Ueda et al., 2010)

The endocannabinoid 2-AG is released from post-synaptic neurons and acts retrograde on pre-synaptic neurons to modulate cellular signaling (Katona, Urban et al. 2006). 2-AG acts as full agonist at CB_1 and CB_2 and is the most potent agonist toward both CB receptors (Hillard 2000; Savinainen, Jarvinen et al. 2001). The K_i values of 2-AG are 472 ± 55 nM at CB_1 and 1400 ± 172 nM at CB_2, respectively (Mechoulam, Ben-Shabat et al. 1995). 2-AG is generated by immune cells, microglia, astrocytes and by neurons (Stella, Schweitzer et al. 1997; Walter, Dinh et al. 2004). The concentration of 2-AG in brain tissue is approximately 200-fold higher than the concentration of anandamide. Both eCB are distributed in the following brain areas: highest in brainstem, striatum and hippocampus and lower in cortex, diencephalon and cerebellum (Bisogno, Berrendero et al. 1999).

1.4 Endocannabinoid synthesis and degradation

Control of CB receptor activation is determined by eCB synthesising and hydrolyzing enzymes. Due to the lipophilic character of eCB, they are synthesised on demand from precursor molecules which are stored in the cell membrane (Di Marzo, 1994). Two enzymatic steps are required for NEA synthesis, the first of which is N- acylation of phosphatidylethanolamine (PE) by the calcium dependent N-acyltransferase (NAT). The acyl group of a glycerophospholipid is transferred from the sn-1 position to the amino group of the PE. Then, NEA and phosphatidic acid are formed by hydrolysis of N-arachidonoyl PE through the N- acylphosphatidylethanolamine-selective phospholipase D (NAPE-PLD), which limits the biosynthesis of NEA by its availability (Sugiura, Kobayashi et al. 2002; Okamoto, Morishita et al. 2004). Alternatively, direct synthesis of NEA from arachidonic acid and ethanolamine has also been described (Ueda, Kurahashi et al. 1995), as evidence exists that anandamide tissue levels remained unchanged in NAPE-PLD knockout mice compared to wild-type animals (Leung, Saghatelian et al. 2006).

Generally, NEA are signaling transmitters with a short half-time as they are quickly and selectively degraded. The best characterised enzyme, fatty acid amide hydrolase (FAAH) degrades NEA, favoring anandamide (Cravatt, Giang et al. 1996; Ueda 2002). FAAH degrades NEA intracellularly to arachidonic acid and ethanolamine (Cravatt, Giang et al. 1996; Ueda 2002). The optimal function of FAAH is around a pH of nine in vitro (Bisogno, De Petrocellis et al. 2002; Ueda 2002) and is found in rat neuronal cells (Di Marzo, Fontana et al. 1994). More recently, FAAH has been reported also in adult rat DRG, sciatic nerve and spinal cord (Lever, Robinson et al. 2009).

Another hydrolyzing enzyme of NEA is N-acylethanolamide-hydrolyzing acid amidase (NAAA), which was recently discovered with a preference for poly unsaturated fatty acids like PEA (Ueda, Tsuboi et al. 2010). There is no sequence homology between NAAA and

FAAH, while rat, mouse, and human NAAAs show high homology (33–34% identity and 70% similarity at amino acid level over their entire length) with acid ceramidases of the same respective animal species (Ueda, Tsuboi et al. 2010). The optimal reaction of NAAA occurs at pH of four to five, indicating NAAA cleavage only after the transportation from the Golgi apparatus to endosomes/lysosomes (Ueda, Tsuboi et al. 2010). The pH profiles of NAAA and FAAH differ from each other and can be used to differentiate the activities of these two enzymes (Sun, Tsuboi et al. 2005). Regarding substrate specificity, NAAA can hydrolyse various NAE with C_{12}–C_{20} fatty acids. PEA is the most active substrate of NAAA (Ueda, Yamanaka et al. 2001; Tsuboi, Sun et al. 2005). The activity of NAAA with anandamide was less sensitive and NAAA was inactive towards 2-AG, unlike FAAH (Ueda, Tsuboi et al. 2010).

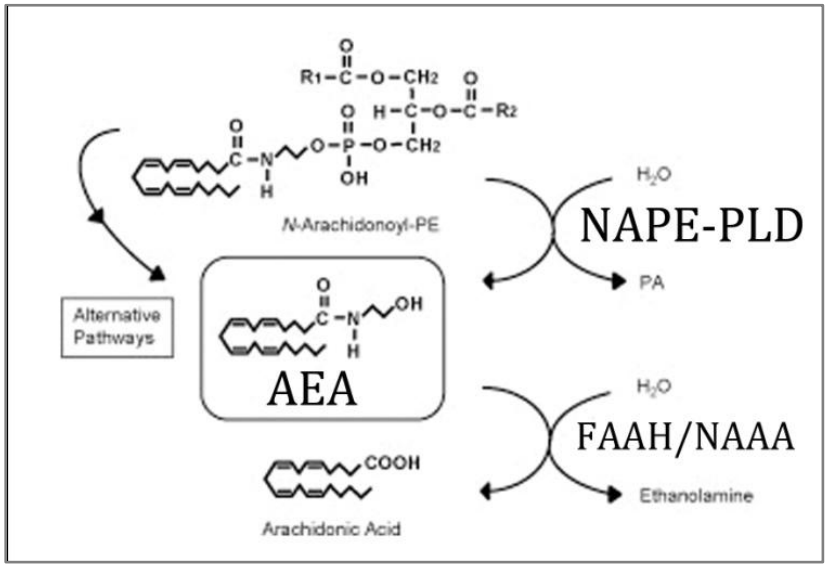

Figure 1.2 Schematic drawing of the synthesis and hydrolysis of anandamide

The major synthesising pathway involves NAPE-PLD and FAAH and NAAA as the main hydrolyzing enzyme. (Adapted and modified from Wang and Ueda, 2009)

Sn-1-diacylglycerol lipase alpha (DAGL) is the primary biosynthetic enzyme of 2-AG, found at the post-synapse of neurons (Bisogno, Howell et al. 2003).

2-AG can be synthesised from inositol phospholipids or phosphatidylcholine by the phospholipase C and subsequently by DAGL. 2-AG might also be generated through the combined actions of phospholipase A1 and phospholipase C (Stella, Schweitzer et al. 1997; Sugiura, Kobayashi et al. 2002; Bisogno, Howell et al. 2003).

The principal 2-AG hydrolyzing enzyme is monoacylglycerol lipase (MAGL), ascribed for 85% of total 2-AG hydrolysis, and was unable to metabolize anandamide (Dinh, Carpenter et al. 2002; Blankman, Simon et al. 2007). MAGL has an optimum pH of 8 and was found on membranes as in cytosolic fractions (Ghafouri, Tiger et al. 2004). Homology of mouse and human MAGL was greater than 80 % (Karlsson, Reue et al. 2001). Further studies suggested that the serine hydrolase α-β-hydrolase domain 12 (ABHD12) is highly expressed in microglia and accounts for approx. 9 % of total brain 2-AG hydrolysis (Savinainen, Saario et al. 2012). ABHD12 was suggested as adequate MAGL analogue for brain microglia as well as in related cell types of peripheral tissues (Fiskerstrand, H'Mida-Ben Brahim et al. 2010). It was also suggested that FAAH was able to hydrolyse 2-AG into arachidonic acid and glycerol (Sugiura, Kobayashi et al. 2002). However, in FAAH knockout mice 2-AG levels remained stable (Lichtman, Hawkins et al. 2002) and selective FAAH inhibitors failed to enhance 2-AG levels (Kathuria, Gaetani et al. 2003).

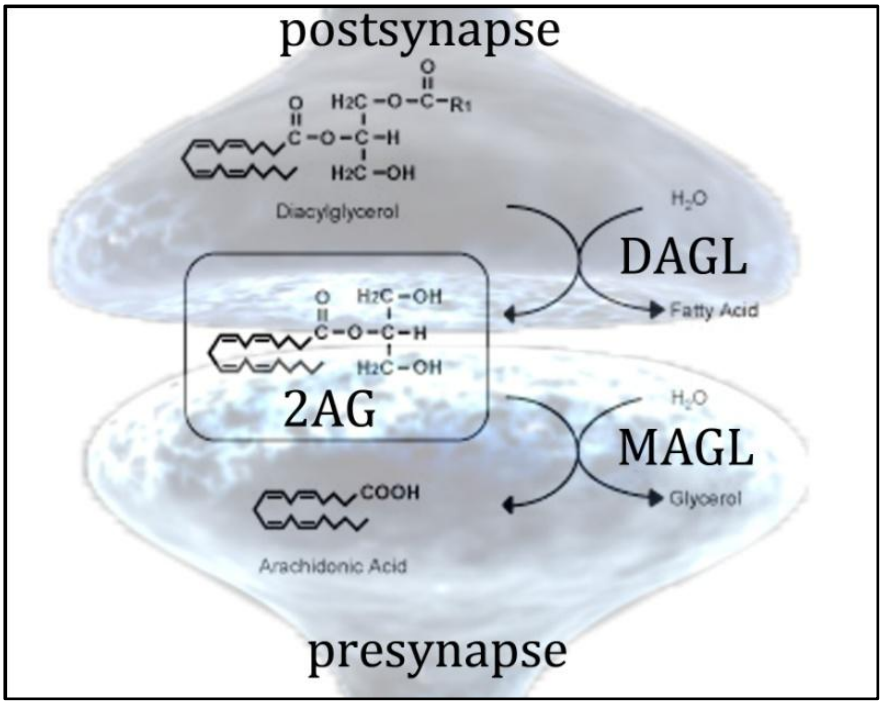

Figure 1.3 Schematic drawing of the 2-AG metabolism

2-AG acts retrograde, synthesised from DAGL at the post-synapse, towards the pre-synapse, where 2-AG is hydrolysed by MAGL. Adapted and modified from Wang and Ueda, 2009)

1.5 Modulative properties of (endo)cannabinoids in neuronal degeneration

Central nervous system (CNS) damage resulting from the acute lesion and the magnitude of secondary damage determines the outcome of individual neurological impairments. The most common neuronal injuries like SCI, TBI or stroke include long-range projections destruction. Although the lesion site might be regional restricted and moderate, healthy neuronal tissue can be destroyed despite not being involved in the initial lesion. The period after the initial insult includes the so called secondary damage, lasting from hours to weeks, and may lead together with the first traumatic source to persistent clinical and social disabilities for the patients (Blight 1985; Signoretti, Vagnozzi et al. 2010). Secondary damage is associated with different inflammatory and cell activating factors as neuronal cell death, reactive astrogliosis

and microglia proliferation and activation (Dumont, Okonkwo et al. 2001; Yakovlev and Faden 2004; Faden and Stoica 2007).

In the healthy organism eCB are expected to maintain basic physiological processes, sustained by the constitutive levels of eCB in the organism. However, in pathologic changes tremendous alteration in eCB concentrations was seen (Mackie 2006). This led to the discovery that the eCBS possess the potency to favor functional sustainment and cellular repair. Still, the eCBS is one of many different systems reflecting a major modulating signaling machinery influencing neuronal damage and leading to either destructive or protective results (Piomelli 2003). Understanding the changes in the eCBS during pathologic conditions, allows to influence and possibly recovering the system. There also exists evidence in vitro and in vivo that the eCBS modulates embryonic and adult neurogenesis and neural progenitor proliferation (Aguado, Monory et al. 2005; Jiang, Zhang et al. 2005; Hill, Kambo et al. 2006). In the present paragraph the known literature of the eCB, also investigated in the present dissertation, and their influence on CNS diseases will be presented.

N-ethanolamines (NEA)

In several reports enhanced anandamide levels have been detected after various pathological events, as well as in human studies (Hansen, Schmid et al. 2001; Maccarrone, Gubellini et al. 2003; Marsicano, Goodenough et al. 2003). Elevated anandamide levels were measured in the cerebrospinal fluids of patients with Parkinson disease or after stroke and were directly associated with brain damage (Schabitz, Giuffrida et al. 2002; Pisani, Fezza et al. 2005). Anandamide protected *in vitro* cerebral rat cortical neurons from ischemia (Sinor, Irvin et al. 2000), indicating a compensatory mechanism to brain damage. Investigations on organotypic hippocampal slice cultures described no protective effect of anandamide and THC in dentate gyrus neurons (Kreutz et al., 2007). N-arachidonoyl dopamine (NADA) and PEA reduced the

number of degenerating neurons. It was shown that NADA activated CB_1 and PEA activated PPARα in microglia and neurons to restrict neuronal damage (Kreutz, Koch et al. 2009; Grabiec, Koch et al. 2011; Koch, Kreutz et al. 2011; Koch, Kreutz et al. 2011). Furthermore, anandamide as a CB_1 agonist is able to decrease NO release and reduce over-activation of microglia by down-regulation of MAPK through mitogen-activated protein kinase phosphatase-1 (MKP-1) induction (Dommergues, Plaisant et al. 2003; Eljaschewitsch, Witting et al. 2006). However, Stella and his group found an increase in microglia motility by anandamide in BV-2 cells (Franklin, Parmentier-Batteur et al. 2003) and neurotoxic events like ischemic conditions or glutamate supplementation induced enhanced anandamide and PEA levels, demonstrating neuroprotective properties under both conditions (Rodriguez De Fonseca, Gorriti et al. 2001; Conti, Costa et al. 2002; Koch, Kreutz et al. 2011). One underlying mechanism seems to be an enhanced receptor binding capacity of anandamide not only at the CB_1 receptor but also at the vanilloid receptor, due to decreased anandamide hydrolysis caused by increased PEA levels, which represents the so called entourage effect (De Petrocellis, Davis et al. 2001). Further, PEA is reported to protect neurons via activation of PPARα in neurons, microglia (Koch, Kreutz et al. 2011) and astrocytes (Raso, Esposito et al. 2011). PPARs are nuclear membrane-associated transcription factors belonging to the nuclear receptor family which exert anti-inflammatory properties in brain injury (Straus and Glass 2007). OEA, as the third N-acylethanolamine, is suggested as a modulator of satiety, inflammation, lipid metabolism and antinociceptive effects, due to its activity at receptors such as TRPV1, GPR119 or PPAR gamma (Rodriguez De Fonseca, Gorriti et al. 2001; Fu, Gaetani et al. 2003; Suardiaz, Estivill-Torrus et al. 2007; Thabuis, Tissot-Favre et al. 2008). Neuroprotective properties mediated by OEA were seen in dopaminergic neurons in the substantia nigra after application of 6-hydroxidopamine in rats simulating a parkinson model (Galan-Rodriguez, Suarez et al. 2009). Enhanced OEA levels were found to reduce microglia

activation (Coffey, Perry et al. 1990; Topper, Gehrmann et al. 1993), however no direct comparison of AEA and OEA to stimulate microglia was performed.

2-Arachidonoylglycerol

2-AG is proposed to reduce excitotoxic damage by acting as a retrograde neurotransmitter decreasing neuronal firing (Katona and Freund 2008). GABAergic interneurons are also involved in long term depression of excitation (Peterfi, Urban et al. 2012). NMDA provokes presynaptic Ca^{2+} accumulation, which is one of the early post-injury events leading to the activation of 2-AG (Piomelli, Beltramo et al. 1998) and subsequently to the involvement in analgesia and anti-inflammation in the CNS (Panikashvili, Simeonidou et al. 2001; Panikashvili, Mechoulam et al. 2005; Kreutz, Koch et al. 2009). Pre-synaptic CB_1 receptors on nerve terminals are activated by 2-AG and inhibit glutamate release, subsequently decreasing excitotoxicity (Katona, Urban et al. 2006).

After TBI, glutamate is released and leads to ROS production within minutes and hours (Chan, Doctor et al. 2001) and inflammatory cytokine release initiates brain inflammation (Shohami, Ginis et al. 1999; Ziebell and Morganti-Kossmann 2010). In vivo models of closed head injury and focal ischemia in mice reported intrinsic elevated 2-AG levels after 4 and 1 to 24 hours post lesion (Panikashvili, Simeonidou et al. 2001; Degn, Lambertsen et al. 2007). 2-AG administration decreased edema formation, reduced blood brain barrier permeability and the production of TNF alpha, IL-1β, IL-6 and NO. Also the general survival and health of the treated mice were increased after 2-AG treatment (Panikashvili, Shein et al. 2006; Degn, Lambertsen et al. 2007). Only a single administration of 2-AG 1 h after closed head injury improved the recovery of mice significantly and was sustained up to 3 month, the end of the follow up study (Shohami, Cohen-Yeshurun et al. 2011). 2-AG was as well potent to reduce TNF-α levels in LPS stimulated mice in vivo (Gallily, Breuer et al. 2000). In line with TNF- α

down-regulation, 2-AG inhibited NF-kB activation after TBI by CB_1 receptor activation (Panikashvili, Mechoulam et al. 2005).

Another enzyme that is involved in 2-AG regulation is COX-2. COX-2 has been shown to catalyze 2-AG oxygenation (Kozak, Rowlinson et al. 2000). Increased 2-AG levels by COX-2 inhibition showed favored outcomes in a rat model of traumatic brain injury (Gopez, Yue et al. 2005). However, prolonged 2-AG stimulation in coronal brain section was found to internalize or down-regulate CB_1 receptors (Schlosburg, Blankman et al. 2010). Chronic and high 2-AG overload by MAGL inactivation led to compensatory desensitization of CB_1 in the brain, as CB_1 density and functional responses were attenuated (Schlosburg, Blankman et al. 2010). Administration of 2-AG had consequently no effect on the pathophysiology of TBI in CB_1-/- mice (Panikashvili, Mechoulam et al. 2005).

The CB_2 receptor, expressed only marginal in healthy brain tissue, can be up-regulated under neuroinflammatory conditions (for review: Stella, 2010). Microglia mainly express CB_2 receptors and can produce high amounts of 2-AG under pro-inflammatory circumstances by the activation of ionotropic P2X7 receptors (Walter, Franklin et al. 2003; Onaivi 2009). 2-AG can also trigger microglia proliferation in vitro and can lead to reduced levels of pro-inflammatory cytokines (Carrier, Kearn et al. 2004). Several authors have highlighted the importance of 2-AG on the regulation of microglia during disease (Franklin, Parmentier-Batteur et al. 2003; Carrier, Kearn et al. 2004; Nunez, Benito et al. 2004). It was also shown that microglia possess the abn-CBD receptor and are sensitive to 2-AG mediated neuroprotection by enhanced microglia migration via this receptor (Franklin, Parmentier-Batteur et al. 2003; Walter, Franklin et al. 2003; Kreutz, Koch et al. 2009).

1.6 Organotypic entorhinal hippocampal slice cultures

The organotypic entorhinal hippocampal slice culture (OHSC) is an excellent model to study neuronal plasticity, long-range projections and neuronal damage. The cytoarchitecture and the synaptic circuit of the hippocampal formation remain intact and the interaction of neurons, astrocytes and microglia can be investigated in an organotypic surrounding, close to that in vivo (Stoppini, Buchs et al. 1991; Gahwiler, Capogna et al. 1997; Holopainen 2005). In OHSC neurons, astrocytes and microglia maintain their morphologic characteristics and show the same structure as in vivo conditions (Kunkler and Kraig 1997). The hippocampal formation incorporates the cornu ammonis (CA), the dentate gyrus (DG), the hilusregion (HI), the subiculum and the entorhinal cortex (EC). Distinct laminated structures characterise the hippocampus, like the stratum pyramidale and the stratum granulosum, composed of the pyramidal CA region 1-3 (CA1-CA3) neurons and the granule cell layer of the DG (Amaral 1978; Amaral, Ishizuka et al. 1990; Forster, Zhao et al. 2006). In Fig.4 an overview of the following synaptic connection is shown. The neuronal excitation enters from the layers II and III of the EC via the perforant pathway (PP) mainly to the outer molecular layer, towards the dendrites of the granule cell layer of the DG while some fibers project from the layer III to the CA1 region. The mossy fiber pathway extends then towards the CA3 pyramidal cells, creating a rich connection between the granular cells and the pyramidal neurons of the CA3 region. By the Schaffer collaterals, the excitation is led from the CA3 region to the CA1 pyramidal neurons and the loop is made back to the EC. Axons leave the hippocampus via the subiculum back to the EC (Coulter, Yue et al. 2011).

The hippocampal circuit is excitatory in nature and uses glutamate as its primary neurotransmitter (Lothman, Bertram et al. 1991) while the final output of this excitatory loop is modulated and fine-tuned by the inhibitory GABAergic interneurons at different steps (Staiger, Zilles et al. 1996). Recent studies showed that the connection fibers from the EC are

also connected directly to the entire CA 1-3 region, although in a lesser extent than to the DG (Coulter, Yue et al. 2011). OHSC in general are made according to the method published by Stoppini et al., (1991).

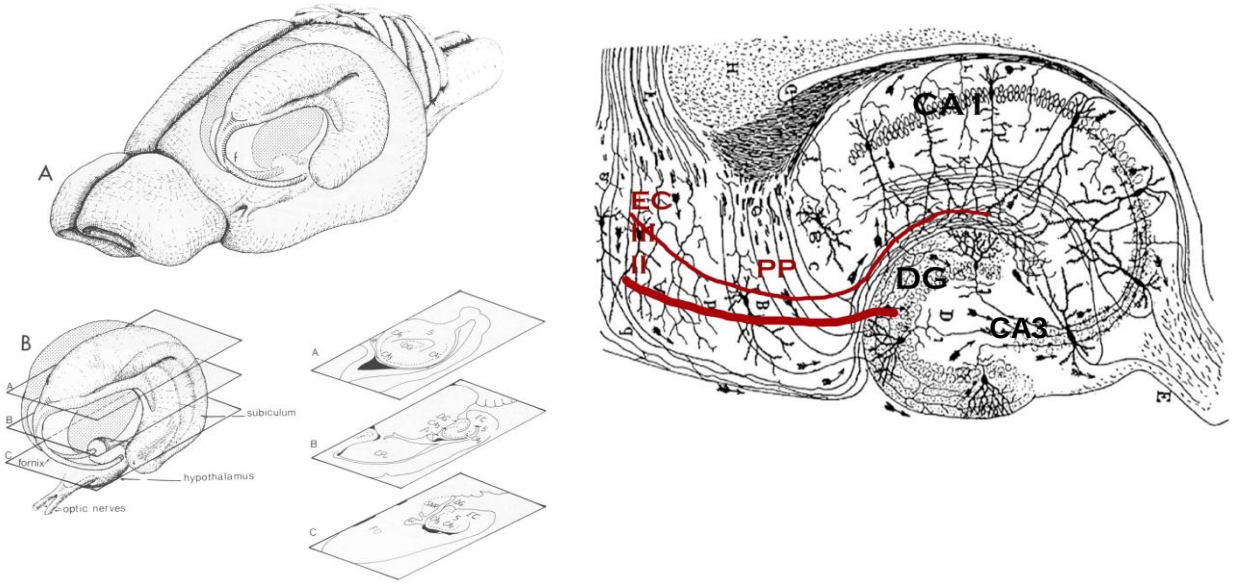

Figure 1.4 Illustration of a horizontal slice of the hippocampal formation

The trisynaptic pathway signal propagates from the layer II of the entorhinal cortex (EC) to the dentate gyrus (DG) through the perforant path (PP). DG projects to CA3 via mossy fibers. CA3 neurons interconnect via a recurrent network to the CA1 through the Schaffer collaterals and back to the EC. The hippocampus contains another excitatory input, called the temporoammonic pathway, in which a signal propagates from layer III of EC directly to CA1 distal dendrites. (Figures adapted and modified from Amaral and Witter, 1989 and Ramòn y Cajal, 1911)

OHSC are used in the present dissertation due to their unique organotypic preservation. After preparation of OHSC the tissue re-organizes and obtains a stable structure of functional neurons, astrocytes and microglia after five days in vitro. Therefore this model is qualified to investigate cellular interaction without influence of the entire organism. The insights can then be applied for specific testing under in vivo conditions.

Neuronal damage in OHSC

OHSC are mostly used to investigate pharmacological compounds or to study neuronal cell damage in vitro due to the maintenance of functional cellular connections. Microglia become highly activated after neuronal insults but can hardly be studied in vitro, as single microglia cultures are difficult to maintain and their behavior changes depending on culture conditions. In cultured OHSC microglia regain their normal morphology and display a healthy surrounding like under in vivo conditions.

Long range projection transection

Disruption of long range projection fibers causes detrimental functional deficits. Projection fibers connect developmentally distinct brain areas and allow highly specialized motor but also mental functions. Disconnection of the originating and target areas is often a result of CNS pathologies like SCI, TBI or stroke. The neuroprotective properties of eCB, involving analgesia and anti-inflammation in the CNS but also in the periphery, might therefore also be involved in fiber damage. OHSC offer a system to study long range projection fibers as they exist in spinal cord and other important areas of the CNS. Here, the perforant pathway was used to investigate the precise regulation of eCB after fiber damage. The perforant pathway fibers originate in the EC and terminate in the molecular layer of the DG, allowing the precise dissection of the projecting fiber tract (Stoppini, Buchs et al. 1991; Deller 1997; Frotscher,

Heimrich et al. 1997; Ramirez 2001; Kovac, Kwidzinski et al. 2004). Transection of the perforant pathway (PPT) is a well-accepted tool to gain insight to inflammatory processes, not only at the lesion site but also in the surrounding and connected tissue.

Excitotoxicity

Excitotoxic lesion is the most frequent neuronal damage used in OHSC, either by kanaic acid or *N*-Methyl-*D*-Aspartat (NMDA). Increased excitation provokes neuronal cell death and is one of the main causes to acute and delayed cell death that is seen in vascular, traumatic and degenerative diseases in the CNS (Choi, Koh et al. 1988). Activation of NMDA receptors leads to intracellular Ca^{2+} entry promoting various effects like nitrogen monoxide increase, cytoplasm and nuclear processes that finally mediate cell death. The CA3 pyramidal neurons are together with the CA1 neurons the most vulnerable cell type of the hippocampal formation followed by the DG granule cells. (Holopainen, Lauren et al. 2001; Kristensen, Noraberg et al. 2001).

1.7 Aim of the research

The involvement of the eCB regulation within the different glial cells during neuronal insults and the temporal alteration of eCB are still unknown. However, the involvement of the eCBS in various processes of neuronal insults is indicated as described previously. Here, the precise temporal regulation of the eCB after neuronal excitotoxicity and lesion of the long-range projection in the hippocampus is investigated. OHSC were used to study the different lesion models as the anatomical structure allows differentiating neuronal subpopulations and site-specific effects. The perforant pathway, as long-range projections, allows to investigate the differentially (anterograde or retrograde) lesioned regions. The EC, DG, and the CA1 are included in the present study.

The excitotoxic lesion model of OHSC induces a neuronal inflammation initiated by neuronal over-stimulation. In the investigated areas of OHSC, neuronal populations displaying diverse vulnerabilities (from low to high; CA1, DG, EC) to excitation can be differentiated. Thus, the eCB regulation of differentially lesioned neuronal populations is determined.

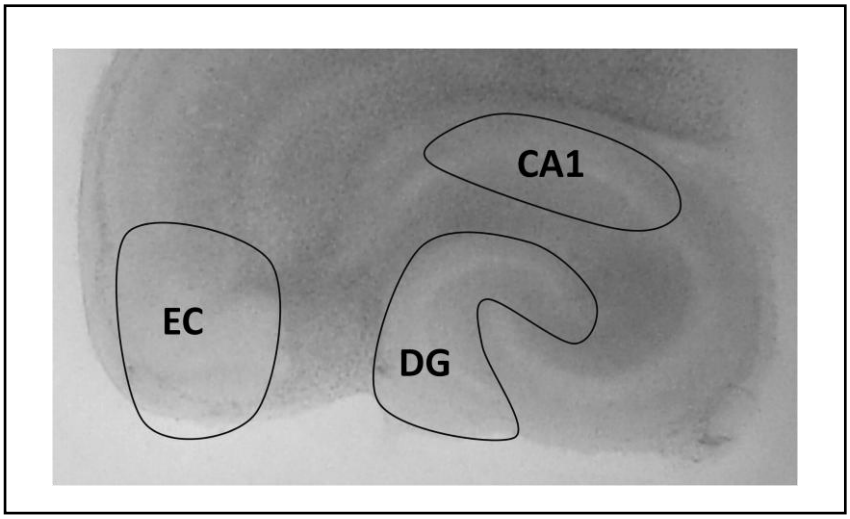

Figure 1.5 Dissected areas of OHSC

The differentiated regions in OHSC, which are analysed after PPT and excitotoxic lesion in the present study. Entorhinal cortex (EC), dentate gyrus (DG), cornu ammonis region 1 (CA1)

The main synthesising and hydrolysing enzymes of the eCB were studied up to 72 hours after excitotoxicity and PPT in OHSC as well. The intrinsic enzymatic regulation is determined to investigate the involved cell populations in eCB regulation. Moreover, the respective cell type being responsible for eCB metabolism, namely neurons, microglia or astrocytes, are analysed in primary cell cultures as well as in lesioned OHSC to clarify their ability to regulate eCB and their synergistic effects in tissue culture. Like other CB receptors which were shown to be involved in protective mechanisms after neuronal lesion, the possible CB_3 GPR55 is

investigated in excitotoxically lesioned OHSC on its impact on neuronal protection after excitotoxic lesion.

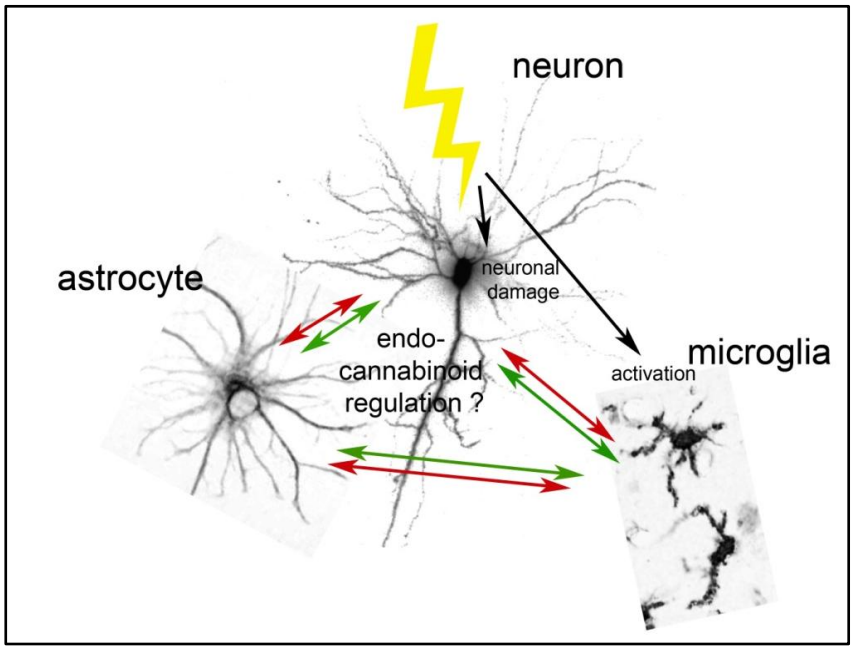

Figure 1.6 Schematic drawing of cell types present in OHSC

In the present dissertation the shown cell types and their involvement in endocannabinoid regulation are investigated.

Hypotheses:

A. Are NEA intrinsically and cell-dependently regulated after PPT in rat OHSC?

B. Is 2-AG intrinsically and cell-dependently regulated after PPT in rat OHSC?

C. Is 2-AG an overall neuroprotective modulator after excitotoxicity and PPT?

D. Does GPR55 excert neuroprotective effects in excitotoxically lesioned OHSC ?

2. Materials and Methods

2.1 Materials

All substances used were treated following producers recommendations. Substances were dissolved in DMSO or ethanol and stored at -20°C (Tab. 2.1). The final concentration of DMSO or ethanol was 0.1% (v/v) or below. To exclude any interference of the used solvents, equivalent concentrations of DMSO and ethanol were used for control experiments.

Table 2.1 Canabinoid/GPR55 agonists and antagonists and deutered standards used for the experiments

substance	specification	concentration	solvent	manufacturer
AM281	synthetic CB1 antagonist/inverse agonist	0.1 µM 10 µM	DMSO	Tocris (Cat no. 1115)
JZL184	MAGL inhibitor	10 µM	DMSO	Gift from J. Long (La Jolla, USA)
L-alpha-Lysophosphatidyl-inositol (LPI)	GPR55 agonist	0.01, 0.1, 1.0, 10 µM	DMSO	Sigma- Aldrich (Cat no. L7635)
WIN-55,212-2 mesylate	CB1 and CB2 agonist	1 µM	ethanol	Tocris (Cat no. 1038)
AEA-d_8	Arachidonoyl ethanolamide-d_8 (AEA-8) contains eight deuterium atoms at the 5, 6, 8, 9, 11, 12, 14, and 15 positions	5 ng/ml	ethanol	Cayman Chemical (Cat no. 390050)

Continue of Tab 2.1: Canabinoid/GPR55 agonists and antagonists and deutered standards used for the experiments

substance	specification	concentration	solvent	manufacturer
PEA-d_4	Palmitoyl ethanolamide-d_4 (PEA-d_4) contains four deuterium atoms at the 7, 7', 8, and 8' positions	10 ng/ml	ethanol	Cayman Chemical (Cat no. 10007824)
OEA-d_2	Oleoyl ethanolamide-d_2 (OEA-d_2) contains two deuterium atoms at the 11 position	20 ng/ml	ethanol	Cayman Chemical (Cat no. 10007823)
2-AG-d_5	2-Arachidonoyl glycerol-d_5 (2-AG-d_5) contains five deuterium atoms at the 1, 1, 2, 3, and 3 positions of the glycerol moiety	10 ng/ml	ethanol	Cayman Chemical (Cat no. 362162)
1-AG-d_5	1-Arachidonoyl glycerol-d_5 (1-AG-d_5) contains five deuterium atoms at the 1, 1, 2, 3, and 3 positions of the glycerol moiety	10 ng/ml	ethanol	Cayman Chemical (Cat no. 362152)

Antibodies were stored following manufacturers recommendations and applied with the dilution factor tested individually for each antibody (Tab. 2.2)

Table 2.2 Antibodies and stainings listed in alphabetic order

antibody	blocking peptide	dilution IHC	dilution WB	secondary AB	manufacturer
ß-actin **monoclonal mouse antibody directed against human**			1:40 000	anti-mouse IgG, 1:4000	Sigma-Aldrich (Cat. no A1978)
CB_1 **guinea pig polyclonal antibody against murine**		*1:100*	*1:2000*	*Goat anti guinea pig 568*	Frontier Science, (Cat no. CB1-G P-Af530-1)
DAGL **alpha rabbit polyclonal antibody against human**		1:200	*1:1000*	*Goat anti rabbit 568*	Frontier Science, (Cat no. DGLa-Rb-Af380-1)
FAAH **rabbit polyclonal antibody against human**	FAAH (Cat no 301600)	*1:200*	*1:1000*	*Goat anti rabbit 568*	Cayman Chemical (Cat no. 101600)
GFAP **monoclonal mouse antibody**	5% (v/v) Roti	*1:200*		*Goat anti mouse 633*	BD Pharmingen (Cat no. 556330)
Hoechst 33342		*1:50 000*		*405*	Sigma-Aldrich (Cat no. B2261)
IsolektinB4 **Griffonia simplicifolia (IB_4)**		*1:50*		FITC conjugated (488)	Vector Labs (Cat no. FL-1201)

Continue of Tab 2.2 Antibodies listed in alphabetic order

antibody	blocking peptide	dilution IHC	dilution WB	secondary AB	manufacturer
***MAGL* rabbit polyclonal antibody against human**		*1:200*		*Goat anti rabbit 568*	Cayman Chemical (Cat no. 100035)
***MAGL* rabbit polyclonal antibody against human**	developed by K. Mackie`s lab		*1:200*	anti-rabbit, 1:1000	gift from K. Mackie, Indiana, USA
***NAAA* rabbit polyclonal antibody against rat**	developed by Ueda`s lab	*1:1000*	1:5000	*Goat anti rabbit 568*	gift from N. Ueda, Kagawa, Japan
***NAPE-PLD* rabbit polyclonal antibody against human**	NAPE-PLD peptide, cat.-No 10303	*1:200*	*1:1000*	*Goat anti rabbit 568*	Cayman Chemical (Cat no. 10305)
***NeuN* mouse monoclonal antibody**	5% (v/v) Roti	*1:200*		*Goat anti mouse 633*	Millipore (Cat no. MAB377)
***Propidium Iodide* (PI)**		5µg/ml		*536*	Sigma-Aldrich (Cat no. 25535-16-4)
***PPARα* rabbit polyclonal antibody against murine**	PPARα, cat.-No PEP-025	*1:1000*	*1:1000*	*Goat anti rabbit 568*	Thermo Scientific (Cat no PA1-822A)
***Vglut1* guinea pig polyclonal antibody**			1:1000	*Goat anti guinea pig 488*	Synaptic Systems (Cat no. 135304)

The following table shows the buffer solutions used in the experiments. The amounts are calculated for one liter of distilled water.

Table 2.3 Main puffers used

Phosphate buffer (PB) 0,1M (pH 7.4):		**PB 0,2M (pH 7.4):**		**PBS/Triton:**	
Na2HPO4	11,36 g	Na2HPO4	22,72 g	PBS	1 L
KH2PO4	2,72 g	KH2PO4	5,44 g	Triton X-100	3 ml
PBS (pH 7.4):		**TBS (pH 7.4)**		**TBS/Triton**	
NaCl	9,00 g	NaCl	8,76 g	TBS	1 L
KH2PO4	0,54 g	Tris	6,05 g	Tween-20	3 ml
Na2HPO4	2,27 g				

Gel electrophoresis for western blot analysis was conducted with gels described in table 2.4. Further cell and slice culture media as well as western blot buffers are described in Tab. 2.5.

Table 2.4 Gel electrophorese was conducted with following gels

	separating gel (7,5 %)	**separating gel (12,5 %)**	**stacking gel (5 %)**
Aqua dest.	7,45 ml	4,95 ml	3,05 ml
1,5 M Tris-HCl (pH 8,8) +SDS	3,75 ml	3,75 ml	-
1,5 M Tris-HCl (pH 6,8) +SDS	-	-	1,25 ml
Acrylamid/Bis 30%	3,75 ml	6,25 ml	650 µl l
10% Ammoniumpersulfat	45 µl	45 µl	25 µl
TEMED	10 µl	10 µl	10 µl

Table 2.5 Culture media and Western Blot buffers

Slice culture media (pH 7.4)				**Cell culture media 10 % and 2 %**	
Minimal essential Media (MEM, Gibco)	50 % (v/v)	Streptomycin (sigma-Aldrich)	0.1mg/ml	DMEM	88% (v/v)
Hanks' balanced salt solution (HBSS, Gibco)	25 % (v/v)	Penicillin (sigma-Aldrich)	100 µg/ml	Glutamine	1 % (v/v)
Normal horse serum (NHS, Gibco)	25 % (v/v)	Ascorbic acid (Sigma-Aldrich)	0.8 µg/ml	Penicillin	1 % (v/v)
Glutamine (Braun)	2 % (v/v)	Insulin (Boehringer)	1 µg/ml	Feutal bovine serum	10% (v/v) or 2 % (v/v)
Glucose (Braun)	1.2 mg/ml				

Lysis buffer		**Elektrophorese buffer**		**Transferbuffer**	
Tris	80 mM	Tris	3 g	Tris	3 g
Sodium dodecylsulfate–polyacrylamide (SDS)	70 mM	Glycin	14,4 g	Glycin	14,4 g
Saccharose	300 mM	10 % SDS	10 ml	10 % SDS	10 ml
Sodium orthovanadate (SOV)	3 mM	Aqua dest.	1 L	Methanol	200 ml
Phenylmethylsulfonyl fluoride (PMSF)	0.5 mM			Aqua dest.	800 ml

2.2 Methods

2.2.1 Cell culture

Ethic statement

All animal experiments have been approved by the ethics committees of the German federal states of Hessen or Saxonia and were performed in accordance with the Policy on Ethics and the Policy on the Use of Animals in Neuroscience Research as approved by the European Communities Council Directive (89/609/EEC) amended by the directive 2010/63/EU of the European Parliament and of the Council of the European Union on the protection of animals used for scientific purposes. The animals were hold in a 12 hour light, 12 hour dark cycle with water and standard food ad libitum. The animals were decapitated at postnatal day 0-2 (p 0-2) for cell cultures and at p8 for OHSC.

Primary cell cultures

Primary cultures of hippocampal neurons were prepared using a modified method originally described by Brewer and colleagues under aseptic conditions (Brewer, Torricelli et al. 1993). Wistar rat pubs (p0) were decapitated and brains were prepared by removing the skin and the cranium with small scissors. Subsequently, brains were placed carefully with forceps into a solution of ice-cold HBSS. The hippocampi were dissected with an applicator and placed in Neurobasal Medium (Gibco) containing BSA (Sigma-Aldrich) and papain (1 mg/ml, Sigma-Aldrich) for 20 min at 37 °C. Then neurons were isolated by tissue dissociation using a Pasteur pipette until tissue homogenisation. The obtained homogenate was centrifuged for 10 min (45 g) and plated onto poly-L-lysine-coated coverslips. Cells were maintained in Neurobasal medium supplemented with B-27 (Gibco), GlutaMAX (Gibco) and penicillin/streptomycin at 37 °C in a humidified atmosphere with 5 % (v/v) CO_2 for 2 weeks.

Primary microglia and astrocyte cell cultures were isolated from cerebral cortices of p 1-2 neonatal Wistar rats. Brains were removed as described above and placed into a solution of ice cold HBSS. The meninges were removed with thin forceps and after 5 min incubation with Ca^{2+}/Mg^{2+}-free HBSS, containing trypsin (4mg/ml, Boehringer) and DNAse (0.5mg/ml, Worthington, Bedford, MA, USA) the cerebral cortices were dissociated. Cells were plated into poly-L-lysine (Sigma-Aldrich) coated 75 cm^2 tissue culture flasks (Falcon) containing 10 % cell culture media. To obtain a proper glial culture astrocytes and microglia were cultured for 10 days in a mixed culture. The cell culture media was changed every other day. Culture media is optimised for glial cells, neurons do not survive the cultivation procedure, using that procedure astrocyte-microglia cultures were obtained.

Microglia were isolated from the astrocytic monolayer by gentle shaking of the culture flasks with fresh culture media for 20 min. The microglia in the culture media was centrifugated for 5 min at 150 g. The supernatant was removed and the obtained cells were cultured in 2 % cell culture media into 6 or 24-well dishes coated with poly-L-lysine one day prior to experiments.

Astrocyte cultures were obtained after microglia were removed for at least three times by the procedure described above. The astrocytes were then washed with serum free media and were incubated with 2 ml of trypsin/EDTA for 5 min. Trypsin was stopped with 10 % cell culture media and cells were transferred in a 15 ml falcon tube (Greiner) for centrifugation for 5 min at 150 g. Supernatant was removed and the obtained cells were cultured in 2 % cell culture media. One day prior to all experiments, primary cultures of astrocytes were transferred into 6 or 24-well dishes coated with poly-L-lysine.

Organotypic entorhinal hippocampal slice cultures

OHSC were prepared from 8-day old Wistar rats. Animals were decapitated and the brains were dissected under aseptic conditions. Brains were removed as described above and placed into a solution of ice cold HBSS. Subsequently the cerebellum and the frontal lobe were removed with a vertical cut using a scalpel and brains were placed in 4 °C minimal essential medium (MEM) containing 1 % (v/v) glutamine (Gibco). The brains were cleaved with tissue adhesive (Histoacryl, Braun, Melsungen, Germany) to a vibratome dish prepared with an aseptic agar block to stabilise the brains during the slicing procedure. The vibratome dish with the brain was placed in ice-cold MEM on a sliding vibratome (Leica VT 1200S, Leica Microsystems AG, Wetzlar, Germany), which was used to cut the brain horizontally in 350 µm-thick slices. The hippocampi were dissected under a binocular (Zeiss) and were immediately placed on cell culture inserts (pore size 0.4 µm; Millipore, Schwalbach/Ts., Germany) for 6-well culture dishes (Falcon, BD Biosciences Discovery Labware, Bedford, MA). The dishes contained 1 ml slice culture medium per well. OHSC were cultured at 35 °C in a fully-humidified atmosphere with 5 % (v/v) CO_2. The culture medium was changed every second day.

2.2.2 Neuronal lesion models

Perforant Pathway Transection

The PPT was mechanically set on day *in vitro* (div) 6 by use of a disposable ophthalmic scalpel equipped with a stainless steel blade (Feather, Osaka, Japan). Under a binocular (Zeiss, Jena, Germany), PPT was performed within OHSC through the perforant pathway following the sulcus between the hippocampus and the entorhinal cortex (EC) as visualised in Fig 2.1. The EC, the DG and the CA1 regions were dissected 0, 1, 6, 12, 24, 48 or 72 hours post lesion (hpl).

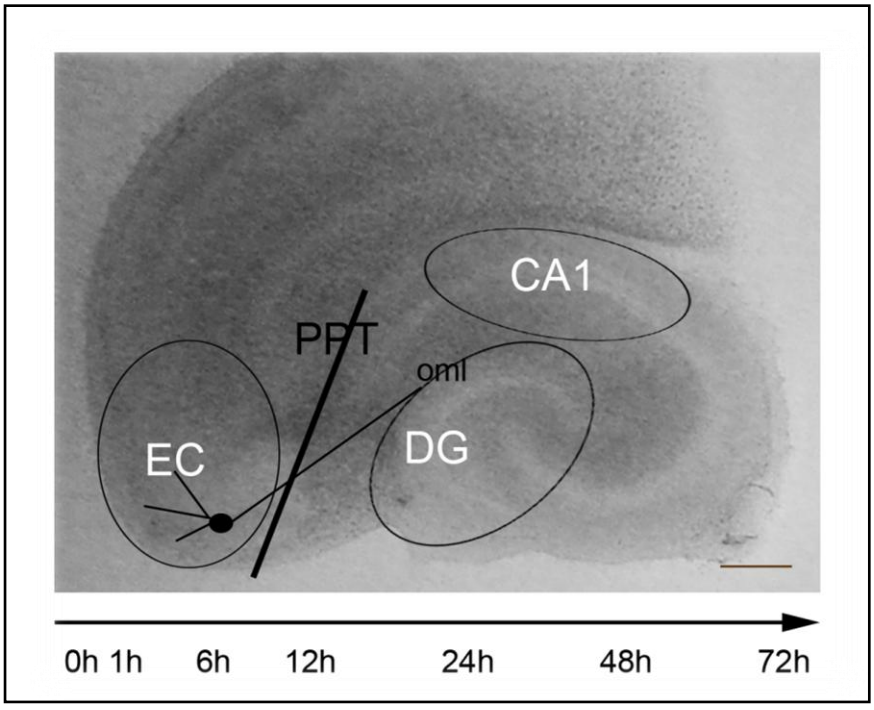

Figure 2.1 Overview of the perforant pathway transection (PPT) in OHSC

The black line indicates the transection of the axons originating from layers II and III of entorhinal cortex (EC) and projecting to the outer molecular layer (oml) of the dentate gyrus (DG). The areas of EC, DG and cornu ammonis (CA)1 were dissected as visualised by the open cycles. OHSC were kept in culture for 6 days before PPT was set and tissue of the highlighted areas was collected 1 h, 6 h, 12 h, 24 h, 48 h and 72 h post lesion. Bar= 500 µm.

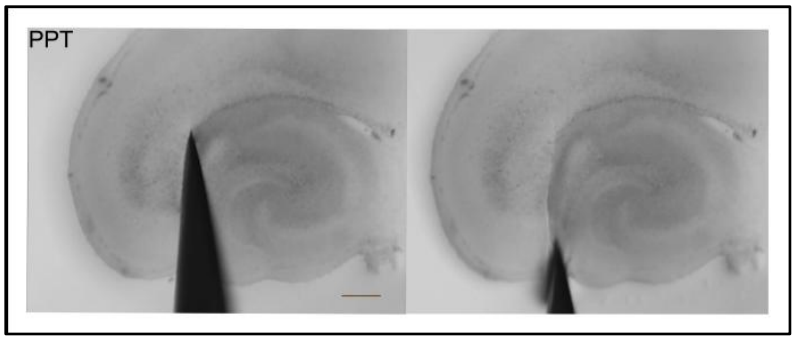

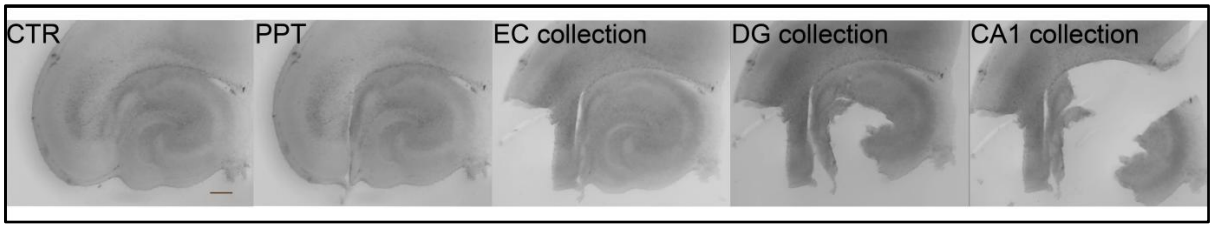

Figure 2.2 Visualisation of the PPT and tissue collection

The PPT is set between the EC and the DG to cut all the connecting axonal fibers from the EC to the outer molecular layer of the DG. The EC, DG and the CA1 tissue is collected after the respective time of interest.

Excitotoxic lesion and treatment protocol

After OHSC preparation, the tissue cultures were spread over the different experimental groups as described below. The control group was incubated with culture media from div 0 until div 9, the day of fixation. They were used as negative controls. Substances were supplemented to the culture media at div6 until div 9 to control for effects of the substances themselves. Excitotoxic lesion was conducted on div 6. 50 µM NMDA was added to the culture media for 4 h. Thereafter, tissue cultures were washed once with culture media and cultured until div9 in culture media which was changed every day from the NMDA lesion on. This condition was used as positive control.

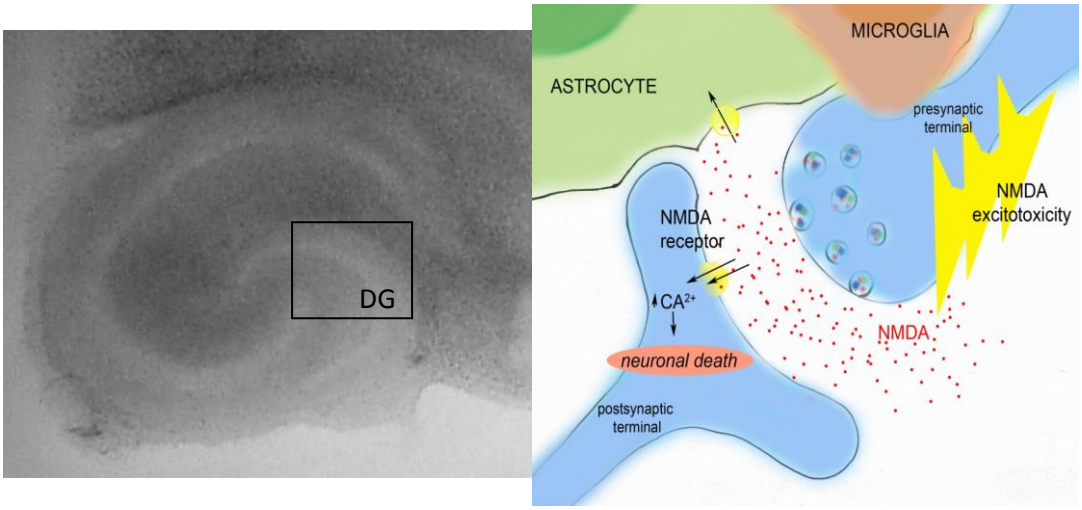

Figure 2.3 Excitotoxicity in OHSC by NMDA

During excitotoxic lesion, neurons become activated and intracellular calcium and nitric oxygen become altered, leading finally to cell death through apoptosis and necrosis. The black box indicates the area of analysis. DG, dentate gyrus.

LPI and Win55,212 were supplemented to the culture media 120h and 24h before excitotoxic lesion took place to study preconditioning. The treatment with LPI and Win55,212 was applied also during NMDA lesion and also thereafter until div7 or div9. These conditions served to find optimal conditions for neuronal protection and to identify the substance involvement in secondary damage.

AM281 is a GPR55 agonist with less potency and a CB1 antagonist/inverse agonist (Henstringe, 2011). AM281 was supplemented to OHSC after NMDA lesion with and without LPI.

siRNA transfection

MAGL gene silencing was carried out using Magl siRNA vs. rat:

(target sequence: 5'-CAGCGTGCTGTCTCGGAACAA-3';

sense strand: 5'-GCGUGCUGUCUCGGAACAATT-3';

antisense strand: 5'-UUGUUCCGAGACAGCACGCTG-3'; cat. no.: SI03067736, Qiagen, Hilden, Germany). For transfection GeneSilencer siRNA transfection reagent (Genlantis-BioCat, Heidelberg, Germany) for 6-well-culture plates were used. The following sequences were used for Gpr55 siRNA vs. rat:

target sequence: 5'- CACGTGGAGTGCGAGAGTCTT-3';

sense strand: 5' CGUGGAGUGCGAGAGUCUUTT-3';

antisense strand: 5'-AAGACUCUCGCACUCCACGTG-3', (cat. no.: SI03004708, Qiagen, Hilden, Germany). AllStars Negative Control siRNA (Qiagen) was used as a negative control. 25 µl culture medium and 5 µl GeneSilencer per well were preincubated for 5-10 min at RT. Then 15 µl culture medium was mixed with 25 µl siRNA Diluent and 1 µg siRNA or AllStars Negative Control siRNA (per well) and were incubated for 5 min at RT. Next, the transfection mix was prepared by combining the diluted GeneSilencer with siRNA mixture and incubated for 10 min at RT. The entire mixture was added directly to the hippocampal slice cultures on 5 div and the slices were cultured in serum-containing medium (1 ml/well). After 24 h culture medium was exchanged with standard culture medium.

2.2.3 OHSC staining for determining neuronal death and microglia determination

To analyse neuronal cell death in the dentate gyrus, the medium of OHSC was supplemented with 5 µg/ml propidium iodide (PI) 2 h prior to fixation with 4 % (w/v) paraformaldehyde (PFA) (Sigma-Aldrich) in 0.1 M phosphate buffer (PB). PI is a non damaging fluorescent stain that enriches in dead cell nuclei by adhesion to DNA. At div9 culture media was

removed and 4 % PFA was added for at least 4 h, the cultures were washed twice with PB and stored in PBS buffer at 4 °C until further handling. Using Isolectin B4 (IB_4) combined with fluorochrom FITC, microglia were visualised. To achieve this, OHSC were incubated 30 min in normal goat serum (1:20 in PBST) followed by an incubation with IB_4 ((1:50 in 0,5 % (w/v) BSA in PBST) over night. On the next day, OHSC were washed two times for 10 min in PBS and once in distilled water and were then embedded with Dako fluorescent mounting medium (Dako Diagnostika GmbH, Hamburg, Germany) and stored at 4 °C for at least 4 h. To analyse cell death and microglia accumulation z-stacks (2 µm) with 20 fold magnification of OHSC were generated by an inverse Zeiss LSM 510 Meta confocal laser scanning system (Zeiss, Göttingen, Germany). ImageJ software (U.S. National Institutes of Health, http://rsb.info.nih.gov/ij/download.html) was used for counting degenerating PI positive neuronal nuclei in the different EC, DG and CA1 regions.

2.2.4 Endocannabinoid analysis of OHSC by LC-MS/MS

Tissues of 3 OHSC were pooled, immediately shock frozen in liquid nitrogen and stored at -80 °C. Homogenisation was performed on ice to prevent degradation of eCB or internal standards. The extraction of eCB was conducted with a 9:1 (v/v) ethylacetate/n-hexan solution (Bishay, Schmidt et al. 2010). The tissue was homogenised first in 70 µl ice cold H_2O in a mixer mill 400 (Retsch, Haan, Germany) for 90 seconds at 25 Hz. As a next step, 20 µl were taken away from the homogenates to quantify the protein amount of beta-actin by Western Blot analysis (see below). 50 µl of the tissue samples were again homogenised together with 25 µl of internal standards, 50 µl ethylacetate/n-hexan and 50 µl H_2O. After 3 minutes of centrifugation at 10.000 g, the organic phase was collected and the extraction procedure was repeated. The ethylacetate phases were evaporated under a gentle stream of nitrogen and assimilated in 25 µl acetonitril in glass vials. Finally, 10µl were injected into the LC-MS/MS

system (API, 5000, AB SCIEX, California, USA). For accuracy, quality standards were always extracted with the samples.

The reconstituted samples were analysed for anandamided, OEA and PEA. The respective deuterated AEA-d_8, OEA-d_2 and PEA-d_4 were used as internal standards. HPLC analysis was performed under gradient conditions using a Luna HST C18 (2) column (100 mm L x 2 mm ID, 2.5 µm particle size; Phenomenex, Aschaffenburg, Germany). MS and MS/MS analysis was performed on an API 5000 triple quadrupole mass spectrometer with a Turbo V source (Applied Biosystems, Darmstadt, Germany) in the negative ion mode. Precursor-to-product ion transitions of m/z 346→259 for AEA, m/z 354→86 for AEA-d_8, m/z 324→86 for OEA, m/z 326→86 for OEA-d_2, m/z 298→268 for PEA and m/z 302→258 for PEA-d_4 were used for the multiple reaction monitoring (MRM) with a dwell time of 70 milliseconds. Concentrations of calibration standards, quality controls and unknowns were evaluated by Analyst software (version 1.4; Applied Biosystems). Variations in accuracy and intra-day and inter-day precision were <15 % over the range of calibration. Endocannabinoid values were expressed in relation to ß-actin levels obtained by Western Blot analysis (Image J 1.43, imagej.nih.gov/ij/download/). In each experiment, protein extracts from controls and corresponding PPT time matches were run on the same gel to ensure similar conditions for both groups. ECB values were then normalised and values obtained from controls were set as 100 %. Changes after PPT were described in relation to corresponding time controls.

2.2.5 Western Blot analysis

For Western Blot analysis the tissue was collected and immediately stored in lysis buffer at -80 °C. Protein extracts were obtained by sonication of tissues in lysis buffer containing 80 mM Tris, 70 mM SDS, 0,3 M Saccharose, 3 mM sodium orthovanadate and 0.5 mM phenylmethylsulfonyl fluoride (PMSF) at pH 7.4. Cell debris was removed by centrifugation for 10 min at 3000 g. Protein concentrations of the supernatants were determined by BCA test (Thermo Fisher Scientific, Rockford, USA). Equal protein amount of 5 µg were loaded onto a 12,5 % or 7,5 % (w/v) sodium dodecylsulfate–polyacrylamide (SDS) gel. After gel electrophoresis, proteins were electrotransferred to nitrocellulose membranes. After blocking non-specific protein-binding sites for 1 h with 5 % (w/v) milk (Carl Roth, Karlsruhe, Germany) or 5 % (v/v) Roti-block solution (Carl Roth, Karlsruhe, Germany) in TBST, the membranes were incubated over-night with the respective following primary antibodies diluted in 5 % (w/v) milk or 5 % (v/v) Roti block in TBST. The next day, membranes were washed three times with TBST for 10 min and the secondary horse radish peroxidase-conjugated antibodies (anti-rabbit, 1:1000; cat.-No PI 1000, Vektor laboratories, Burlingame, CA; anti-guinea pig 1:1000;cat.-No P0141, DAKO Diagnostika GmbH, Hamburg, Germany or anti-mouse IgG, 1:4000; cat.-No CP01, Millipore, Billerica, USA) were added for 1 h. Membranes were finally exposed to enhanced chemiluminescence (ECL detection system, Millipore) and the signal of bound antibody was visualised with radiographic films (Kodak, Stuttgart, Germany). Finally, semiquantification of the immunoreactive bands was performed with ImageJ image analysis software.

Specificity tests for the antibodies used

The specificity of the antibodies was tested by preabsorption with the corresponding blocking peptides. For preabsorption, each primary antibody was diluted in 5 % (w/v) milk or 5 % (v/v) Roti block in TBST and incubated with a five to ten-fold excess (by weight) of its blocking peptide for 1 h at room temperature with gentle shaking. Thereafter, the antibody-blocking peptide solution was applied to the Western Blot membranes and the subsequent procedures followed as in the above described Western Blot protocol. The CB_1 antibody was tested on CB_1 (-/-) knock-out mice (kindly provided by Beat Lutz, Mainz, Germany).

2.2.6 Immunocytochemistry

The OHSC were fixed with a 4 % (w/v) paraformaldehyde solution in 0.1 M PB for at least 4 h. After fixation, OHSC were washed in PB and incubated for at least 4 h in 15 % (w/v) sucrose, followed by 30 % (w/v) sucrose, respectively. Using a cryostat 3050 S (Leica, Wetzlar, Germany), the OHSC were sectioned (14 µm) and mounted on superfrost microscope slides (Thermo Scientific). To block unspecific binding sites, sections were preincubated with normal goat serum for 30 min (1:20 in PBS/Triton) followed by incubation with primary antibodies for 16 h in PBS/Triton containing 0.5 % (w/v) bovine serum albumin. Binding of the primary antibodies was visualised by means of the ABC method with a biotin-conjugated anti-rabbit IgG (diluted 1:100; cat-No B7389 Sigma-Aldrich) as the secondary antibody, a horseradish peroxidase (HRP)-conjugated streptavidin complex (diluted 1:100; cat.-No E2886 Sigma-Aldrich) and 3, 3-diamino-benzidine as the chromogen. For immunocytochemical characterisation of different cell populations within OHSC, the following primary antibodies were used: NeuN as a neuronal marker, GFAP as a marker for astrocytes and IB_4 as a marker for microglia.

For triple-immunofluorescence staining, the primary antibodies against NAPE-PLD, FAAH, NAAA, CB_1 or PPARα were combined with IB_4 and either with antibodies against NeuN or GFAP respectively. After incubation with primary antibodies for 16 h at room temperature, sections were washed three times with PBS followed by application of secondary antibodies Alexa fluor dye 568 (goat-anti rabbit IgG, 1:500, cat.-No A-11011, Invitrogen) and Alexa fluor dye 633 (goat anti-mouse IgG, 1:100, cat.-No A21050, Invitrogen, Karlsruhe, Germany) for 1 h. The preparations were finally coverslipped with Dako fluorescent mounting medium (Dako) and analysed using a Zeiss LSM 510 Meta confocal laser scanning system.

2.2.7 Semi-quantitative real time PCR

All primers were synthesised by MWG Biotech, Eversberg, Germany and diluted to 10 pmol/µl. Cells or OHSC were harvested and stored in RTL*later* (Qiagen) at -80 °C until further use. Total RNA was extracted from the cells using TRIzol reagent (invitrogen) according to the manufacturers instructions. For RNA extraction, the cells and the tissues were collected and immediately stored in 50 µl RLT*later* at -80 °C until further use. Tissue rupture was obtained by sonication 3x 3 sec in 1 ml Trizol reagent (invitrogen) on ice. The samples were centrifuged for 10 min at 10.000 rpm at 4 °C. The supernatant was transferred into a new Eppendorf tube and 200 µl chloroform were added to obtain RNA. After 3 min at room temperature, the tubes were centrifuged at 13.000 rpm for 15 min and the upper phase (500 µl) was transferred into a new tube. 600 µl of ice cold isopropanol were added and incubated 10 min at RT for protein precipitation.

Table 2.6 Primer sequences

Gene product (rat)	**mRNA accesion**	**Nucleotide sequence 5´-3´**	**°C**
DAGL	NM_001005886.1	sense TGAGCCCCACTGAGGTAGAC antisense GGACAGCAGCAACAGCTCTA	**61**
MAGL	NM_138502.2	sense: ATATCCTTGGGGCGCATCGA antisense: GATGAGTGGCTCGGAGTTGT	**57**
GPR55	XM_001063474.1	sense: CTGCCACAAGTGAAGTCC antisense: GACCACGAAGACGACAAG	**61**
GAPDH	NG_028301.1	sense: ATGGTGAAGGTCGGTGTGA antisense: AAGATGGTGATGGGCTTCC	**57-61**

After centrifugation for 15 min at 11 000 g, supernatant was discarded and RNA was washed with 75 % (v/v) ethanol and dissolved in 20 µl DPC water. RNA measurement was done by photometric analysis. The mesomeric structures of purin and pyrimidin that are part of the nucleic acid are excited by UV-light. The absorption was measured at 260 nm and 280 nm. The quotient of the measured absorption represents the purity of the RNA extracted and must be above 1.7 (OD 260/280). Total RNA was immediately reversely transcribed (Superscript II, Invitrogen) with oligo(dT) primer cDNA. 50 ng of total RNA were subjected to rtPCR using Platinum-SYBR Green® qPCR Supermix (Invitrogen). Oligonucleotide primers (Tab.2.4) were designed with the Primer3 software to flank intron sequences. All primers were synthesised by MWG Biotech, Eversberg, Germany and diluted to 10 pmol/µl. Quantitative rtPCR was performed by an CFX9 (Bio Rad laboratories, München, Germany) using the following protocol: 3 min at 95 °C and 40 cycles of 10 sec at 95 °C and 30 s at

57-61 °C. A product melting curve was recorded to confirm the presence of a single amplicon. The correct amplicon size and identity were additionally confirmed by agarose gel electrophoresis. Standard curves with serial dilutions of cDNA were generated for each primer pair to assert linear amplification. Threshold cycle (C_t) values were set within the exponential phase of the PCR. After normalisation to rodent glyceraldehyde 3-phosphate dehydrogenase (GAPDH) primer, ΔC_t values were used to calculate the relative expression levels. Gene regulation was statistically evaluated by subjecting the $\Delta\Delta C_t$ values derived from each preparation samples to a one way Anova.

2.2.8 Statistical Analysis

Data from at least three independent experiments were expressed as mean values (± standard error of the mean (SEM)). Data were statistically analysed using one way ANOVA, followed by Bonferroni posttests. Results with $p < 0.05$ were considered as significant. Analysis was conducted with Graph Pad Prism software 5 (GraphPad software, La Jolla, USA).

3. Results

Endocannabinoid regulation in different OHSC models of neuronal damage

3.1 Perforant pathway transection and neuronal damage

After div 6, rat OHSC were lesioned by following the sulcus between the EC and the hippocampal formation to secure that all projecting fibers of the EC were disconnected. PPT is an indirect dendritic lesion, as the projecting axonal fibers were mechanically transsected without direct dendritic damage. The determination of neuronal cell death by counting the numbers of propidium iodide (PI) positive nuclei, revealed very few PI positive nuclei in the EC, the DG and the CA1 region. There was no significant change in the number of PI positive nuclei or IB_4 positive microglia in investigated regions (EC, DG, CA1) at all time-points assessed ($p > 0.05$). No difference was found between controls and PPT slices ($p > 0.05$, $n = 3$).

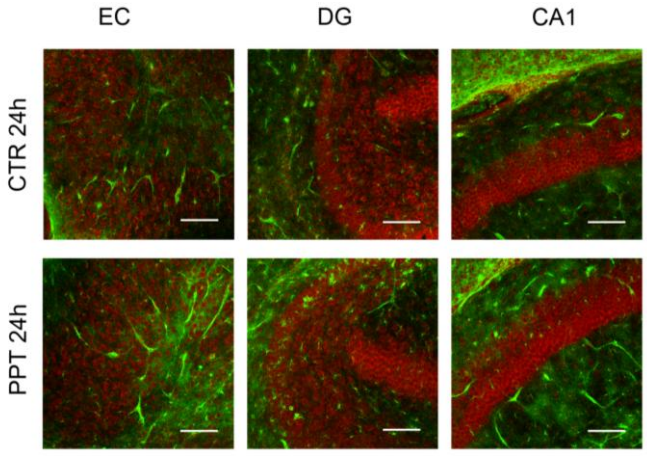

	EC CTR		EC PPT		DG CTR		DG PPT		CA1 CTR		CA1 PPT	
	PI	IB_4	PI	IB_4	PI	IB_4	PI	IB_4	PI	IB_4	PI	IB_4
0 hpl	0.0	16	0.0	22	0.0	6	0.3	19	0.0	11	0.0	14
1 hpl	0.0	19	0.3	26	0.3	17	0.7	23	0.0	14	0.3	11
6 hpl	0.0	32	0.0	23	0.3	9	0.0	15	0.0	10	0.0	16
12 hpl	0.0	25	0.0	17	0.3	18	1.7	24	0.0	8	0.0	12
24 hpl	1.7	10	1.3	26	0.7	15	1.7	28	0.0	17	0.3	13
48 hpl	1.7	24	1.7	33	1.0	16	1.3	25	0.7	18	0.7	15
72 hpl	0.0	28	0.0	18	0.0	18	2.0	30	0.0	15	1.0	17

Figure 3.1 Neuronal damage in PPT

72 h after PPT, neuronal damage was hardly observed. Microglia were not significantly enhanced in the EC, DG and CA1 region in OHSC.

3.2 Endocannabinoid regulation after neuronal damage in the hippocampal formation

The different regions were pooled by three OHSC to obtain a net tissue weight of approximately 1 mg per tissue. The data obtained by investigating the eCB levels after PPT and excitotoxic (10 and 50 µM NMDA) damage at different time points up to 72 hpl are shown.

3.2.1 Endocannabinoid measurement

The eCB levels of non lesioned controls (CTR) were set to 100 % and the PPT data was expressed in relation to their time controls, respectively. The actin content of each sample was examined to control for the collected amount of tissue.

3.2.2 Endocannabinoid levels after PPT

Axonal dissection/ dendritic denervation as induced by PPT, led to a site-specific intrinsic up-regulation of AEA, PEA, OEA and 2-AG levels in the DG. Under control conditions the following absolute values for NEA and 2-AG were found in the investigated areas: AEA: EC, 0.01 ng/ml; DG, 0.01 ng/ml; CA1, 0,02 ng/ml; PEA: EC, 1.00 ng/ml; DG, 1.40 ng/ml; CA1, 1.00 ng/ml; OEA: EC, 0.50 ng/ml, DG, 0.50 ng/ml, CA1, 1.00 ng/ml, 2-AG: EC, 6.71 ng/ml; DG, 5.45 ng/ml; CA1, 6.06 ng/ml respectively.

Entorhinal Cortex: In the EC region, no significant changes of the measured endocannabinoid levels were observed after PPT. Values are given in Tab 3.1 and shown in Fig. 3.2A. AEA levels in the EC remained at control levels. Only at 1 hpl a non significant elevation to 139 % was observed. At all time points investigated, no significant changes were detected for PEA, OEA or for 2-AG levels in the EC ($p > 0.05$).

Dentate Gyrus: Values are given in Tab. 3.1. In the DG, AEA levels did not differ significantly from controls up to 12 hpl. At 24 hpl, mean AEA levels were significantly increased compared to controls (24 hpl, 261 %; $p < 0.001$). Thereafter, AEA levels declined and were below the respective time control at 72 hpl (Fig. 3.2B). PEA levels in the DG did not differ significantly from controls up to 6 hpl. At 12 hpl, the PEA levels were elevated (12 hpl, 193 %, $p < 0.05$) and reached the maximum at 24 hpl (24 hpl, 352 %, $p < 0.001$). PEA levels then declined and were found to be reduced at 72 hpl without reaching the significant threshold. OEA levels after PPT in the DG were comparable to control levels up to 12 hpl. At 24 hpl, OEA levels were maximal elevated (24 hpl 299 %; $p < 0.001$). Thereafter, OEA levels declined and were lowered at 48 hpl and 72 hpl compared to the respective time controls (Fig. 3.2B). 2-AG levels did not differ significantly from controls up to 12 hpl in the DG. At 24 hpl mean 2-AG levels were significantly increased compared to controls (Fig. 3.2B, 24 hpl, 172.20 %; $p < 0.05$). Thereafter, 2-AG levels declined to control levels.

Cornu ammonis 1 In the CA1 region, no significant changes were observed in AEA levels (Fig.3.2C). PEA levels remained close to the control levels until 12 hpl. At 24 hpl (24 hpl, 70 %; $p> 0.05$), PEA levels were below control levels reaching the significant threshold at 48 hpl (48 hpl, 38 %; $p < 0.05$). OEA levels in the CA1 region were comparable to the control levels up to 24 hpl. At 48 hpl the OEA levels decreased significantly compared to the control levels (48 hpl, 44 %; $p < 0.05$; Fig. 3.2C). No significant changes were observed in 2-AG levels in the CA1 region.

Table 3.1 Endocannabinoid values after PPT

EC	*AEA (%)*	*PEA (%)*	*OEA (%)*	*2-AG (%)*
0 hpl	*115; p>0.05*	*116; p>0.05*	*106; p>0.05*	*122; p>0.05*
1 hpl	*139; p>0.05*	*160; p>0.05*	*157; p>0.05*	*118; p>0.05*
6 hpl	*74; p>0.05*	*96; p>0.05*	*86; p>0.05*	*94; p>0.05*
12 hpl	*121; p>0.05*	*143; p>0.05*	*130; p>0.05*	*119; p>0.05*
24 hpl	*112; p>0.05*	*111; p>0.05*	*121; p>0.05*	*134; p>0.05*
48 hpl	*82; p>0.05*	*66; p>0.05*	*75; p>0.05*	*87; p>0.05*
72 hpl	*79; p>0.05*	*85; p>0.05*	*99; p>0.05*	*91; p>0.05*
DG	*AEA (%)*	*PEA (%)*	*OEA (%)*	*2-AG (%)*
0 hpl	*113; p>0.05*	*111; p>0.05*	*101; p>0.05*	79; *p>0.05*
1 hpl	*122; p>0.05*	*132; p>0.05*	*129; p>0.05*	107; *p>0.05*
6 hpl	*90; p>0.05*	*124; p>0.05*	*131; p>0.05*	114; *p>0.05*
12 hpl	*142; p>0.05*	*193; p<0.05*	*143; p>0.05*	120; *p>0.05*
24 hpl	*261; p<0.001*	*352; p<0.001*	*299; p<0.001*	172; *p<0.01*
48 hpl	*79; p>0.05*	*56; p>0.05*	*61; p>0.05*	98; *p>0.05*
72 hpl	*82; p>0.05*	*76; p>0.05*	*81; p>0.05*	101; *p>0.05*
CA1	*AEA (%)*	*PEA (%)*	*OEA (%)*	*2-AG (%)*
0 hpl	*114; p>0.05*	*92; p>0.05*	*84; p>0.05*	89; *p>0.05*
1 hpl	*107; p>0.05*	*119; p>0.05*	*112; p>0.05*	82; *p>0.05*
6 hpl	*113; p>0.05*	*111; p>0.05*	*132; p>0.05*	93; *p>0.05*
12 hpl	*66; p>0.05*	*76; p>0.05*	*77; p>0.05*	77; *p>0.05*
24 hpl	*90; p>0.05*	*70; p>0.001*	*64; p>0.015*	74; *p>0.05*
48 hpl	*59; p>0.05*	*38; p<0.05*	*44; p<0.05*	80; *p>0.05*
72 hpl	*106; p>0.05*	*92; p>0.05*	*98; p>0.05*	138; *p>0.05*

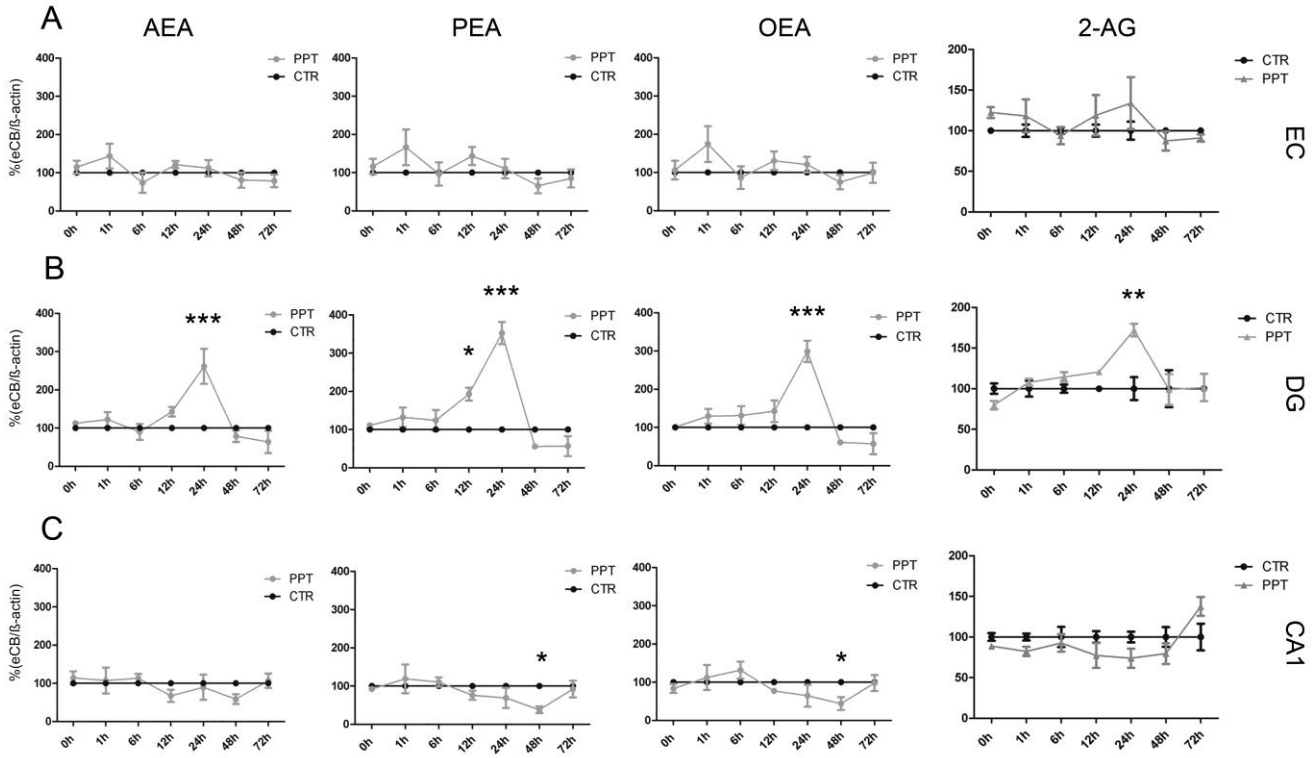

Figure 3.2 Endocannabinoid (eCB) levels after PPT in EC, DG and the CA1 region

ECB levels (grey cycles) were related to control conditions (CTR, black cycles) of each time-point respectively and CTR was set to 100 %. In the EC, no alteration of the eCB levels was observed. In the DG, all investigated eCB were significantly increased after 24 hpl. PEA was also 12 hpl increased compared to the respective control. In the CA1, AEA and 2-AG showed no changes after PPT. PEA and OEA decreased after 48 hpl (n = 4, *p < 0.05, **p < 0.01, ***p < 0.001).

3.2.3 Endocannabinoid levels after excitotoxicity

ECB levels are regulated in a site specific and time dependent manner after excitotoxic lesion and PPT. The eCB levels of non lesioned controls (CTR) were set to 100 %. The NMDA and PPT data were expressed in relation to their time controls, respectively. Exciotoxic NMDA lesion led to an intrinsic up-regulation of eCB levels in the EC, DG and in the CA1 region after low and high excitotoxic lesion (NMDA, 10 µM and 50 µM, Fig. 3.3).

Entorhinal cortex: AEA levels were enhanced 24 hpl in the EC after low and high NMDA concentrations shown in Tab. 3.2 and Fig 3.3A. At 24 hpl, high NMDA application AEA levels were significantly enhanced compared to low NMDA treatment (10 µM: 24 hpl, 579 % vs. 50 µM: 24 hpl, 1298 %; $p < 0.05$). PEA levels were not increased at low NMDA concentration, whereas after high NMDA supplementation at 24 hpl, an up-regulation was observed in the EC region. At 24 hpl, high NMDA application PEA levels were significantly enhanced compared to low NMDA treatment (10 µM: 24 hpl, 557 % vs. 50 µM: 24 hpl, 1274 %; $p < 0.05$). OEA levels were enhanced after 24 hpl in the EC after high NMDA application. At 24 hpl, high NMDA application OEA levels were significantly enhanced compared to low NMDA treatment (10 µM: 24 hpl, 635 % vs. 50 µM: 24 hpl, 1355 %; $p < 0.05$). 2-AG levels remained at control levels in the EC after 10 µM NMDA and after high NMDA treatment. No differences were seen between low or high NMDA application.

Dentate gyrus: AEA levels in the DG were significantly up-regulated at all time points measured after low NMDA application. At high NMDA concentration, the measurements became significant at 24 hpl. High NMDA application enhanced AEA levels significantly 24 hpl compared to low NMDA treatment (10 µM: 24 hpl, 340 % vs. 50 µM: 24 hpl, 653 %; $p < 0.05$). PEA levels in the DG were significantly up-regulated at all time points measured independently from the used NMDA concentration. 24 and 72 hpl high NMDA application enhanced PEA levels significantly compared to low NMDA treatment (10 µM: 24 hpl, 330 % vs. 50 µM: 24 hpl, 705 %, $p < 0.05$ and 10 µM: 72 hpl, 640 % vs. 50 µM: 72 hpl, 1008 %, $p < 0.05$). OEA levels in the DG were significantly up-regulated at all time points measured, independent from the used NMDA concentration. 24 and 72 hpl, high NMDA application enhanced OEA levels significantly compared to low NMDA treatment (10 µM: 24 hpl, 356 % vs. 50 µM: 24 hpl, 738 %, $p< 0.001$ and 10 µM: 72 hpl, 560 % vs. 50 µM: 72 hpl, 804 %, $p < 0.001$). 2-AG levels In the DG were enhanced 72 hpl by low NMDA (308 %; $p < 0.001$, vs. CTR) but not at 4 hpl and 24 hpl. 50 µM of NMDA increased 2-AG levels from 24 hpl on (Fig. 3.3A)

Cornu ammonis 1: AEA levels were enhanced 24 and 72 hpl in the CA1 region after low NMDA concentrations and 24 hpl after high NMDA treatment. 24 hpl, high NMDA application enhanced AEA levels significantly compared to low NMDA treatment (10 µM: 24 hpl, 890 % vs. 50 µM: 24 hpl, 1628 %; $p < 0.001$). PEA levels were enhanced 24 and 72 hpl in the CA1 region after low and high NMDA concentrations. 24 hpl, high NMDA application enhanced PEA levels significantly compared to low NMDA treatment (10 µM: 24 hpl, 902 % vs. 50 µM: 24 hpl, 1732 %; $p < 0.001$). OEA levels were enhanced 24 and 72 hpl in the CA1 region after low NMDA concentrations and 24 hpl after high NMDA treatment. 24 hpl, high NMDA application enhanced OEA levels significantly compared to low NMDA treatment (10 µM: 24 hpl, 937 % vs. 50 µM: 24 hpl, 1711 %; $p < 0.001$). 2-AG levels of the

CA1 region treated with 10 µM NMDA showed a significant increase 72 hpl (364 %; $p < 0.001$, vs. CTR). After treatment with 50 µM NMDA, 2-AG was enhanced after 24 and 72 hpl. 24 hpl, high NMDA application enhanced AEA levels significantly compared to low NMDA treatment (10 µM: 24 hpl, 185 % vs. 50 µM: 24 hpl, 290 %; $p < 0.05$).

Table 3.2 Endocannabinoid values after excitotoxic lesion

EC	*AEA (%)*		*PEA (%)*		*OEA (%)*		*2-AG (%)*	
	10 µM	*50 µM*	*10 µM*	*50 µM*	*10 µM*	*50 µM*	*10 µM*	*50 µM*
4 hpl	333; p>0.05	142; p>0.05	500; p>0.05	309; p>0.05	521; p>0.05	296; p>0.05	94; p>0.05	63; p>0.05
24 hpl	579; p<0.05	1298; p<0.001	557; p>0.05	1274; p<0.001	635; p>0.05	1355; p<0.001	68; p>0.05	87; p>0.05
72 hpl	148; p>0.05	129; p>0.05	379; p>0.05	336; p>0.05	262; p>0.05	255; p>0.05	114; p>0.05	103; p>0.05
DG	*AEA (%)*		*PEA (%)*		*OEA (%)*		*2-AG (%)*	
	10 µM	*50 µM*	*10 µM*	*50 µM*	*10 µM*	*50 µM*	*10 µM*	*50 µM*
4 hpl	279; p<0.01	234; p>0.05	397; p<0.01	399; p<0.01	453; p<0.001	433; p<0.001	140; p> 0.05	124; p>0.05;
24 hpl	340; p<0.001	653; p<0.001	330; p<0.05	705; p<0.001	356; p<0.05	738; p<0.001	147; p>0.05	198; p<0.01;
72 hpl	375; p<0.001	462, p<0.001	640; p<0.001	1008; p<0.001	560; p<0.001	804; p<0.001	308; p<0.001	324; p<0.001,
CA1	*AEA (%)*		*PEA (%)*		*OEA (%)*		*2-AG (%)*	
	10 µM	*50 µM*	*10 µM*	*50 µM*	*10 µM*	*50 µM*	*10 µM*	*50 µM*
4 hpl	245; p>0.05	164; p>0.05	396; p>0.05	341; p>0.05	495; p>0.05	382; p>0.05	63; p>0.05	114; p>0.05
24 hpl	890; p<0.001	1628; p<0.001	902; p<0.001	1732; p<0.001	937; p<0.001	1711; p<0.001	185; p>0.05	290; p<0.001
72 hpl	502; p<0.01	414; p>0.05	635; p<0.01	545; p<0.05	592; p<0.05	487; p>0.05	364; p<0.001	307; p<0.001

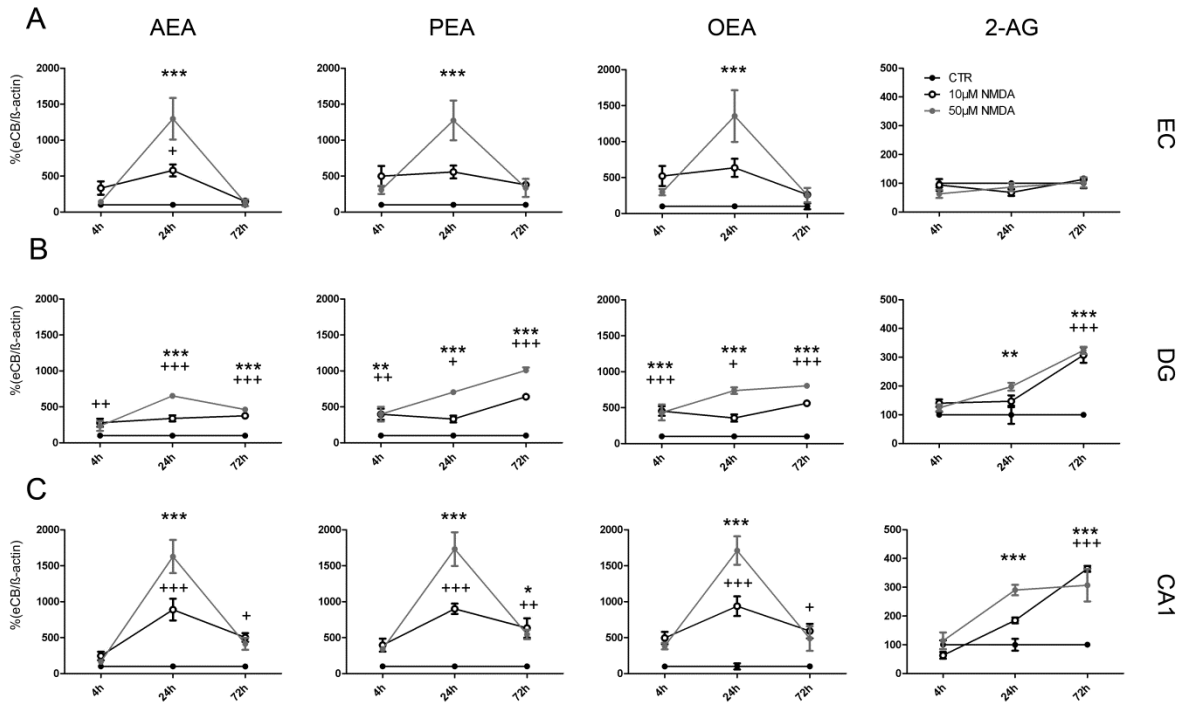

Figure 3.3 Endocannabinoid levels after excitotoxicity

Endocannabinoid levels after excitotoxicity in EC, DG and the CA1 region. 10 µM of NMDA (open cycles) and 50 µM of NMDA (grey cycles) were related to control conditions (CTR, black cycles) of each time-point, respectively and CTR was set to 100 %. In the EC, AEA, PEA and OEA levels were increased 24 hpl and decreased at 72 hpl back to control levels. 2-AG did not show any alteration in comparison to the respective CTR in the EC. In the DG, all investigated eCB were significantly increased after 10 µM of NMDA treatment and were even further increased after 50 µM NMDA. In the CA1, AEA, PEA and OEA showed a dose dependent peak to NMDA treatment 24 hpl. 2-AG increased 24 hpl at both concentrations of NMDA and remained up-regulated after 72 hpl. (n = 3, $*/^{+}p < 0.05$, $**/^{++}p < 0.01$, $***/^{+++}p < 0.001$).

3.3 Differential regulation of enzymes and receptors of NEA after PPT

The site-specific and time-dependent changes in enzymes, namely NAPE-PLD, FAAH, NAAA as well as receptors CB_1 and PPARα were analysed by Western blot. The specificity of the used antibodies was tested by means of preabsorption. The CB_1 antibody showed no signal in $CB_1^{-/-}$ animals. For densitometric analysis, the PPT data was expressed relative to their time-controls respectively and the control levels were set to 100 %.

3.3.1 CB_1 and PPARα receptor regulation after PPT

Entorhinal Cortex: After PPT, CB_1 protein (0 hpl, 86 %; 1 hpl, 94 %; 6 hpl, 129 %; 12 hpl, 92 %; 24h, 101 %; 48 hpl, 108 %; 72 hpl, 132 %; $p > 0.05$; Fig. 3.4) was significantly increased 1 hpl (129 %; $p < 0.05$) and 72 hpl (132 %; $p < 0.05$) in the EC only. PPARα (0 hpl, 83 %; 1 hpl, 105 %; 6 hpl, 93 %; 12 hpl, 112 %; 24h, 76 %; 48 hpl, 112 %; 72 hpl, 111 %; $p > 0.05$; Fig. 3.4) showed no alteration in PPT compared to the respective time control.

Dentate Gyrus: The protein amount of CB_1 did not differ from the time control (0 hpl, 119 %; 1 hpl, 101 %; 6 hpl, 77 %; 12 hpl, 107 %; 24h, 123 %; 48 hpl, 105 %; 72 hpl, 109 %; $p > 0.05$, Fig. 3.4). The PPARα protein amount did not change in comparison to the time controls (1 hpl 102 %, 6 hpl 107 %, 12 hpl 114 %, 24h 87 %, 48 hpl 107 %, 72 hpl 92 %, $p > 0.05$, Fig. 3.4).

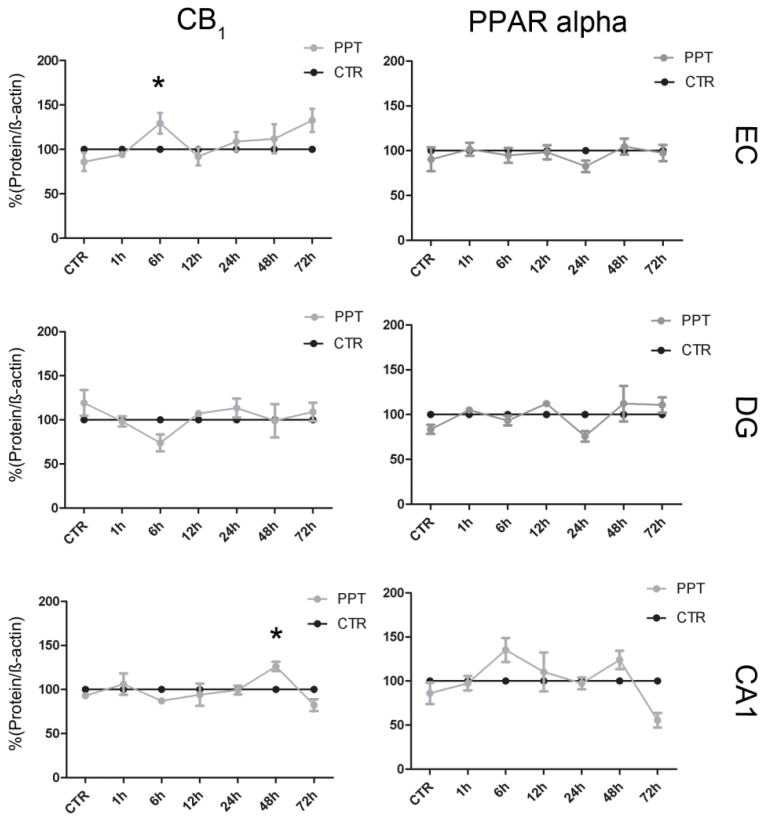

Figure 3.4 CB_1 and PPARα receptor regulation after PPT

The amount of CB_1 protein was significantly elevated 6 hpl whereas PPARα was not altered.

Cornu ammonis 1: In PPT, CB_1 (0 hpl, 93 %; 1 hpl, 106 %; 6 hpl, 87 %; 12 hpl, 94 %; 24h, 99 %; 48 hpl, 126 %; 72 hpl, 82 %; $p > 0.05$; Fig. 3.4) as well as PPARα (0 hpl, 86 %; 1 hpl, 97 %; 6 hpl, 135 %; 12 hpl, 110 %; 24h, 97 %; 48 hpl, 124 %; 72 hpl, 69 %; $p > 0.05$; Fig. 3.4) were not altered after PPT in CA1 as compared to the respective time controls.

3.3.2 Enzymatic regulation of NEA after PPT

Entorhinal Cortex: No change in NAPE-PLD was detectable after axonal damage in the EC (0 hpl, 98 %; 1 hpl, 114 %; 6 hpl, 105 %; 12 hpl, 114 %; 24h, 102 %; 48 hpl, 111 %; 72 hpl, 119 %; $p > 0.05$; Fig. 3.5). Neither FAAH (0 hpl, 83 %; 1 hpl, 115 %; 6 hpl, 104 %; 12 hpl, 98 %; 24h, 88 %; 48 hpl, 97 %; 72 hpl, 90 %; $p > 0.05$; Fig. 3.5) nor NAAA (0 hpl, 88 %; 1 hpl, 89 %; 6 hpl, 79 %; 12 hpl, 98 %; 24h, 101 %; 48 hpl, 100 %; 72 hpl, 105 %; $p > 0.05$; Fig. 3.5) were significantly changed.

Dentate Gyrus: An increase of NAPE-PLD protein amount was observed in DG from 1 hpl to 6 hpl (0 hpl, 97 %; $p>0.05$; 1 hpl, 140 %; 6 hpl, 133 %; $p < 0.05$; Fig. 3.5). Thereafter, NAPE-PLD protein decreased to control levels (12 hpl, 133 %; 24h, 118 %; 48 hpl, 117 %; 72 hpl, 99 %; $p > 0.05$). The FAAH protein amount remained close to control levels up to 24 hpl (1 hpl, 110 %; 6 hpl, 108 %; 12 hpl, 106 %; 24 hpl, 111 %; $p > 0.05$). At 48 hpl, (120 %; $p < 0.05$) a significant peak of FAAH was observed that was not visible anymore at 72 hpl (113 %; $p > 0.05$; Fig. 3.5). No change in the NAAA enzyme was detectable after dendritic denervation in the DG (1 hpl 101 %, 6 hpl 98 %, 12 hpl 95 %, 24h 128 %, 48 hpl 105 %, 72 hpl 111 %, $p > 0.05$).

Cornu ammonis 1: In the CA1 region, no alterations in NAPE-PLD were detected (0 hpl, 89 %; 1 hpl, 100 %; 6 hpl, 112 %; 12 hpl, 109 %; 24h, 86 %; 48 hpl, 100 %; 72 hpl, 86 %; $p > 0.05$; Fig. 3.5). FAAH (0 hpl, 111 %; 1 hpl, 100 %; 6 hpl, 97 %; 12 hpl, 114 %; 24h,

94 %; 48 hpl, 87 %; 72 hpl, 102 %; p> 0.05; Fig. 3.5) and NAAA (0 hpl, 111 %; 1 hpl, 105 %; 6 hpl, 107 %; 12 hpl, 102 %; 24h, 99 %; 48 hpl, 106 %; 72 hpl, 81 %; p > 0.05) remained unchanged after PPT.

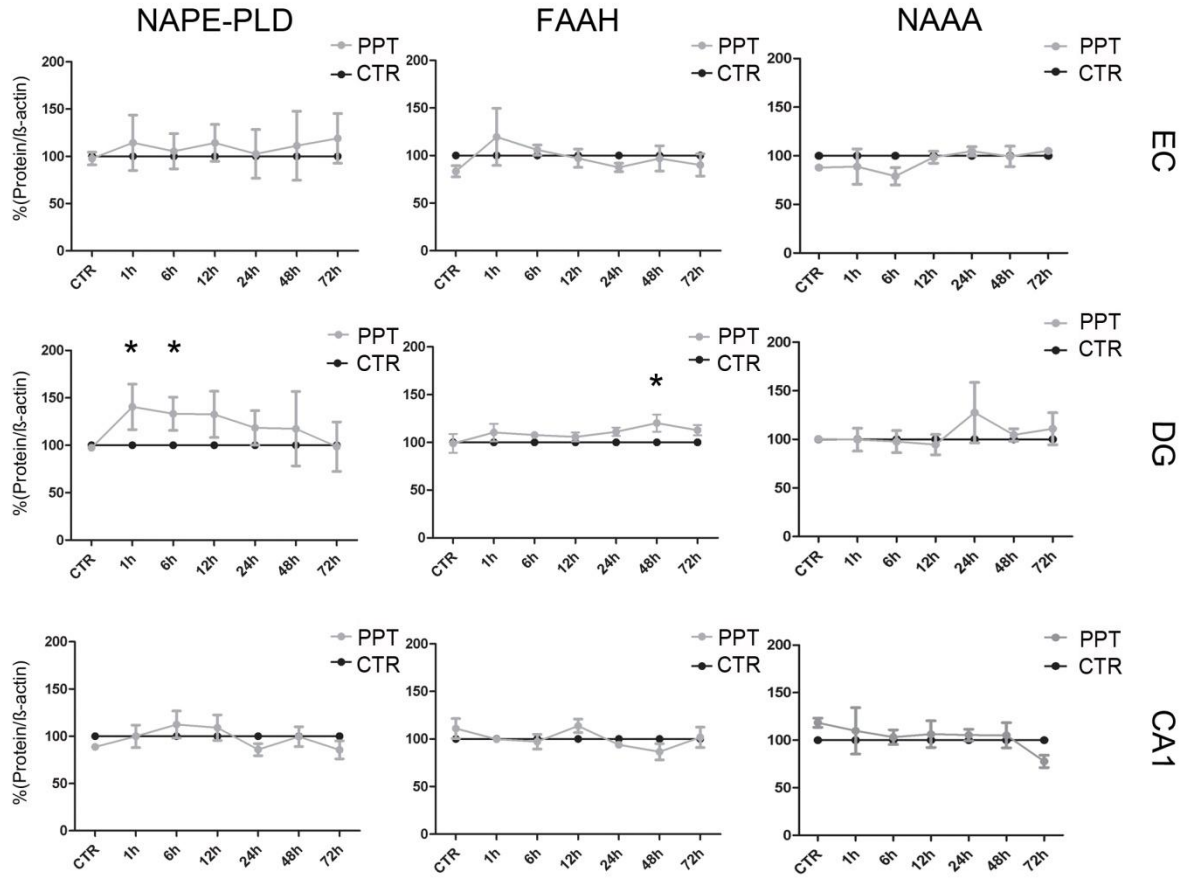

Figure 3.5 Enzymatic regulation of NEA after PPT

Relative amount of NAPE-PLD, FAAH and NAAA after PPT compared to respective time controls (CTR) set to 100 %. NAPE-PLD, FAAH and NAAA remained constant after PPT in EC. In DG, NAPE-PLD was increased 1 and 6 hpl. FAAH showed elevated levels 48 hpl, whereas NAAA did not show any alteration after PPT. In CA1, NAPE-PLD, FAAH and NAAA remained unchanged after PPT. (n = 4, *p < 0.05)

3.4 Enzymatic and transcriptional regulation of 2-AG after PPT

Western Blot analysis and semi-quantitative real time PCR (rtPCR) were used to investigate the intrinsic regulation of the synthesising (DAGL) and the hydrolyzing (MAGL) enzymes of 2-AG in the different regions over time.

3.4.1 Enzymatic regulation of 2-AG after PPT

Entorhinal cortex: No changes of DAGL and MAGL protein were observed in the EC region after PPT compared to the time control OHSC (DAGL: 0 hpl, 101 %; 6 hpl, 85 %; 12 hpl, 79 %; 24 hpl, 119 %; 48 hpl, 101 %; $p > 0.05$; MAGL: 0 hpl, 105 %; 6 hpl, 112 %; 12 hpl, 103 %; 24 hpl, 99 %; 48 hpl, 98 %; $p > 0.05$, Fig. 3.6).

Dentate gyrus: DAGL protein was decreased 24 hpl significantly (Fig. 3.6, 24 hpl, 66 %; $p < 0.05$) related to the respective controls (0 hpl, 102 %; 6 hpl, 101 %; 12 hpl, 107 %, 48 hpl, 84 %; $p > 0.05$). MAGL expression did not show significant changes (MAGL: 0 hpl, 104 %; 6 hpl, 120 %; 12 hpl, 123 %; 24 hpl, 115 %; 48 hpl, 95 %; $p > 0.05$).

Cornu ammonis 1: In the CA1 region no significant changes were observed in DAGL or MAGL protein expression (DAGL: 0 hpl, 92 %; 6 hpl, 114 %; 12 hpl, 88 %; 24 hpl, 97 %; 48 hpl, 99 %; $p > 0.05$, MAGL: 0 hpl, 110 %; 6 hpl, 109 %; 12 hpl, 117 %; 24 hpl, 130 %; 48 hpl, 103 %; $p > 0.05$, Fig. 3.6).

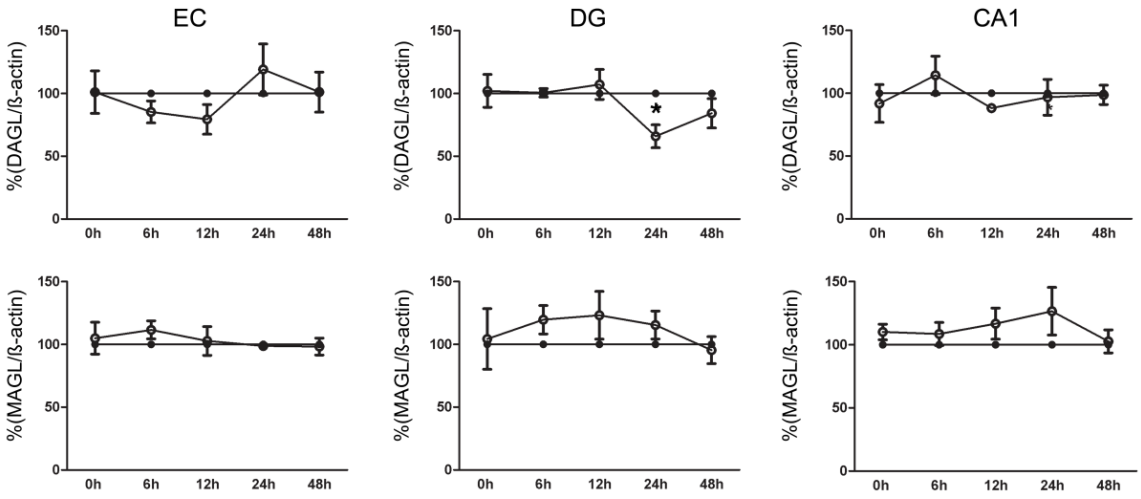

Figure 3.6 Enzymatic regulation of 2-AG after PPT

DAGL and MAGL protein (open cycles) regulation after PPT in the entorhinal cortex (EC) and the hippocampus (DG, CA1) normalized to time controls (closed cycles). DAGL was decreased 24 hpl in the DG. After PPT no further changes could be observed (n = 3, *p < 0.05).

3.4.2 Transcriptional regulation of DAGL and MAGL after PPT

Entorhinal cortex: In the EC region, no changes of both enzymes were observed after PPT. DAGL and MAGL expression were not significantly increased compared to the control OHSC (DAGL: 6 hpl, 55 %; 12 hpl, 87 %; 24 hpl, 70 %; 48 hpl, 107 %; p > 0.05; MAGL: 6 hpl, 68 %; 12 hpl, 103 %; 24 hpl, 112 %; 48 hpl, 137 %; p > 0.05, Fig. 3.7).

Dentate gyrus: In the DG, DAGL expression was significantly enhanced 24 hours after PPT (24 hpl, 175 %; p < 0.05, Fig. 3.7) related to the respective controls (6 hpl, 132 %; 12 hpl, 108 %, 48 hpl, 65 %; p > 0.05). MAGL expression did not show significant changes (MAGL: 6 hpl, 78 %; 12 hpl, 76 %; 24 hpl, 76 %; 48 hpl, 113 %; p > 0.05).

Cornu ammonis 1: In the CA1 region, no significant changes were observed in DAGL or MAGL expression (DAGL: 6 hpl, 77 %; 12 hpl, 92 %; 24 hpl, 92 %; 48 hpl, 77 %; $p > 0.05$, MAGL: 6 hpl, 157 %; 12 hpl, 83 %; 24 hpl, 111 %; 48 hpl, 123 %; $p > 0.05$, Fig. 3.7).

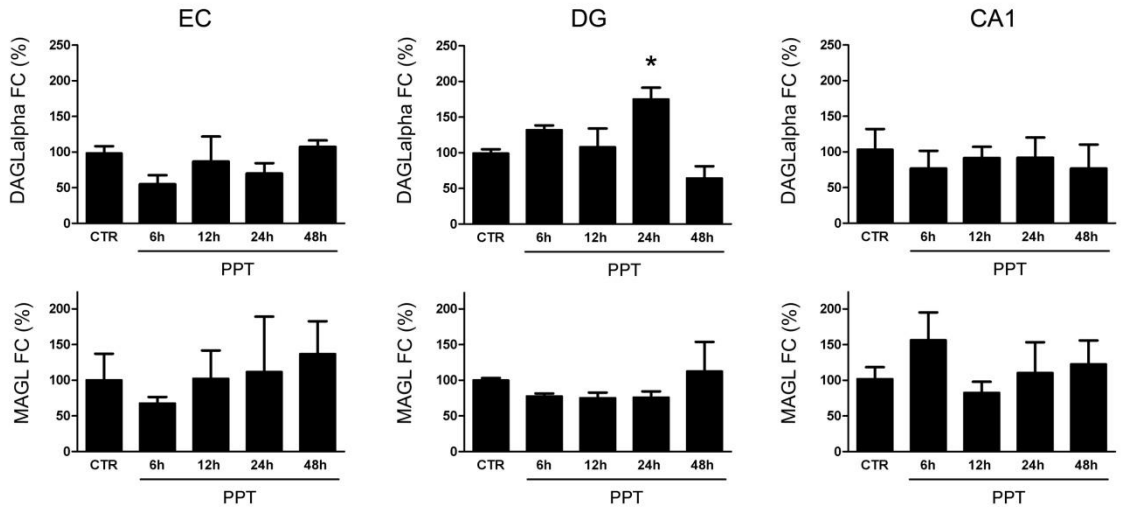

Figure 3.7 DAGL and MAGL transcription after PPT

DAGL and *MAGL* mRNA regulation after PPT in the entorhinal cortex and the hippocampus. *DAGL* was increased 24 hpl in the DG ($n = 3$, $*p < 0.05$).

3.5 Immunohistochemical analysis of eCB regulating enzymes in OHSC

3.5.1. CB1 and PPARα after PPT in OHSC

A strong CB_1 immunosignal was detected in the inner and outer molecular layer of the DG. CB_1 was present in some morphologically characterised inter-neurons of the hilus. Whereas IB_4 positive microglia displayed a positive immunosignal for CB_1, this reaction was weak when GFAP immunoreactive astrocytes were examined. PPARα was found in NeuN immunoreactive neurons, IB_4 positve microglia and GFAP positive astrocytes. PPARα was localised in vesicular structures close to the cell nucleus, apparently reflecting the Golgi apperatus throughout the entire OHSC.

3.5.2 NAPE-PLD, FAAH, and NAAA after PPT in OHSC

Localisations of NAPE-PLD, FAAH, NAAA, CB_1 and PPARα immunoreactions (IR) were investigated by immunohistochemical staining with NeuN, GFAP and IB_4 in sections obtained from OHSC at 24 hpl shown in Fig 3.8. NAPE-PLD immunoreaction was found to be co-localised with NeuN positive neurons and a subset of IB_4 positive microglia. GFAP positive astrocytes did not show a NAPE-PLD immunoreaction. FAAH immunoreactions showed a robust cytoplasmic distribution in neuronal cells. Neither microglial cells nor GFAP positive astrocytes exhibited a detectable amount of FAAH. Co-localszation of NAAA immunoreaction with NeuN positive neurons was observed, mainly in the perikarya. In addition, some nuclei showed positive immunoreactions for NAAA. There was no overlap of NAAA immunoreaction with IB_4 or GFAP positive cells.

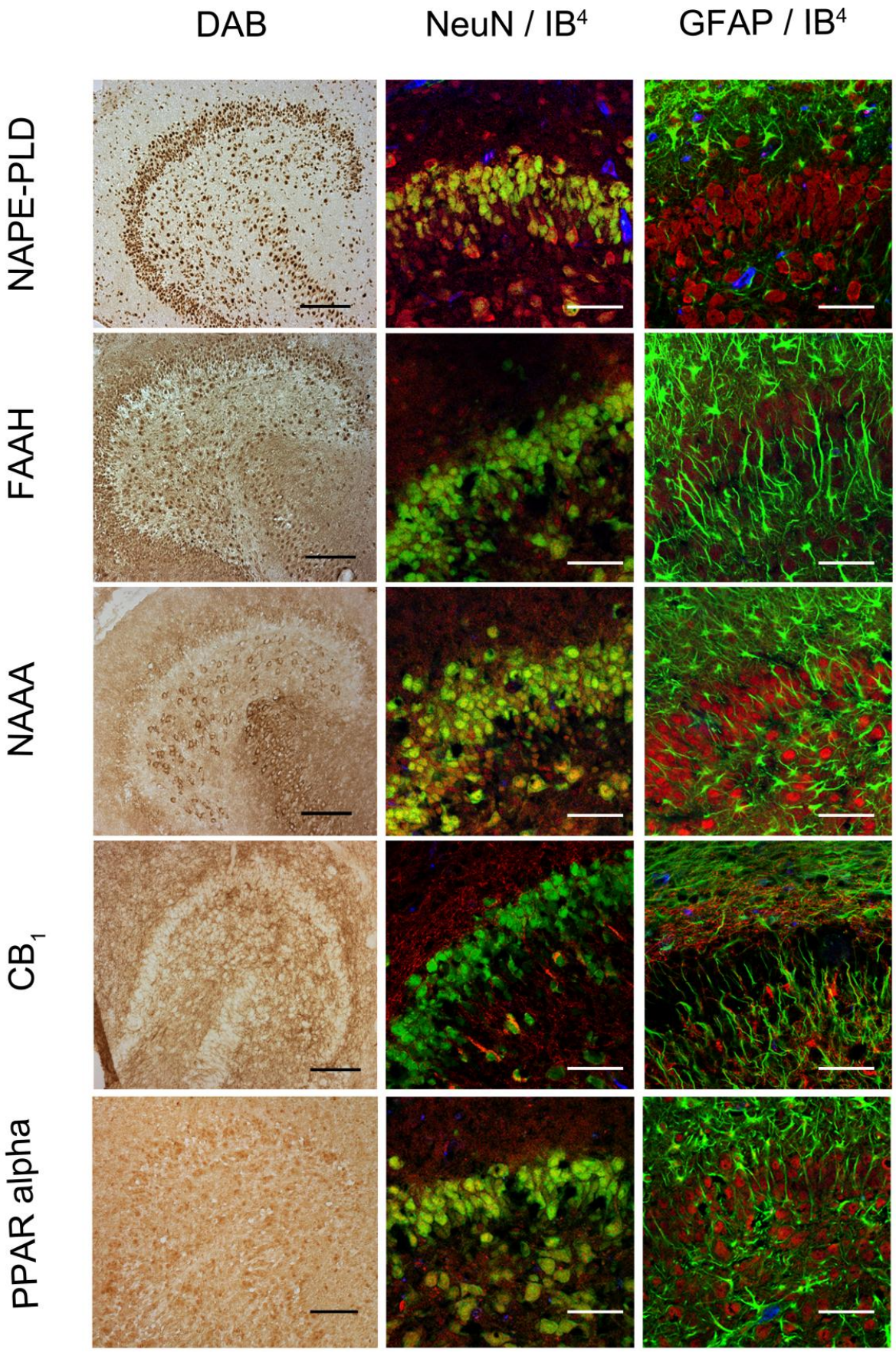
DAB
NeuN / IB4
GFAP / IB4
NAPE-PLD
FAAH
NAAA
CB1
PPAR alpha

Figure 3.8 Immunocytochemical analysis of OHSC

Immunocytochemical analysis of NAPE-PLD, FAAH, NAAA, CB_1 and PPARα in the dentate gyrus of OHSC 24 hpl. Left column: DG in overview after DAB staining. Middle column; Triple staining of eCB system related proteins with NeuN and IB_4. Right column; Triple staining of OHSC with eCB system related proteins in combination with NeuN and GFAP. The granular cell layer of the DG and interneurons in the hilus region showed a strong immunoreaction for NAPE-PLD. No overlap was observed with GFAP or IB_4. The granular cell layer of the DG and especially interneurons in the hilus region were strongly immunoreactive for FAAH. No overlap was observed with GFAP or IB_4. Please note the similarity of staining pattern of NAPE-PLD and FAAH immunoreactions. NAAA was found in perikarya and nuclei of neurons. In addition to the granular cell layer of the DG and hilar neurons, the CA3 region was strongly labeled. Astrocytes and microglia seem to be not NAAA immunoreactive. The entire molecular layer of the dentate gyrus showed a positive CB_1 immunoreaction. CB_1 was present in microglia and to a lesser extent in astrocytes. PPARα was observed in perikarya and nuclei of neurons. Microglia and astrocytes showed a positive immunoreaction for PPARα (n = 3, bars: left column = 100 µm, middle and right columns = 50 µm).

3.5.3 DAGL and MAGL in excitotoxically and dendritic lesioned OHSC

DAGL protein was found in the cytoplasm of NeuN positive cells. Also, co-localisation of DAGL with GFAP positive astrocytes was observed but no immunoreaction was seen in IB_4 positive cells (Fig.3.9).

No changes could be found in PPT OHSC until 12 hpl. The DAGL IR remained in the cytoplasm of neurons and astrocytes. 24 hpl reorganization of DAGL IR was observed, the tight organisation of the granular cell layer dispersed and DAGL IR was found in the outer third of the granular layer but vanished in the inner half of the granular layer. MAGL immunoreactions showed only a weak punctual distribution in NEUN positive cells. GFAP positive astrocytes expressed strong co-localisation with the MAGL protein. Microglia displayed only weak MAGL IR in OHSC (Fig.3.9). Over time, microglia did not show a change of MAGL expression as expected after cell culture experiments. Some co-localisation

of IB_4 and MAGL could be due to phagocytosis of cell vesicles by microglia. At 24 hpl MAGL IR was less expressed in GFAP positive cells. No other changes in cellular distribution were observed over time.

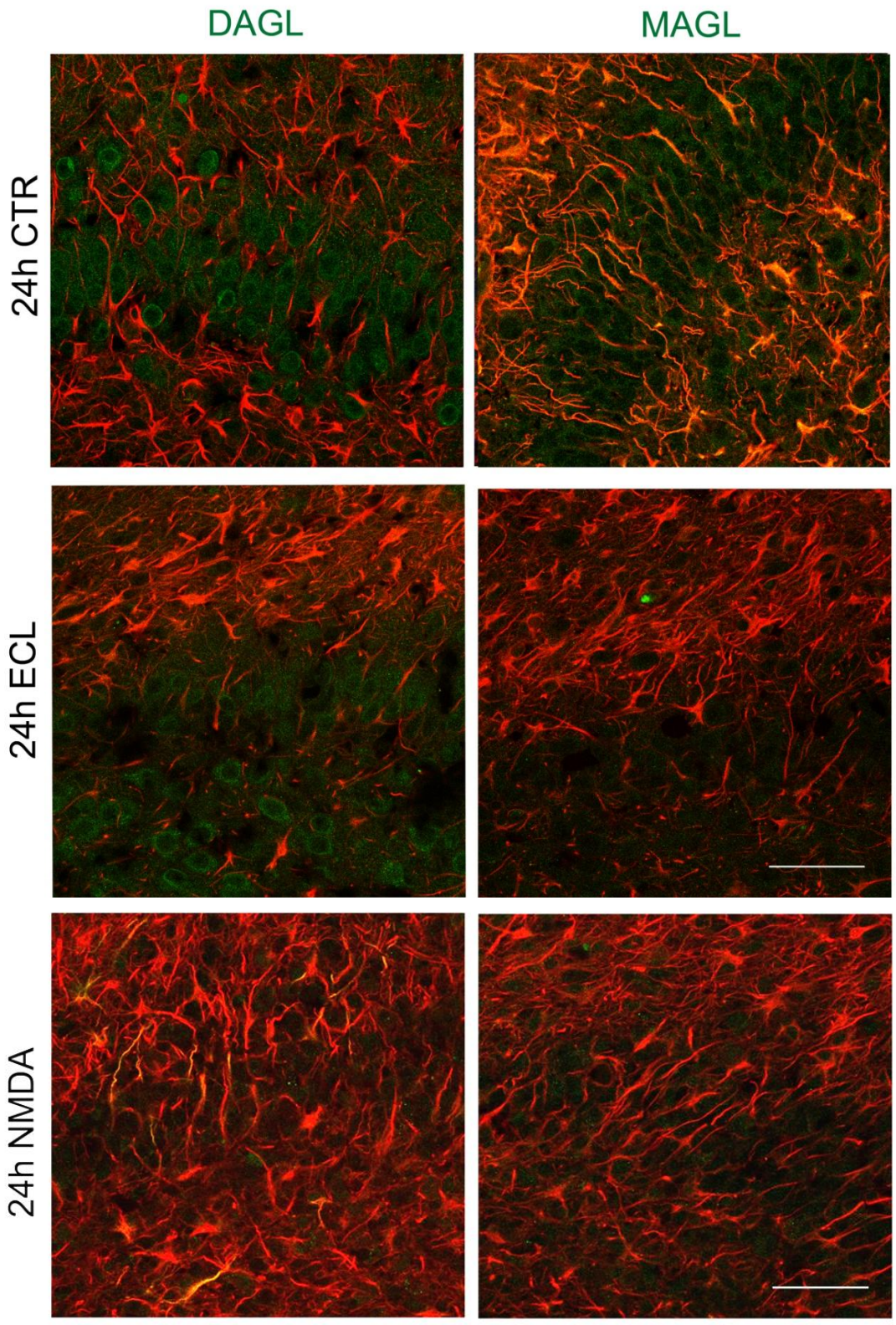

Figure 3.9 Immunocytochemical analysis of MAGL and DAGL in OHSC

DAGL and MAGL immunoreaction in OHSC 24 h after PPT. DAGL was co-localised with GFAP positive cells IB_4 positive microglia were not DAGL IR. After PPT, a reorganisation of DAGL IR was seen. The outer half of the granular cell layer kept immunoreactive whereas the inner half of the granular cell layer was not DAGL IR 24 hpl. GFAP positive cells expressed strong co-localisation with the MAGL protein. Microglial cells displayed little MAGL IR in OHSC. 24 hpl, MAGL protein was less expressed in astrocytes. No other alteration in cellular distribution was seen. (bar = 50 µm)

3.6 Immunohistochemical analysis of eCB regulating enzymes in primary cell culture

Cell cultures often demonstrate different expression patterns and activation states as in tissue culture or in vivo. To analyse each cell type precisely, primary neurons, microglia and astrocyte cultures were investigated whether they express receptors and enzymes of the eCB.

3.6.1 Cellular distribution of CB_1 and PPARα in primary rat neurons, microglia and astrocytes

Neurons showed a strong CB_1 immunoreaction in perikarya, primary and secondary neuronal processes and spines. Primary microglia culture and primary astrocytes demonstrated a clear CB_1 immunoreaction at the membrane and processes, although the immunoreaction in astrocytes was very weak. PPARα immunoreaction was detectable in primary neurons, microglia and astrocytes. In neurons, PPARα was scattered over the entire perikarya, whereas in glial cells, PPARα was found close to the nuclei respectively.

3.6.2 Cellular distribution of NAPE-PLD, FAAH and NAAA in primary rat neurons, microglia and astrocytes

In isolated primary neuronal cell cultures, NAPE-PLD immunoreaction was observed within neuronal perikarya and processes (Fig. 3.10).

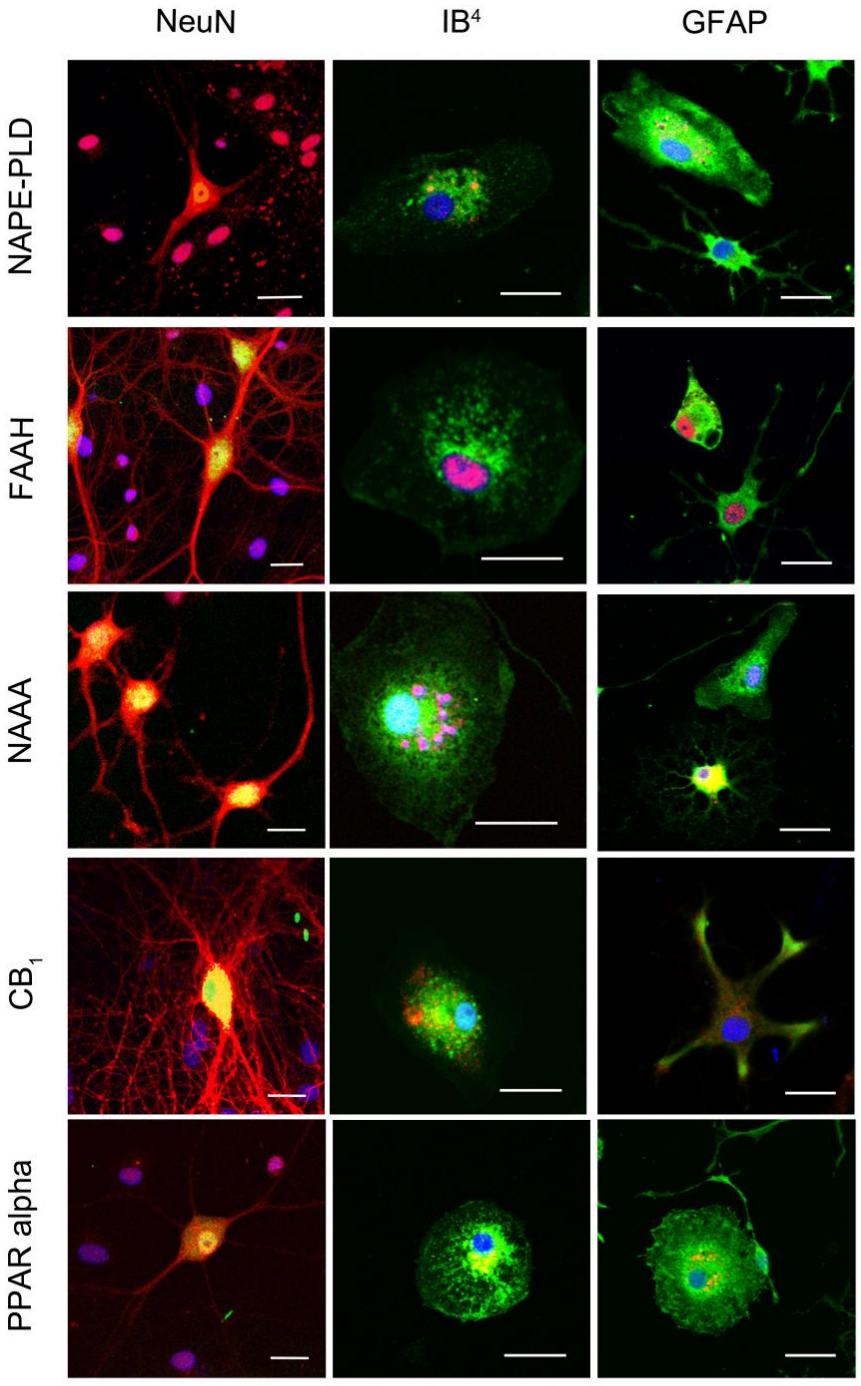

Figure 3.10 Immunocytochemical analysis of primary cell cultures

Immunocytochemical analysis of NAPE-PLD, FAAH, NAAA, CB_1 and PPARα in primary neuronal (left column), microglia (middle column) and astrocyte (left column) cell cultures**.** In neurons, NAPE-PLD was distributed in the perikarya but not in neuronal processes. In microglia, NAPE-PLD immunoreactions were detectable in small vesicles closely located to the nucleus. NAPE-PLD was not found in protoplasmic astrocytes, whereas fibrillary astrocytes showed an immunosignal comparable to microglia. The immunosignal for FAAH in primary neurons was localised in the cell bodies as well as in the primary branches of the neurites. In microglia and astrocytes, FAAH was localised within the nucleus respectively. In fibrillary astrocytes a FAAH immunoreaction was additionally observed in vesicles. NAAA was clearly found in neurons but was barely found in microglia and astrocytes. In microglia NAAA showed a vesicular staining pattern close to the nucleus. Protoplasmic astrocytes were immunoreactive for NAAA, whereas fibrillary astrocytes did not show any NAAA immunosignal. A robust CB_1 immunoreaction was found in neurons. To a lower extent, CB_1 immunosignals were detectable in microglia and astrocytes. Primary neurons showed a strong PPARα immunoreaction in their Perikarya and nuclei. Microglia and astrocytes were positive for PPARα immunoreaction in a vesicular pattern. (n = 3, bar = 20 µm)

Similar to OHSC, NAPE-PLD was found close to the nuclei in microglial cells. In primary astrocyte culture fibrillary astrocytes displayed a weak, protoplasmic astrocytes a robust NAPE-PLD immunoreaction. Primary neurons, microglia and astrocytes showed a FAAH immunoreaction that was localised close to the nuclei respectively (Fig. 3.10). In addition, nuclear labeling was observed in microglia and astrocytes. Isolated primary neurons showed a NAAA immunoreaction that was found to be distributed in the perikarya and the secondary branches. Microglia was labeled with the NAAA antibody close to the nucleus. Fibrillary astrocytes displayed NAAA immunoreactions within their cell bodies and to a minor extent in their processes (Fig. 3.10).

3.6.3 Cellular distribution of DAGL and MAGL in primary rat neurons, microglia and astrocytes

In isolated primary neuronal cultures DAGL IR were observed within neuronal perikarya and processes. The double staining of DAGL and VGUT1 showed punctual co-localisation (Fig. 3.11). MAGL IR was not observed to be co-localised with VGLUT1 in primary neuronal cell culture. In primary microglia cultures DAGL IR were located in the cell body that became more intense after LPS treatment (Fig. 3.11). DAGL was differentially expressed in astrocyte subtypes whereas fibrillary astrocytes showed a weak DAGL IR, especially after LPS treatment. Protoplasmic astrocytes displayed punctual immunoreactions spread throughout the cell body under both, control and LPS treated conditions. In IB_4 positive microglia, MAGL was found in the cytoplasm and at the cell borders. Interestingly MAGL IR disappeared after LPS treatment. Fibrillary astrocytes displayed MAGL immunoreactions within their cell bodies. In LPS treated cells, MAGL IR was seen in the cell bodies and to a minor extent in their processes. The immunoreaction of MAGL in protoplasmic astrocytes was weak, no alteration was observed between the control and the LPS treated condition (Fig. 3.11).

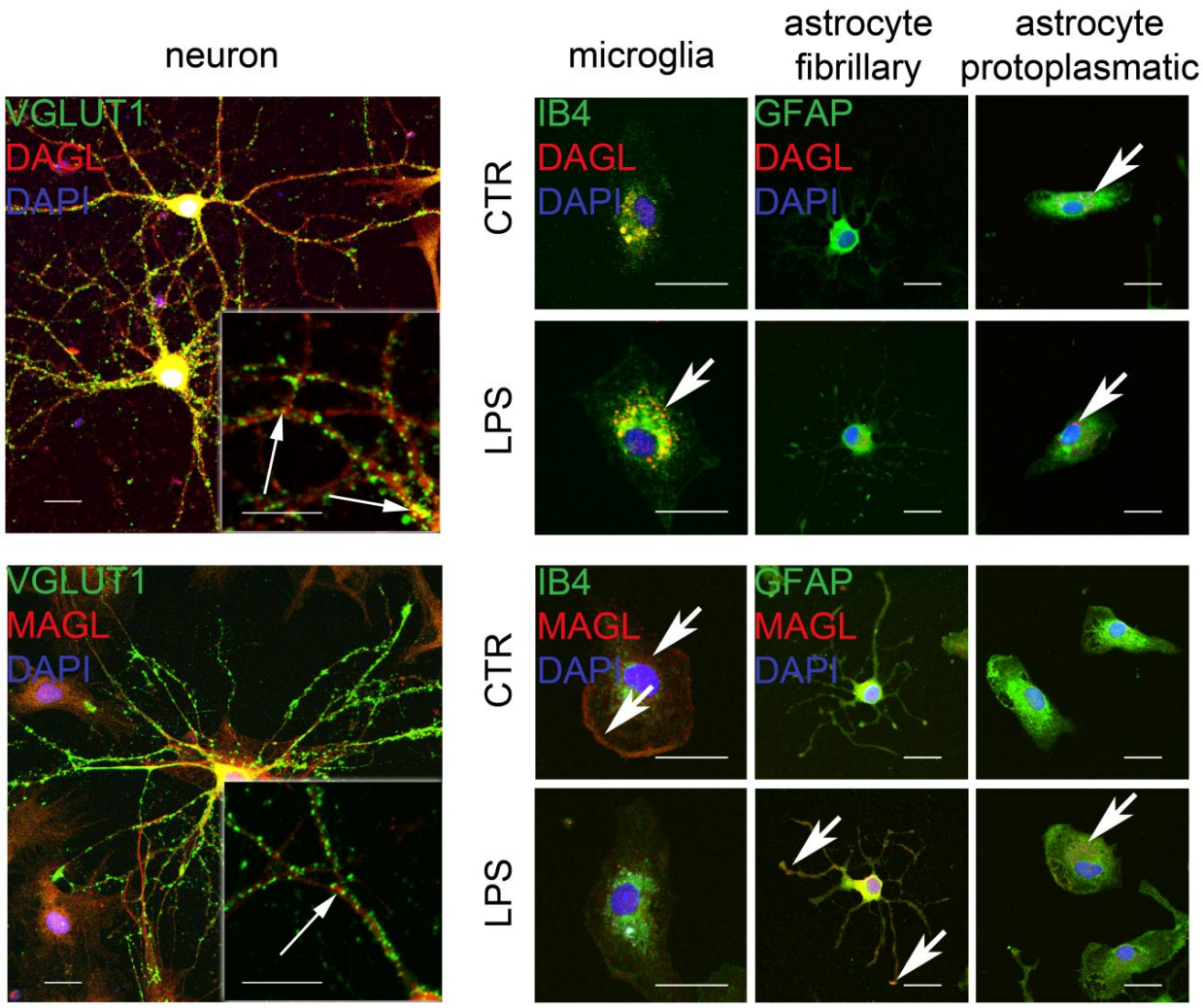

Figure 3.11 Immunocytochemical analysis of DAGL and MAGL in primary cell culture

Immunocytochemical analysis of DAGL and MAGL in primary neuronal (left column), microglia, (middle column) and astrocyte (left columns) cell cultures**.** In neurons, DAGL was distributed in the perikarya and in neuronal processes. VGLUT1 was co-localised with DAGL suggesting a close surveillance of glutamate by DAGL. (white arrow). MAGL was distributed in primary neuronal cultures but displayed no overlap with VGLUT1. Microglia were labeled with DAGL in the cell body, after LPS treatment DAGL expression was stronger than in controls. However, MAGL expression in microglia was clearly visualised under control condition at the outer edges of the cells but disappeared in the LPS treated condition. DAGL IR was not found in fibrillary astrocytes under control condition, but little DAGL IR was seen after LPS treatment in fibrillary astrocytes, whereas protoplasmic astrocytes displayed DAGL IR in control and stimulated condition visualised in droplets throughout the cell body. MAGL IR was stimulated in LPS conditioned fibrillary and protoplasmic astrocytes. Under control conditions, only some MAGL IR was found in fibrillary astrocytes (n = 3, bar = 20 µm).

3.7 Neuroprotection after intrinsic 2-AG upregulation

3.7.1 Intrinsic upregulation of 2-AG after MAGL inhibition by JZL184 in OHSC

To determine the intrinsic regulation of 2-AG after neuronal damage, 2-AG levels were measured after MAGL inhibition. Raw values of 3 pooled OHSC (EC, DG or CA1) were about 3-5 ng/ml for 2-AG under control condition. The obtained 2-AG values were corrected for their ß-actin content and were then given in % of the respective controls. After JZL184 (1 µM) supplementation for 4 h, 2-AG could increase up to 35-45 ng/ml in OHSC and was significantly elevated in all studied regions (EC, 736 %; $p < 0.01$; DG, 688 %; $p < 0.01$, CA1, 570 %; $p < 0.05$, Fig.3.12).

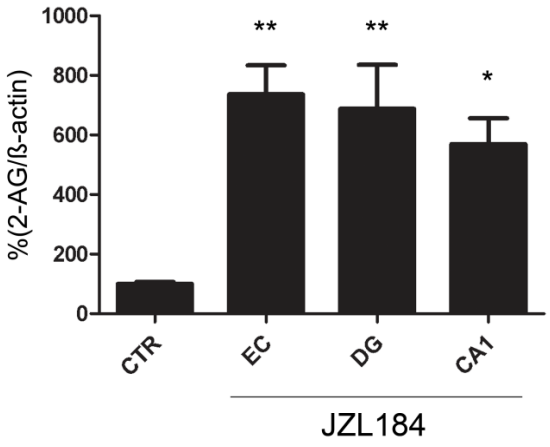

Figure 3.12 Regulation of 2-AG after JZL184 regulation

Regulation of 2-AG in EC, DG and CA1. A significant increase of 2-AG levels in all three regions of the Hippocampus (DG and CA1) and the entorhinal cortex (EC) after supplementation of JZL 184 for 72 h to the culture media (n = 4).

3.7.2 JZL184 protected dentate gyrus granule cells after excitotoxic lesion in OHSC

Non-lesioned control OHSC exhibited a good neuronal preservation with almost no PI positive neuronal nuclei. All conditions were normalised to the positive NMDA control and given in % (Fig. 3.13A). The application of 1 µM JZL184 did not lead to any significant alterations within the number of PI positive neuronal nuclei compared to the negative control

(JZL184, 0 %, $p > 0.05$). Treatment of OHSC with 50 µM NMDA for 4 hours at 6 div strongly increased the numbers of PI positive cells in the dentate gyrus (DG) granule cell layer (GCL) (NMDA, 156±26 PI postitive neuronal nuclei, 100 %, $p < 0.001$ vs. negative CTR) as compared to untreated OHSC. Application of 1 µM JZL184 to NMDA-lesioned OHSC led to a significant reduction of PI positive neuronal nuclei compared to NMDA alone (NMDA+1 µM JZL184, 51 %; $p < 0.05$ vs. NMDA, Fig.3.13A).

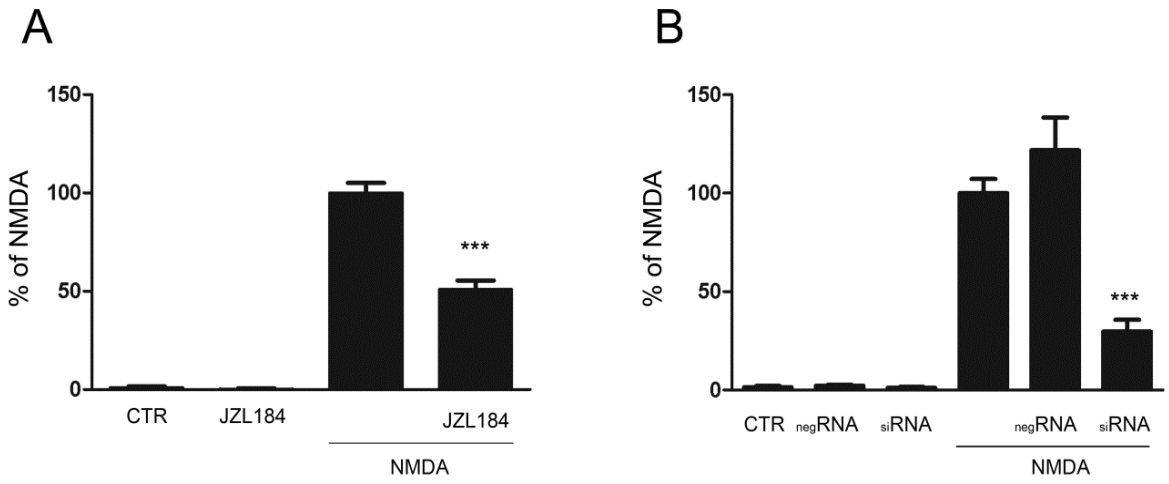

Figure 3.13 MAGL inhibition protects neuronal cell death

MAGL inhibition led to neuroprotection and increased intrinsic 2-AG levels. (A) To investigate wheather 2-AG increase is neuroprotective, we increased 2-AG levels by MAGL inhibition and received significantly less PI positive neurons in the DG after NMDA (50 µM) lesion and JZL 184 (1 µM) treatment then in the NMDA control OHSC (as former research of our lab showed as well with 2-AG suplementation, Kreutz, 2009). (B) Also the MAGL knock down by siRNA reduced the damaged neurons significantly.

3.7.3 MAGL knock down by siRNA protected NMDA lesioned OHCS

All conditions were normalised to the positive NMDA control and given in % (Fig. 3.13B). Non-lesioned OHSC treated with negRNA or siRNA (negRNA, 0 % siRNA, 0 %) exhibited no different neuronal preservation than the control OHSC. Treatment of OHSC with 50 µM NMDA for 4 hours at 6 div, strongly inducted the numbers of PI positive neuronal nuclei (NMDA, 100 %, $p < 0.001$ vs. CTR) as compared to untreated CTR. Application of negRNA to NMDA-lesioned OHSC showed no changes (NMDA+negRNA, 122 %; $p > 0.05$ vs. NMDA), but the application of siRNA led to a significant reduction of PI positive neuronal nuclei compared to OHSC treated with NMDA alone (NMDA+siRNA, 33 %; $p < 0.05$ vs. NMDA, Fig. 3.13B).

3.8 LPI protected dentate gyrus granule cells and reduced the number of microglia after excitotoxic lesion in OHSC

All conditions were normalised to the positive NMDA control, 136.47±15.82 PI positive cells/GCL and 27.25±1.83 IB_4 positive cells/GCL. Non-lesioned control OHSC exhibited a good neuronal preservation with almost no PI positive neuronal nuclei (CTR, 1 %) and IB_4 positive microglial cells (CTR, 13 %) Compared to CTR, the application of 1 µM LPI did not led to any significant alterations within the number of PI positive neuronal nuclei (LPI, 2 %, $p > 0.05$ vs. CTR, Fig. 3.14A) and IB_4 positive microglial cells (LPI, 5 %, $p > 0.05$ vs. CTR, Fig. 3.14B). Treatment of OHSC with 50µM NMDA for 4 hours at 6 div strongly inducted the numbers of PI positive neuronal nuclei (NMDA, 100 %, $p < 0.001$ vs. CTR) and IB_4 positive microglial cells (NMDA, 100 %, $p < 0.001$ vs. CTR). Application of 1 µM LPI to NMDA-lesioned OHSC led to a significant reduction of PI positive neuronal nuclei (NMDA+1 µM LPI, 56 %; $p < 0.001$ vs. NMDA Fig. 3.14A). Treatment of NMDA-lesioned OHSC with 1 µM LPI significantly reduced the number of IB_4 positive microglia as compared to NMDA-lesioned OHSC (NMDA+1µM LPI, 62 %, $p < 0.01$ vs. NMDA, Fig. 3.14B).

3.8.1 Concentration dependent effect of LPI on excitotoxically lesioned OHSC

Application of 1 nM-10 µM LPI to NMDA-lesioned OHSC led to a reduction of PI positive neuronal nuclei, whereas 10 pM-0.1 nM LPI showed no effect as compared to OHSC treated with NMDA alone (NMDA+1 nM LPI, 45 %; NMDA+10 nM LPI, 32 %; NMDA+0.1 µM, 46 %; NMDA+10 µM LPI, 57 %; $p < 0.001$ vs. NMDA, respectively; NMDA; NMDA+100 pM LPI, 106 %; $p > 0.05$ vs. NMDA, respectively Fig. 3.14A). NMDA-lesioned OHSC treated with 0.1 µM-10 µM LPI, showed reduced IB_4 positive microglia as compared

to NMDA-lesioned OHSC whereas 10 pM-10 nM LPI showed no effects (NMDA+0.1 µM, 63 %; NMDA+10 µM LPI, 60; $p < 0.01$ vs. NMDA, respectively., NMDA+100 pM LPI, 94 % NMDA+1 nM LPI, 83 %; NMDA+10 nM LPI, 89 %; $p > 0.05$ vs. NMDA, respectively, Fig. 3.14B).

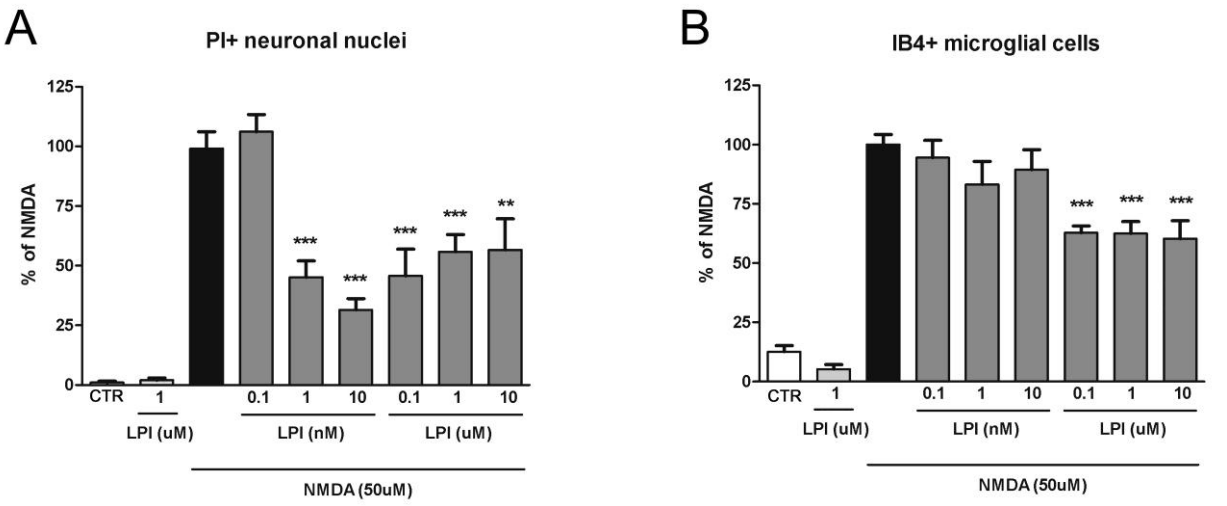

Figure 3.14 GPR55 activation mediates neuroprotection

LPI mediated neuroprotection from 0.1 nM to 10 µM. (A) LPI protected dentate gyrus granule cells in OHSC. LPI (1 nM - 10 µM) significantly decreased the numbers of Propidium Iodite (PI) positive neuronal nuclei after excitotoxic NMDA (50 µM) lesion (**$p < 0.01$, ***$p < 0.001$). The neuroprotective effect could not be observed at 0.1 nM of LPI. (B) Microglial cells were reduced in LPI (0.1- 10 µM) treated OHSC leasioned with NMDA (***$p < 0.001$). No effect on microglia was observed when LPI (0.1 – 10 nM) was applied on NMDA lesioned OHSC.

3.8.2 The neuronal protective effect of LPI is dependent on time and duration of LPI application

Prolonged exposure to 1 µM LPI even could enhance neurotoxicity in OHSC. Application of 1 µM LPI from div 0 until div 6, when excitotoxicity was provoked by NMDA, had no effect on neuronal death and microglia accumulation in the DG of OHSC (LPI (div 0-6)+NMDA, PI: 88 %, $p > 0.05$, IB_4: 101 %, $p > 0.05$, Fig. 3.15). LPI was applied from div 0-6 and after NMDA treatment until div 9, an enhanced neuronal cell death could be observed but no microglia alteration compared to the positive control (LPI (div 0-6)+NMDA+LPI (div 6-9), PI: 130 %, $p < 0.05$, Fig. 3.15, IB_4: 116 %, $p > 0.05$). Applying LPI continuously from div 0, during NMDA application and thereafter up to div 9 no alteration was seen (LPI (div 0-6)+NMDA/LPI+LPI (div 6-9), PI: 105 %, $p < 0.05$, IB_4: 74%, $p > 0.05$). Application of LPI 24 h prior to NMDA application had no effect on neuronal death and microglia accumulation (LPI (24 h)+NMDA, PI: 118 %, $p > 0.05$, IB_4: 76 %, $p>0.05$). 24 h LPI treatment after NMDA lesion showed a marginal decrease in neuronal lesion and microglia accumulation (NMDA+LPI (div 6), PI: 79 %, $p > 0.05$, IB_4: 85 %, $p > 0.05$, Fig.3.15). LPI applied during 4h of NMDA lesion showed no effect (NMDA/LPI, PI: 111 %, $p > 0.05$, IB_4: 98 %, $p > 0.05$). Application of LPI for 9 days in non lesioned OHSC showed no effect (LPI (div 0-9) PI: 1 %, $p > 0.05$, IB_4: 28 %, $p > 0.05$) compared to the control condition.

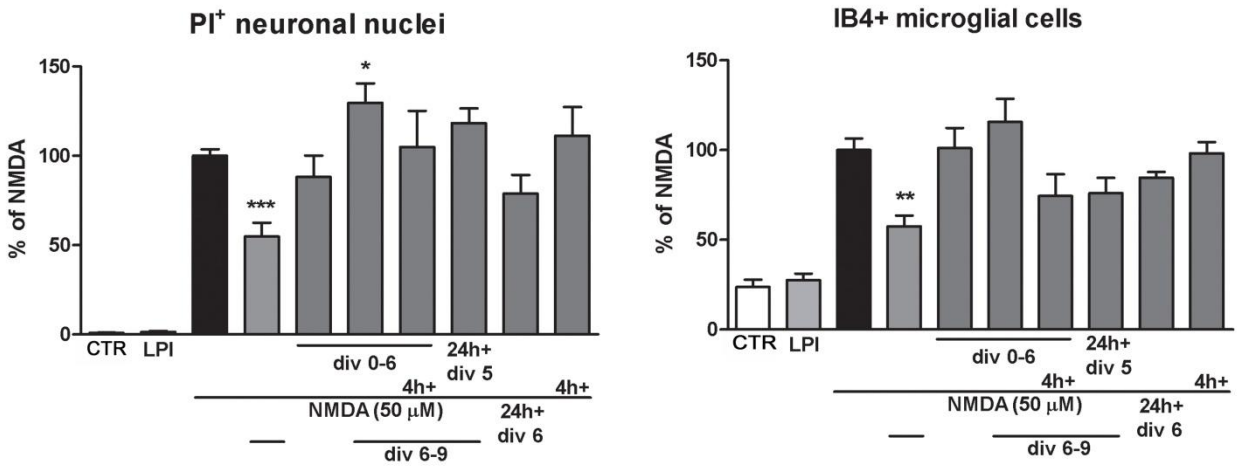

Figure 3.15 Temporal variances of GPR55 activation led to changes in neuronal cell death

Temporal modification of LPI application changes the neuroprotective effect of LPI. 1 µM of LPI was applied prior to NMDA lesion from day in vitro (div) 0-6, together with NMDA (+4 h) and after NMDA application (24 h+ or from div 6-9).

3.8.3 AM281 reduced the effect of LPI on microglia

Application of AM281, a CB_1 receptor antagonist, showed no neuroprotective properties at 0.1 µM AM281 (NMDA+0.1 µM AM281, PI: 74 %, $p > 0.05$, IB_4: 103 %, $p > 0.05$). 10 µM AM281 decreased neuronal cell death but had no effect on microglial cells in the DG of OHSC (NMDA+10 µM AM281, PI: 58 %, $p > 0.05$, IB_4: 73 %, $p > 0.05$). Combination of 10 µM AM281 and 1 µM LPI reduced the neuronal cell death significantly and decreased microglial cells in OHSC (NMDA+10 µM AM281+LPI, PI: 50 %, $p > 0.05$, IB_4: 72 %, $p > 0.05$, Fig. 3.16).

Application of AM281 had no effect on non damaged OHSC (PI: CTR, 2 %; LPI, 2%; 0.1 µM AM281, 1 %, $p > 0.05$; 10 µM AM281, 0 %, $p > 0.05$, 10 µM AM281+LPI, 0 %, $p > 0.05$;

IB_4: CTR, 13 %; LPI, 5%; 0.1 µM AM281, 9 %, p > 0.05; 10 µM AM281, 7 %, p > 0.05, 10 µM AM281+LPI, 8 %, p > 0.05, Fig. 3.16).

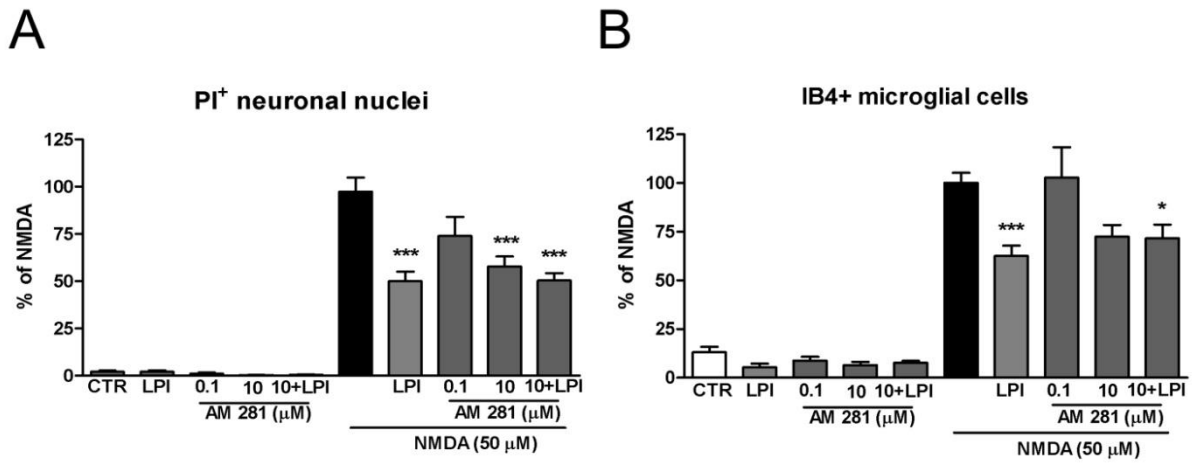

Figure 3.16 GPR55 agonist AM281 reduced neuronal cell death

AM281 (GPR55 agonist, CB_1 receptor antagonist) application on OHSC. LPI (1 µM) and AM281 (0.1 and 10 µM) had no effect on non lesioned OHSC. Neuronal protection was observed in NMDA (50 µM) lesioned OHSC treated with either LPI (1 µM) or AM281 (10 µM). AM281 combined with LPI also reduced the number of PI positive cells in comparison with OHSC treated with NMDA (ANOVA, ***p < 0.001). (B) In microglia, no additional effect of AM281and LPI was seen.

3.8.4 Combined treatment with LPI and WIN55 212-2 (WIN) enhanced neuroprotection

OHSC treatment with NMDA and the CB_1 agonist WIN significantly reduced the PI positive nuclei compared to NMDA (NMDA+WIN, 71 %; p < 0.05 vs. NMDA, Fig. 3.16). The combination of WIN and LPI led to an additional decrease in PI positive nuclei compared to single WIN application after NMDA (NMDA+WIN+LPI, 48 %; p < 0.05 vs. NMDA+WIN, Fig. 3.17A).

IB_4 positive microglia were not decreased when OHSC were treated with WIN (NMDA+WIN, 93 % $p > 0.05$ vs. NMDA, Fig. 3.17B). WIN combined with LPI led to a decrease of microglia in OHSC (NMDA+WIN+LPI, 82 %; $p < 0.05$ vs. NMDA).

WIN alone or in combination with LPI had no effect on negative control OHSC (PI positive nuclei: WIN, 4 %; WIN+LPI, 0 %; $p > 0.05$ vs. CTR; IB_4 positive microglia: WIN, 17 %; WIN+LPI, 22 %; $p > 0.05$ vs. CTR).

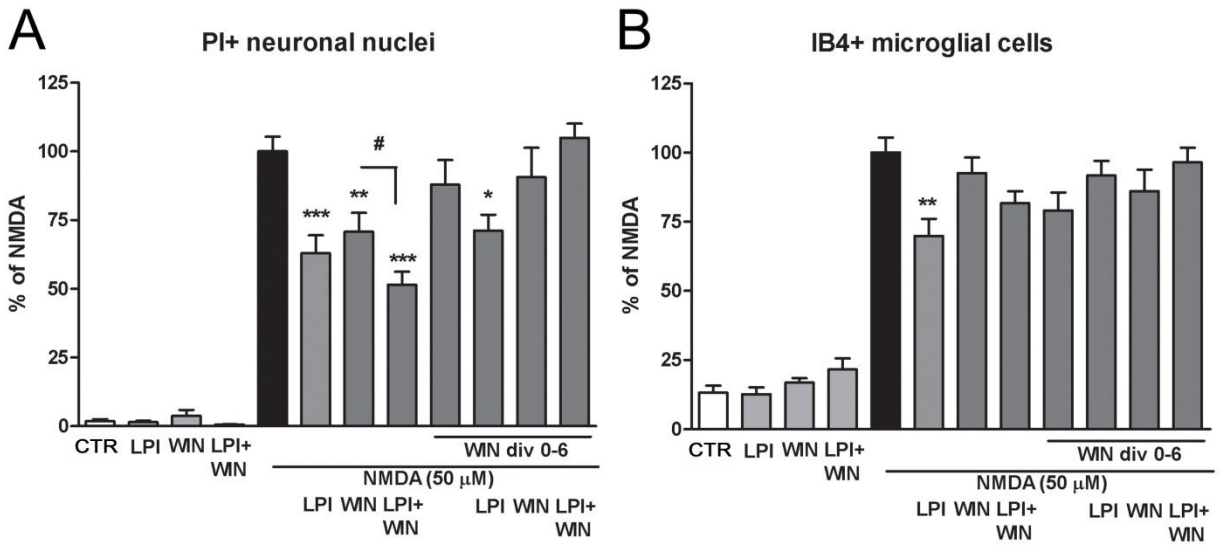

Figure 3.17 CB1 agonist WIN enhanced the neuronal protection of GPR55 activation

Combined treatment with LPI and WIN55 212-2 enhanced neuroprotection. (A) Neuronal protection was observed in NMDA (50 µM) lesioned OHSC treated with either LPI (1 µM) or WIN55 212-2 (1 µM). WIN55 212-2 combined with LPI even reduced the number of PI positive cells in comparison with WIN55 212-2 alone in OHSC treated with NMDA (t-Test, $\#p < 0.05$). (B) In microglial cells, no additional effect of WIN55 212-2 and LPI was seen, confirming the non microglial mediated WIN55 212-2 neuroprotective effect.

3.9 LPI lost its neuroprotective effects after depletion of microglia

Microglial cells were depleted in OHSC with clodronate. The neuronal cell death is increased in clodronate treated OHSC after NMDA application (PI: clodronate + NMDA, 124%; $p < 0.01$ vs. NMDA). LPI lost its neuroprotective effect in clodronate treated OHSC. PI positive nuclei were not decreased after NMDA+LPI treatment in comparison with NMDA in clodronate treated OHSC (PI: clodronat+: NMDA 124 %; NMDA+LPI, 139 %; $p > 0.05$ vs. NMDA, Fig. 3.18). After clodronate treatment, only few microglia could be observed in OHSC (IB_4: clodronate treated OHSC CTR, 4 %; LPI, 3 %; NMDA 3 %; NMDA+LPI, 2 %; $p > 0.05$ vs. NMDA, compared to non clodronate treated OHSC: CTR, 13 %; LPI, 5 %; NMDA+LPI, 70 %, $p < 0.01$ vs. NMDA; Fig. 3.19).

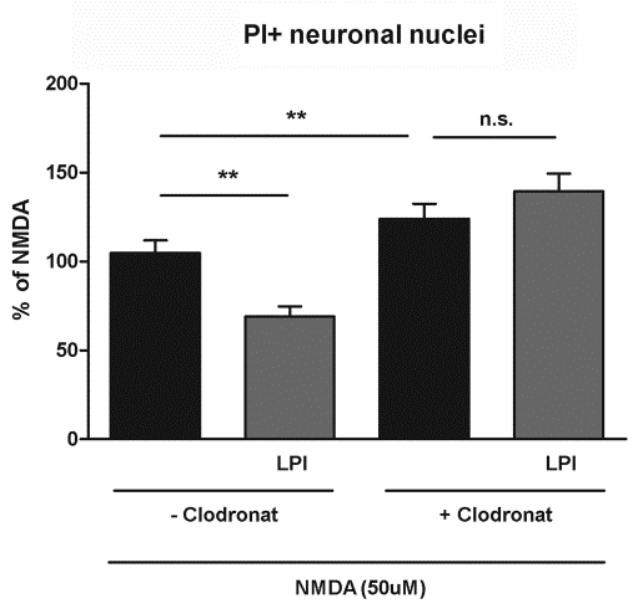

Figure 3.18 GPR55 activation had no effect on microglia depleted OHSC

LPI lost its neuroprotective effects after depletion of microglia. Microglial cells in OHSC were depleted by clodronat treatment. After microglial cell depletion, an enhanced neuronal damage after NMDA (50 µM) treatment was observed (**$p < 0.01$ vs. NMDA). No decrease of neuronal cell death could be seen in microglial depleted OHSC treated with NMDA and LPI (1 µM).

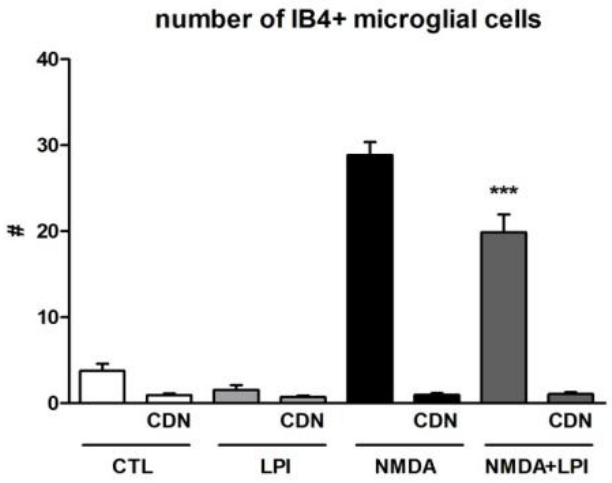

Figure 3.19 Microglia depletion in OHSC

Clodronate depleted microglia from OHSC. Microglial cells were depleted after clodronat treatement. Even after NMDA lesion no microglia activation could be seen.

3.10 LPI-mediated neuroprotection and microglia reduction was reversed by transfection of OHSC with Gpr55 siRNA

Treatment of OHSC with siRNA against GPR55 24 h prior to NMDA application at 6 div diminished the protective effect of LPI. The numbers of PI positive neuronal nuclei at 9 div in NMDA and LPI supplemented OHSC were significantly decreased compared to NMDA treatment alone (NMDA+LPI, 48 %; Fig. 3.20A, $p < 0.001$ vs. NMDA). In LPI supplemented OHSC microglia were decreased as well compared to NMDA (NMDA+LPI, 52 %, $p < 0.01$ vs. NMDA Fig. 3.20B). OHSC treated with negRNA showed a significant decrease of PI positive cells after LPI treatment in comparison with single NMDA application (negRNA treated OHSC: NMDA 77 %; NMDA+LPI, 39 %; $p < 0.01$ vs. negRNA NMDA, Fig. 3.20A). Microglial cells were also reduced in negRNA NMDA and LPI treated OHSC compared to negRNA NMDA treated OHSC (negRNA treated OHSC: NMDA, 76 %; NMDA+LPI, 39 %; $p < 0.05$ vs. negRNA NMDA, Fig. 3.20B). In siRNA treated OHSC, no significant decrease

in PI positive nuclei could be observed after LPI treatment in comparison to the respective NMDA condition (siRNA treated OHSC: NMDA, 78 % and NMDA+LPI, 64 %; p>0.05 vs. siRNA NMDA, Fig.3.20A). Microglia in OHSC treated with siRNA did not decrease significantly after LPI treatment (siRNA treated OHSC: NMDA, 106 % and NMDA+LPI, 81 %; p > 0.05 vs. siRNA NMDA, Fig. 3.20B). Non-NMDA lesioned OHSC treated with LPI demonstrated no alteration in PI positive cells or in the amount of microglia (PI+: CTR was set to 100 %, LPI, 31 %; negRNA CTR, 109 %; negRNA LPI, 71 %; siRNA CTR, 78 %; siRNA LPI, 72 %; p > 0.05 vs. CTR; IB_4 microglial cells: CTR was set to 100 %, LPI, 81 %; negRNA CTR, 98 %; negRNA LPI, 91 %; siRNA CTR, 82 %; siRNA LPI, 69 %; p > 0.05 vs. CTR, data not shown)

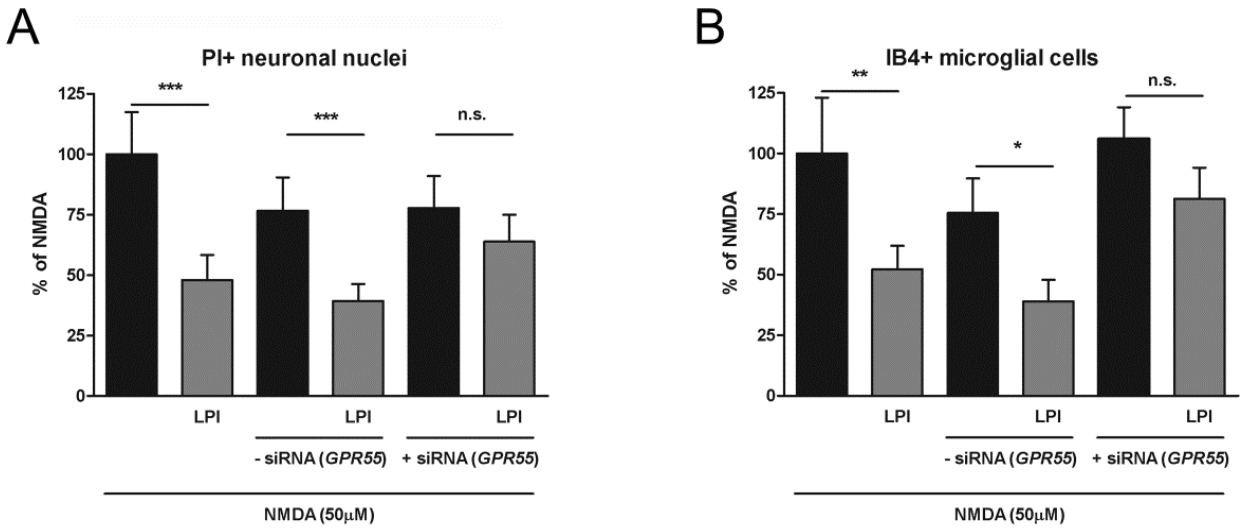

Figure 3.20 Neuronal protection is mediated by GPR55

Neuronal protection was mediated by GPR55. LPI (1 µM) mediated neuroprotection (A) and microglia (B) reduction was reversed by transfection of OHSC with GPR55 siRNA. OHSC treated with negRNA showed neuronal protection and microglia reduction by LPI treatment after NMDA (50 µM) lesion (***p < 0.001 vs. NMDA, **p < 0.01 vs. NMDA, *p < 0.05 vs. NMDA). In GPR55 siRNA treated OHSC, the neuronal protective effect as well as the reduced microglia accumulation vanished.

3.10.1 Successful *Gpr55* siRNA transfection was proven by semi-quantitative rt-PCR

Down-regulation of the GPR55 expression after siRNA transfection was controlled by semi-quantitative rt-PCR. Untreated OHSC served as controls and were set to 100 %. 24 h after siRNA supplementation to the culture media, a significant decrease of *Gpr55* cDNA to 19 % ($p < 0.01$ vs. untreated OHSC, Fig 3.21) was measured. After 96 h of siRNA treatment *Gpr55* cDNA was still decreased to 35 % ($p < 0.05$ vs. untreated OHSC).

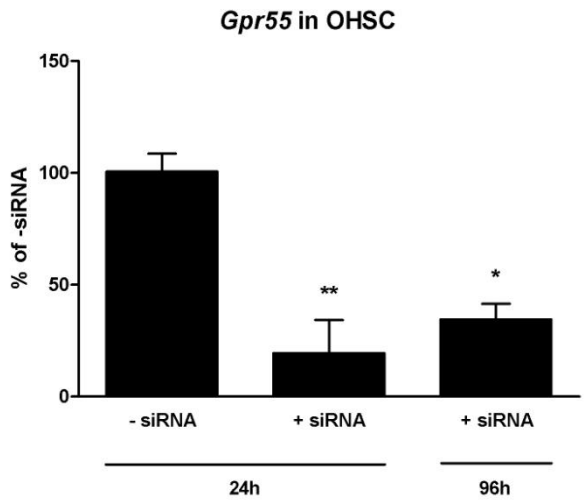

Figure 3.21 GPR55 was down-regulated after siRNA transfection

GPR55 was successfully down-regulated. (A) Successful GPR55 siRNA transfection was proven by semi-quantitative rt-PCR. 24 h and 96 h after GPR55 siRNA transfection GPR55 was downregulated significantly (**$p < 0.01$, *$p < 0.05$, $n = 3$).

3.11 Gpr55 mRNA in OHSC, primary microglia and astroglia after LPI treatment

In primary astrocyte cell culture, GPR55 was down-regulated after 10 ng/ml LPS and 1 µM LPI. Control primary astrocyte cell culture was set to 100 % (LPI, 128 %; LPS, 85 %; $p > 0.05$ vs. CTR, and LPS+LPI, 43 %, $p < 0.05$ vs. CTR independent t-Test, Fig. 3.22A). GPR55 was downregulated in primary microglia culture treated with LPI (1 µM), LPS (10 ng/ml) and LPS+LPI compared to control cultures (LPI, 54 %; LPS, 43 %; LPS+LPI, 55 %, $p < 0.001$ vs. CTR, Fig. 3.22B)

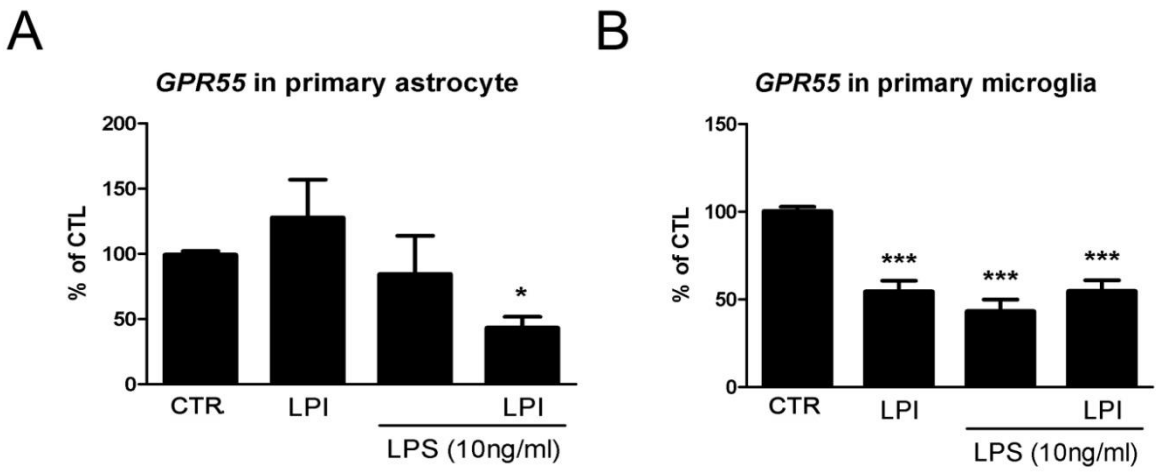

Figure 3.22 GPR55 expression in primary glia cell cultures

LPI influenced GPR55 expression in primary glia cell culture. (A) Primary astrocyte culture was treated with LPI (1 µM), or/and LPS (10 ng/ml) for 6 h. Only LPS in combination with LPI led to a decrease in GPR55 expression (**$p < 0.01$). (B) In primary microglia, LPI and LPS reduced GPR55 expression significantly (*$p < 0.05$). No enhanced GPR55 down-regulation was observed by combined LPS and LPI treatment. (n = 3)

3.12 LPI attenuated ATP- and LPI- induced microglia migration

LPI (1 µM), ATP (100 µM) and LPS (10 ng/ml) increased the migration of primary microglia in Boyden chamber experiments significantly (CTR, 10.48/well; LPI, 21.23/well; ATP, 24.22/well, LPS, 23.55/well $p < 0.01$ vs. CTR). The enhanced motility of ATP and LPS was reduced by LPI addition back to LPI counts (LPI+ATP, 19.41/well; LPI+LPS, 18.57/well; $p < 0.05$ vs. ATP and LPS respectively, Fig. 3.23A,B). Control experiments with equal substance distribution reduced the migration to control levels (CTR, 7.50/well; LPI, 7.33/well; ATP, 6.60/well; LPI+ATP, 6.33/well; $p > 0.05$ vs. CTR, data not shown). The CB_1 antagonist AM281 enhanced migroglia migration but did not change the effect of LPI (CTR, 11.53/well; LPI, 17.26/well; AM281, 18.77/well; LPI+AM281, 17.76/well, $p < 0.05$ vs. CTR, Fig. 3.23C).

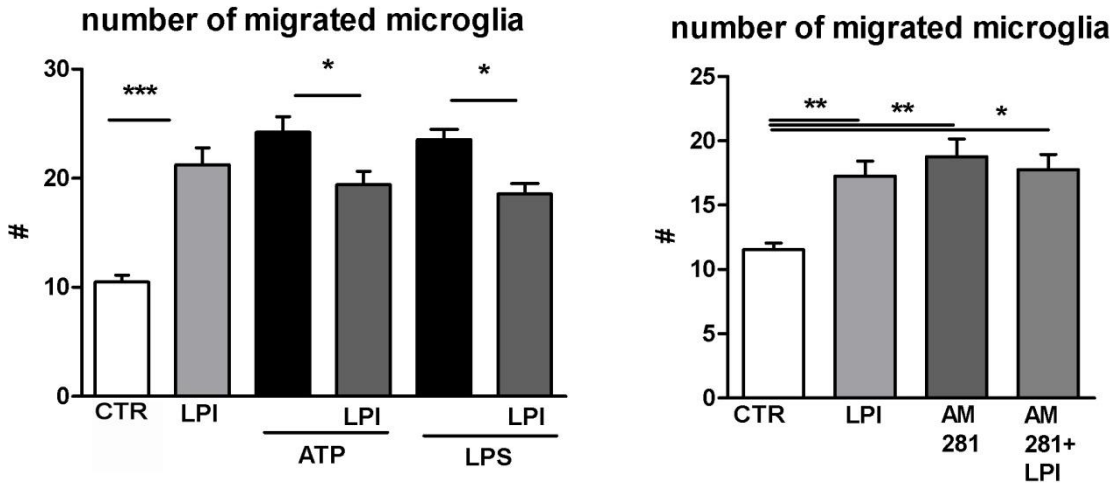

Figure 3.23 GPR55 activation on microglia migration

LPI enhanced primary microglia migration. Using Boyden Chamber, single LPI (1 µM) ATP (100 µM) or LPS (10 ng/ml) supplementation to primary microglial cell culture increased the number of migrating microglial cells compared to untreated control microglial cells (***$p < 0.001$). Combining LPI and ATP reduced the migratory effect of primary microglial cells (*$p < 0.05$). The migratory effect was lost when the substances were applicated in the upper chamber as well. Combining LPI and LPS reduced the migratory effect of primary microglial cells as well as ATP (*$p < 0.05$). (C) No modification of migration induced by LPI was seen when CB_1 antagonist was applied.

4. General Discussion

The present dissertation investigated the regulation of the endocannabinoid system after long range projection damage and excitotoxic lesion and the impact of GPR55, a potent cannabinoid receptor, during excitotoxic lesion. The present studies were conducted with organotypic hippocampal slice cultures (OHSC) in vitro. In OHSC the neuronal circuit is preserved during culture and allows identifying properties of neuronal tissue, neurons and glial cells. (Adamchik, Frantseva et al. 2000; Hailer, Wirjatijasa et al. 2001; Adembri, Bechi et al. 2004).

4.1 Perforant Pathway transection model modification

The PPT model in OHSC has been extended by precise dissection of the affected areas to investigate the intrinsic regulation of endocannabinoids after axonal (retrograde) damage and dendritic denervation (anterograde damage) of the perforant pathway, a long-range projection. The PPT model and the subsequent precise dissection of the anterograd and retrograde lesioned regions was successfully applied and the eCB content could be determined. After denervation neurons undergo complex reorganization processes. It could be shown that the dissection of entorhinal afferents induced dendritic changes of the granular cell layer of the dentate gyrus (Diekmann, Ohm et al. 1996; Vuksic, Del Turco et al. 2011). Neuronal cell death was not induced by deafferentiation of the granular cell layer as also described earlier in an in vivo model (Kovac, 2004). Glial cells became activated and covered the lesion sites, peviously neurite sprouting was observed after astrocyte hypertrophy and astrocyte derived factors were supposed to influence neuronal growth after deafferentiation (Ide, Scripter et al. 1996).

4.2 Endocannabinoid regulation after perforant pathway transection

CNS pathologies induce direct neuronal tissue damage that also involves long range projection deafferentiation, but also indirect lesioned areas become severely affected in secondary damage regulation. Small but not significant changes were observed in the EC, whereas a significant and robust increase in the concentration of all investigated eCB was found 24hpl in the DG. These findings indicate a spatial and temporal regulation of eCB mostly affecting the target area of long-range projections. In several reports enhanced anandamide and 2-AG levels have been detected after various pathological events, like stroke, traumatic brain injury e.g., indicating a compensatory mechanism to brain damage (Hansen, Schmid et al. 2001; Maccarrone, Gubellini et al. 2003; Marsicano, Goodenough et al. 2003).

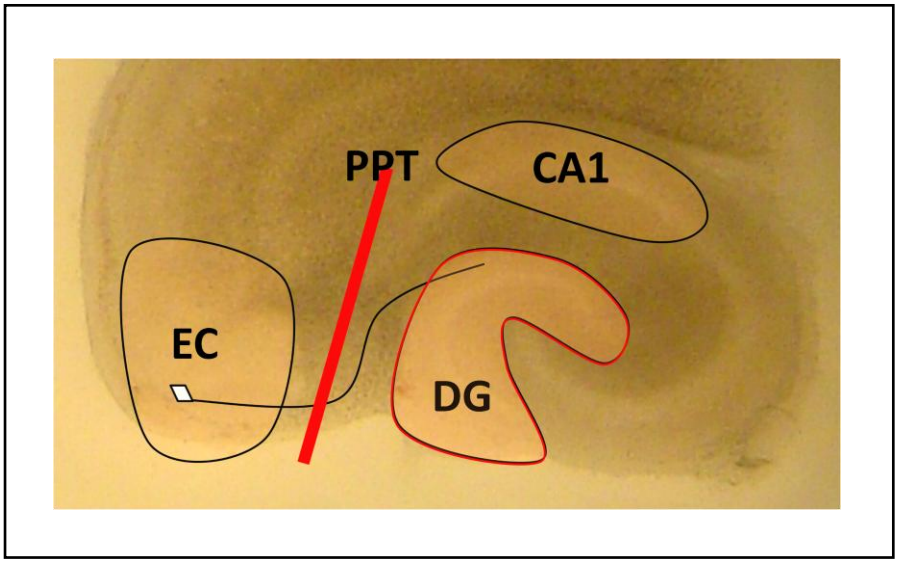

Figure 4.1 Anterograde signallin of endocannabinoids

ECB were up-regulated in the DG, after perforant pathway transection. Only the anterograde lesion site showed an alteration of eCB levels after PPT. EC entorhinal cortex, CA1 cornue ammonis region 1, DG dentate gyrus, PPT perforant pathway transsection.

It was previously shown that anandamide and 2-AG activate MKP-1 in microglia, abolishing NO release and protected against over-activation of microglia (Dommergues, Plaisant et al.

2003; Eljaschewitsch, Witting et al. 2006). Therefore, the increased eCB levels 24hpl in our study might reduce the microglia activation leading to neuroprotective effects. However, cell culture experiments with BV-2 cells showed an increase in microglia motility after anandamide supplementation (Franklin, Parmentier-Batteur et al. 2003). Still, enhanced OEA levels, also observed in the present study were found to further reduce microglia activation (Coffey, Perry et al. 1990; Topper, Gehrmann et al. 1993). The inhibition of reactive microglia by OEA might therefore conduct neuroprotective effects. Also PEA was shown to be potent to prevent neuronal damage by activation of PPARalpha in microglia. PEA however stimulated also PPARalpha in neurons and astrocytes (Koch *et al.*, 2011, Raso *et al.*, 2011).

Similar to the elevated anandamide levels in the cerebrospinal fluids after stroke or in Parkinson disease (Schabitz, Giuffrida et al. 2002; Pisani, Fezza et al. 2005), increased anandamide and PEA levels were observed in the present study 24hpl. Enhanced PEA levels were also measured in inflamed tissues undergoing severe cell damaging processes, ischemic conditions and glutamate induced neurotoxicity demonstrating neuroprotective properties (Rodriguez De Fonseca, Gorriti et al. 2001; Conti, Costa et al. 2002; Koch, Kreutz et al. 2011). The combined up-regulation of anandamide and PEA, the previously described entourage effect could have served also in the present study to enhanced action of anandamide at the CB_1 and the vanilloid receptor (De Petrocellis, Davis et al. 2001). The simultaneously enhanced OEA levels 24hpl in the present study is in line with a previous study, where dopamine neurons of the substantia nigra were protectd by OEA after a treatment with 6-OHDA (Galan-Rodriguez, Suarez et al. 2009). 2-AG regulation after PPT in OHSC, also differentiated clearly the lesion sites. It could be shown that the indirect dendritic lesion resulted in a moderate 2-AG increase in the DG and had no further effects on 2-AG regulation in the CA1 region. 2-AG is commonly accepted as an important component of the endocannabinoid system protecting neurons after neuronal insults by retrograde signaling

decreasing neuronal excitation (Panikashvili, Simeonidou et al. 2001; Marsicano, Moosmann et al. 2002; Milton 2002; van der Stelt and Di Marzo 2005). The elevation observed in the present study might therefore indicate a neuroprotective reaction at the anterograde lesion site after PPT. However, the overall increase of eCB at the anterograde lesion site could further indicate an involvement of eCB in dendtitic re-organisation.

4.3 Endocannabinoid regulation after excitotoxic lesion

The excitotoxicity model with NMDA was used to investigate whether different OHSC regions would respond with different eCB levels to low or high concentrations of NMDA.

Surprisingly, the EC did not react to low or high NMDA lesion with altered 2-AG levels but with enhanced levels of NEA after high NMDA treatment. Enhanced eCB levels were measured 24 hours after low and high NMDA lesion in the DG. Though, low NMDA doses enhanced eCB levels significantly in the CA1 region. Being the region with the highest density of NMDA receptors the CA1 region is the most sensitive region to excitotoxic lesion (Kristensen, Noraberg et al. 2001). Evidence exists that the density of the 2-AG hydrolyzing enzyme, MAGL, is low on the axon terminals of mossy cells and DAGL, the 2-AG synthesising enzyme, was shown to be abundant at the Schaffer collateral CA1 region of the hippocampal formation (Katona, Urban et al. 2006; Ludanyi, Hu et al. 2011; Uchigashima, Yamazaki et al. 2011). This strengthens the relevance of 2-AG in the CA1 region during neuronal stress. Enhanced eCB response to low NMDA excitotoxic damage might be a possible mechanism to counteract the insult in the more susceptible CA1 region. Stimulation of the Schaffer collateral synapses shown by Stella et al. led also to an endogenous 2-AG release in rat OHSC (Stella, Schweitzer et al. 1997) and also short-term synaptic depression was consistently enhanced by inhibition of MAGL (Pan, Wang et al. 2011; Straiker, Wager-Miller et al. 2011) supporting the present data. In vivo models of closed head injury and focal

ischemia in mice reported intrinsic elevated 2-AG levels after 4 and also after 1 to 24 hours post lesion (Panikashvili, Simeonidou et al. 2001; Degn, Lambertsen et al. 2007). This variances in 2-AG regulation might be partly provoked by the blood-brain barrier (BBB) disruption, as enhanced 2-AG levels were shown to reduce BBB permeability 1-4 hours after brain injury (Panikashvili, Shein et al. 2006; Degn, Lambertsen et al. 2007). However, the diverse regulation of eCB in different brain regions after PPT and after excitotoxic lesion demonstrates a specific involvement of eCB in distinct damage regulation in the brain. Whether eCB are involved in different neuronal protection mechanisms needs however further investigation. The difficulty to interpretate PEA and OEA together with anandamide is due to their structural similarity and comparable regulation (Hansen 2010), that is also seen in the present study.

4.4 Enzymatic regulation of eCB after PPT

As a next step the time-dependent and spatial regulation of enzymes responsible for synthesis and hydrolysis of the eCB in the PPT model was investigated, as the lesion sites were clearly differentially regulated.

Enzymatic regulation of NEA

NAPE-PLD, synthesising NEA from NAPE (Okamoto, Morishita et al. 2004; Leung, Saghatelian et al. 2006), was elevated early between 1hpl and 6hpl after PPT but decreased to control levels at 72 hpl. The augmentation of NAPE-PLD might explain the NEA accumulation 24 hours after PPT. However two further enzymes were found that may present an alternative pathway for NEA synthesis and were not investigated in the present study. Phospholipase C (PLC) can synthesise phosphor-NEA, which is then hydrolysed to NEA and the two enzymes phospholipase B (ABDH4) and the phosphodiesterase (GDE1) can together

hydrolyse glycerophospho-NAE (GP-NAE) to NEA (Sun, Tsuboi et al. 2004; Simon and Cravatt 2008). The alternative enzymes were taken into consideration after it could be shown in 2011 by Zhu et al. that mice lacking NAPE-PLD were able to synthesise PEA (Zhu, Solorzano et al. 2011). Whether these alternative pathways become active when NAPE-PLD gain its functionality or whether they display only a compensatory mechanism in NEA synthesis, still remains unclear. In a study with macrophage cell culture, lipopolysaccharide (LPS) reduced the amount of NAPE-PLD and therewith the amount of PEA, subsequently leading to enhanced inflammatory reactions (Zhu, Solorzano et al. 2011). The cellular distribution of NAPE-PLD displayed a clear neuronal localisation that was earlier described (Nyilas, Dudok et al. 2008). NAPE-PLD immunoreactivity was seen in primary microglia in culture and microglia in OHSC, although astrocytes in culture expressed NAPE-PLD but not in OHSC. In a postmortem study of MS patients, NAPE-PLD expression could be found in microglia as well as in astrocytes (Zhang, Hilton et al. 2011). Whether the expression of NAPE-PLD in MS indicates a dysregulated endocannabinoid system or an appropriate response to compensate the pathologic inflammation in these patients remains ambiguous.

The hydrolysing enzyme FAAH was found being predominantly localised in the endoplasmic reticulum (Cravatt, Giang et al. 1996) and is able to hydrolyse all three acylethanolamides investigated in this work (Ueda, Tsuboi et al. 2010). The high FAAH expression observed at 48 hpl might explain the down-regulation of all investigated NEA back to control levels or even decreased levels. The FAAH inhibitors MAFP or URB597 enhance NEA levels in vivo and in vitro and MAFP was found to reduce apoptosis in the neocortex (Maccarrone, Piccirilli et al. 2004) and URB 597 decreased the infarct volume when administered prior to focal cerebral ischemia (Degn, Lambertsen et al. 2007). The amount of FAAH was observed to correlate with neurotoxic properties (Degn, Lambertsen et al. 2007). Other FAAH inhibitors were found to be beneficial for the outcome of neurological diseases as well (Fowler, Rojo et al. 2010). FAAH was clearly expressed in neurons of OHSC, confirming previously reported

data by Cravatt et al. (Cravatt, Giang et al. 1996). In OHSC, FAAH could not be detected in microglia neither in PPT nor in controls, whereas primary microglia cell cultures expressed FAAH as shown previously (Witting, Walter et al. 2004; Tham, Whitaker et al. 2007). A previous report of Alzheimer disease patients showed that FAAH is expressed in astrocytes. In the present study, low FAAH expression in fibrillary astrocytes and high FAAH expression were found in protoplasmic astrocytes of primary cell cultures but not in OHSC (Nunez, Benito et al. 2008). However, further investigations are required to figure out whether the here observed endogenous up-regulation of FAAH determines the eCB involvement in inflammatory reactions and for which reason. Thus, the question remains whether the intrinsic down-regulation of eCB happens due to the inflammatory status or whether prolonged eCB activation could have positive effects as indicated in literature (Fowler *et al.*, 2010).

Another recently discovered enzyme is NAE-hydrolysing acid amidase (NAAA) that was detected in lysosomes of HEK cells (Zhao, Tsuboi et al. 2007). This enzyme is responsible to hydrolyse acylethanolamides of less than 18 carbon atoms, including PEA. However, NAAA protein expression remained unchanged at any time point after PPT in the present study. The imunohistochemical distribution of NAAA in brain tissue is described here for the first time. NAAA was expressed in neurons of OHSC and primary neuronal cultures. Microglia in OHSC showed no NAAA expression although NAAA was described in macrophages as a lysosome associated protein (Ueda, Tsuboi et al. 2010). In primary cultures fibrillary astrocytes showed high NAAA expression whereas protoplasmic astrocytes displayed only weak NAAA in their nuclei only.

Taken together, the different expression patterns of NAPE-PLD, FAAH and NAAA in primary cell culture and OHSC, especially found in microglia, might be due to the tight functional connection of the glia cells and neurons with each other. This interplay determines the state of activation, especially of microglia (Schafer, Lehrman et al. 2012). Thus, NEA can

be synthesised and hydrolysed not only by neurons but also by glial cells under physiological and pathological conditions, indicating the importance of the eCBS in pathological changes and underlining its high dynamic. The present results indicate that the different cell types are potent to alter their eCB content depending on circumstances and environment. The lack of neuronal contact is suggested to lead to enhanced eCB production of glia cells which opens a new perspective of the eCBS and still needs to be investigated.

No obvious redistribution of CB_1 in lesioned dendrites of the molecular layer or glial cells could be observed in slice cultures undergoing PPT. Although eCB and the specific enzymes become altered after PPT in OHSC, the main target receptor of the investigated eCB, $CB_{1,}$ remained quantitatively unchanged. Still, the CB_1 could be re-distributed and more cellular investigation is needed to understand the precise mechanism.

Enzymatic regulation of 2-AG

The involvement of the main synthesising (DAGL) and hydrolysing (MAGL) enzymes of 2-AG were investigated. *Dagl* mRNA amounts were unchanged after PPT in the EC and were enhanced 24 hpl in the DG, whereas *Magl* mRNA remained at control levels. Increased *Dagl* mRNA levels could explain the enhanced 2-AG levels of the anterograde lesion site as suggested by a previous spinal cord study (Garcia-Ovejero, Arevalo-Martin et al. 2009). The investigated DAGL protein levels over time however, showed a decreased DAGL protein expression 24 hours after PPT. Opposed expression of *Dagl* mRNA and DAGL protein expression with increased 2-AG levels might still be explained by DAGL ubiquitination, as DAGL is involved in highly dynamic processes e.g. development, axonal growth and orientation (Bisogno, Howell et al. 2003; Walker, Suetterlin et al. 2010). Therefore, DAGL needs to be expressed in a quickly regulated mechanism like ubiquitination. It was shown that ubiquitination was important in the regulation of fast turnover of signaling events and plays a

fundamental role in signal transduction, cell cycle regulation and transcription (Wickliffe, Williamson et al. 2009; Clague and Urbe 2010). Recently, two enzymes (Phospholipase D1, Cyclooxygenase-1 (COX-1)) involved in arachidonic acid regulation were shown to be ubiquitinated (Yin, Gui et al. 2010; Yazaki, Kashiwagi et al. 2012). In human embryonic kidney cells, intra-cellular calcium concentration COX-1 degradation was shown to be regulated by ubiqitination. (Yazaki, Kashiwagi et al. 2012). As 2-AG is regulated calcium dependent in excitotoxic neuronal damage, this might be another indication for an ubiquitin involved mechanism.

The regulation of DAGL and MAGL was investigated under control and stimulated conditions in OHSC as well as in primary cell cultures on their cellular distribution in neurons, microglia and astrocytes. DAGL could be observed in neurons and only marginal in astrocytes of OHSC. In primary neuronal cultures, DAGL co-localised with Vglut1 at the presynapse. Previously, DAGL was localised in cerebellar, hippocampal and striatal neurons at the dendritic spines in the CA1 subfield, linked to the intracellular surface of the plasma membrane (Katona, Urban et al. 2006; Yoshida, Fukaya et al. 2006; Uchigashima, Narushima et al. 2007; Uchigashima, Yamazaki et al. 2011). A re-organisation of DAGL after PPT towards the lesioned dendrites was observed in the present study, but interestingly the DAGL immunoreactions in astrocytes increased. Gomez et al., showed that GFAP positive cells can be DAGL immunoreactive (Gomez, Arevalo-Martin et al. 2010) sustaining the present data. Further, astrocytes were shown in the epicenter of spinal cord injury to be DAGL positive (Garcia-Ovejero, Arevalo-Martin et al. 2009). The expression of DAGL in astrocytes is in line with previous reports describing an intense 2-AG production of astrocytes when stimulated *in vitro* with inflammatory mediators (Franklin, Parmentier-Batteur et al. 2003; Walter, Franklin et al. 2003). In microglia however, no DAGL IR in OHSC, but in primary microglia culture was observed. In previous studies, 2-AG was also shown to be produced by microglia cultures

in vitro (Walter, Franklin et al. 2003; Witting, Chen et al. 2006). However, in an in vivo study of spinal cord injury no DAGL IR could be observed in microglia (Garcia-Ovejero, Arevalo-Martin et al. 2009) like in the present study.

The distribution of the degrading enzyme MAGL displayed a re-organisation. Most studies focused on the neuronal expression pattern of MAGL, however the cellular expression of MAGL during NMDA lesion and PPT showed a very low expression of MAGL IR in astrocytes compared to the controls. It has been previously reported that astrocytes express the degrading enzyme MAGL as reviewed by Stella (Stella 2004; Fernandez-Ruiz, Pazos et al. 2008). The here observed MAGL expression during neuronal damage demonstrates the high impact of 2-AG and that astrocytes are highly involved in 2-AG break-down. However, this result still needs to be supported by in vivo experiments. Further, it indicates that glia cells might have a greater role in eCB regulation as indicated by literature.

MAGL IR of microglia was not found in OHSC but in primary cell culture. Likewise, the regulating enzymes of NEA microglia are potent to determine eCB regulation but the environmental signals still remain unknown. Studies suggest that approx. 9 % of total 2-AG hydrolysis in brain is ABHD12 dependent, which is highly expressed in microglia (Savinainen, Saario et al. 2012). Further, MAGL and ABHD12 were suggested as analogues for brain microglia or monocytes in related cell types of peripheral tissues (Fiskerstrand, H'Mida-Ben Brahim et al. 2010). ABHD12 was however not investigated in the present study. During different cellular activation state,s DAGL IR and MAGL IR were differentially expressed, suggesting a defined expression pattern. Thus, a highly defined regulation of 2-AG in different neurotoxic conditions is suggested.

4.5 Regulation of CB_1 and PPARalpha after PPT in OHSC

The regulation of CB_1 was enhanced in the EC early after PPT and in the CA1 region at a later time point. However, in the region of eCB up-regulation, the DG, CB_1 showed no alteration. A previous study on rats observed only an up-regulation of CB_1 expression from 2 h after middle cerebral artery occlusion up to 72 h in the direct ischemic region (Jin, Mao et al. 2000). The effect of ischemic insults upon CB_1 however, is unclear and seems to depend on ischemic condition, time and species investigated (Fowler, Rojo et al. 2010). Studies of differentially regulated CB_1 receptors on glutamatergic and GABAergic synapses might clarify these coherences (Marsicano, Goodenough et al. 2003). Recently, evidence showed that GABAergic interneurons of the hippocampus synthesise 2-AG, although a higher excitation stimulus is needed compared with glutamateric neurons (Peterfi, Urban et al. 2012). CB_1 and DAGL are evolutionary related, stating 2-AG as the endogenous ligand for CB_1 (McPartland, Norris et al. 2007; Katona and Freund 2008). This might indicate a synergistic regulation. However, the regulation of CB_1 during neuronal damage needs further investigation. Cravatt et al. showed that after prolonged 2-AG stimulation, compensatory desensitization of the CB_1 receptor in the brain, like CB_1 receptor density and functional responses were attenuated (Schlosburg, Blankman et al. 2010). In the present model however, no up-regulation of DAGL or down-regulation of MAGL was observed. The intrinsic augmentation of anandamide and 2-AG have not influenced the CB_1 expression in the DG, altough the CB_1 alteration in the EC and CA1 region might be a response to axonal re-orientation.

A nuclear receptor for NEA is PPARα (De Petrocellis, Chu et al. 2004; Suardiaz, Estivill-Torrus et al. 2007). Application of exogenous PEA was reported to enhance PPARα activation. Selective NAAA inhibitors were able to up-regulate the endogenous PEA levels and subsequently increase PPARα activity (Lo Verme, Fu et al. 2005; Solorzano, Zhu et al.

2009). However, no alteration of PPARα could be observed after PPT in OHSC although PEA was up-regulated 24 hours post lesion.

4.6 2-AG mediates neuroprotection

2-AG was shown to be endogenously up-regulated at the anterograde lesion site 24 hpl after PPT in OHSC. Supplemented 2-AG is seen as a modulator of neuroprotection which could be shown in a previous study of excitotoxic damage in OHSC (Kreutz, 2009). DAGL -/- mice had reduced 2-AG levels and it was shown that 2-AG was involved in neurogenesis (Goncalves, Suetterlin et al. 2008; Gao, Vasilyev et al. 2010). The anterograde up-regulation of 2-AG after PPT might indicate a further role of 2-AG in dentritic protection, not only after excitation as shown by Kantona and Freund (2008). In a different approach, the MAGL inhibitor JZL184 was used here to induce an endogenous increase in 2-AG levels to reduce neuronal damage. The increase of 2-AG after JZL184 supplementation in the present study was similar to the increase reported in former studies where chronic JZL184 supplementation inactivated MAGL and subsequently led to a 10-fold increase of 2-AG levels in brain and spinal cord tissue (Chanda, Gao et al. 2010; Savinainen, Saario et al. 2012). A lower 2-AG increase in the CA1 region after PPT than in the DG and the EC was observed, supporting the data that less MAGL is present in the CA1 region (Katona, Urban et al. 2006; Ludanyi, Hu et al. 2011; Uchigashima, Yamazaki et al. 2011).

Here, excitotoxic lesioned OHSC were treated with JZL184 or MAGL siRNA to investigate whether this MAGL inhibition indeed can induce neuroprotection. The neuronal damage of the granular cell layer decreased remarkably, as was also shown by other studies, which demonstrates the neuroprotective properties of endogenous and exogenous 2-AG in neuronal excitotoxic models and other cellular settings (Zhao, Yuan et al. 2010; Koch, Kreutz et al. 2011).

Summarizing, the intrinsic activation of the eCBS after neuronal damage by transection of long-range projections and excitotoxic damage within secondary damage regulation, provides a strong time-dependent and site-specific signal for endogenous synthesis of eCB, presumably to prevent or restrict neuronal damage. Furthermore, the regulation of eCB underlines their importance in CNS pathologies that involves a dynamic and complex interplay mainly of astrocytes and neurons, depending on time and cellular organization.

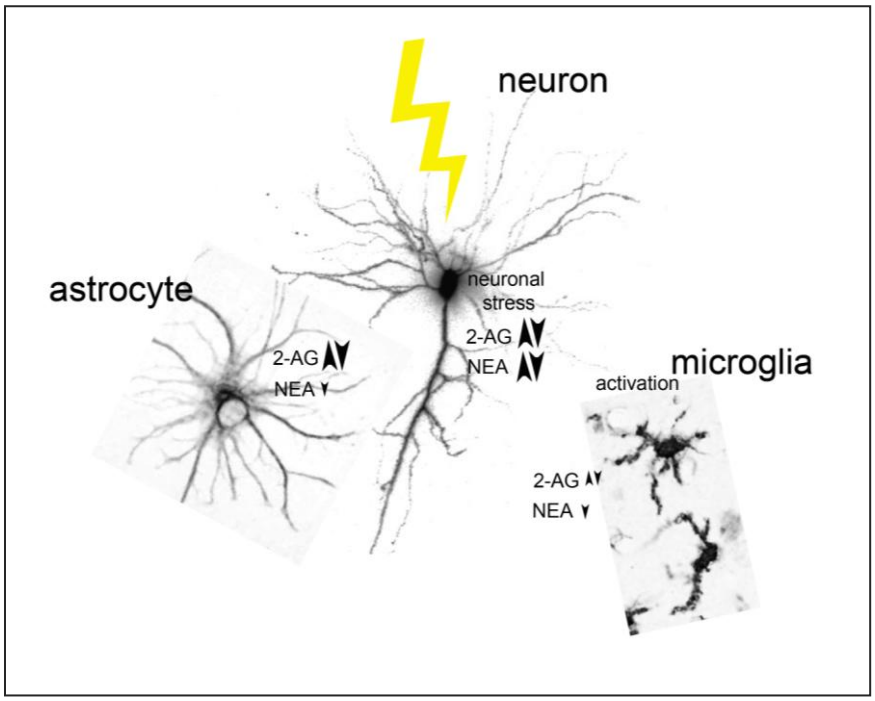

Figure 4.2 Schematic drawing of the endocannabinoid regulation in different cellular populations

Schematic drawing of neurons and glial cells and their potential of eCB regulation after neuronal damage. Neurons, astrocytes and microglia are potent to regulate 2-AG. NEA are regulated by neurons. Glial cells have the capacity to break down NEA. (arrows indicate the degree of potention)

4.7 GPR55 mediates neuroprotection in excitoxically lesioned OHSC through microglia

Besides CB_1 and CB_2, GPR55 has recently been identified to become activated by endocannabinoids and is now discussed as a potential cannabinoid receptor. GPR55 was cloned in 1999 and an in silico screening revealed a ligand-binding region in GPR55 very similar to that of CB_1/CB_2 (Henstridge, Balenga et al. 2010). It was suggested earlier that additional receptor subtypes than CB_1 and CB_2 belong to the targets of eCB and are associated with neuroprotection (Begg, Pacher et al. 2005). Recently, the GPR55 receptor is discussed as a novel CB receptor subtype (Stella 2010). Endocannabinoids activate the CB_1/CB_2 but also the transient receptor potential vanilloid-1 (TRPV1) and yet unknown receptors. The cluster ”endocannabinoids” might therefore be only a superficial categorisation and sometimes even misleading. Lipid signaling network is much more complex and reflects often a broader interaction than the present nomenclature indicates. Therefore, it might be misleading when substances and receptors are directed to one or the other system and provoke the impression that the different systems do not highly interact with each other.

Acute and chronic CNS pathologies lead to intensive searches for drugs and targets that might reduce the detrimental outcome of CNS damage, especially of the secondary damage impact (Dumont, Okonkwo et al. 2001). ECB and the CB receptors are shown to mediate neuroprotection in excitotoxic neuronal damaged OHSC, likewise the GPR55 receptor ligand lysophosphatidylinositol (LPI) was applied to investigate the potency of GPR55 on neuroprotection. GPR55 besides eCB, is also a target of the phospholipid LPI, which has been identified as the best characterised agonist of GPR55, and the onewith the highest activation rate (Oka *et al.*, 2007). Together with the well studied glycerophospholipids and sphingolipids, LPI belongs to the group of lysophospholipids. In brain tissue, considerable levels of LPI (37.5 nmol/g tissue) are present; and GPR55 is expressed at high levels in the

central nervous system (Pineiro and Falasca 2012). Although GPR55 has been studied intensively and pharmacological evidence exists for being an additional cannabinoid receptor, LPI was used in the present model to identify the potential neuroprotective effect of GPR55. Interference with concomitant activation of CB_1/CB_2 by eCB was herewith prevented.

Less neuronal damage and fewer microglial cells were dose-dependently observed after LPI (0.1 nM - 10 µM) treatment. In an earlier study, LPI (10 µM) was observed to mediate neuroprotection in excitotoxic lesioned cultures of cerebellar granule cells and after cerebral ischemia in rats without knowing the specific receptor mediating this effect (Blondeau, Lauritzen et al. 2002). Using *Gpr55* siRNA, it was shown that GPR55 is one responsible receptor for the LPI induced neuroprotection in excitotoxically lesioned OHSC, as no neuronal protection and microglia accumulation could be observed in OHSC any longer.

However, LPI/GPR55 activation was only neuroprotective when applied for three days after excitotoxic damage was induced and lost its neuroprotective effect depending on temporal administration. No protective effect was seen after pre-treatment or simultaneously application of LPI during excitation. After prolonged administration of LPI thoughout the culture periode and the entire experiment, an even enhanced neuronal damage could be observed. It could be assumed that enhanced exposure to LPI decreases cellular sensitivity, disabling important protective mechanisms like calcium regulation mediated by GPR55. Endocannabinoids, phytocannabinoids and synthetic cannabinoids were shown to activate GPR55 in the nM as well as in the µM range when GPR55 was over-expressed in different cell lines (Sawzdargo, Nguyen et al. 1999; Baker, Pryce et al. 2006; Ryberg, Larsson et al. 2007; Pietr, Kozela et al. 2009; Ross 2009). This evidence led to the hypothesis that eCB might influence the effects of LPI/GPR55 but also might influence their own effectiveness. A very recent study suggests the interaction of GPR55 and CB_1, although this study was conducted with HEK cells over-expressing GPR55 and CB_1 (Kargl, Balenga et al. 2012).

AM281, a CB_1 antagonist and potential GPR55 agonist, was tested on excitotoxically lesioned OHSC. AM281 reduced the number of dead neurons independent of LPI administration and microglia were less reduced than compared to LPI treatment. Meanwhile the activity of AM281 is discussed in literature wheather it is a ligand at GPR55 or not, as studies were mostly conducted with transfected cell lines (Sharir and Abood 2010). WIN55 212-2, an approved CB_1 agonist in synergism with LPI enhanced the neuronal protection in OHSC, although microglia were not down-regulated. This suggests that CB_1 and GPR55 independently regulate neuroprotective mechanisms leading to favorable effects. The neuroprotective effect of LPI and the simultaneously decreased microglia, together with the recent finding of GPR55 in the mice microglia cell line BV-2 and in primary microglia (Pietr, Kozela et al. 2009), was followed by the investigation of the role of microglia in excitotoxically lesioned OHSC. Subsequently, the effect of LPI in microglia depleted OHSC on behalf of clodronate was investigated and counteracted the neuroprotective activation of GPR55 by LPI.

In regard to the decreased microglia number in OHSC as well as changes in receptor mRNA level the effect of LPI on migration of primary microglia was investigated. Interestingly, LPI reduced ATP and LPS induced migration, however, LPI was chemoattractive itself, showing migratory effects of LPI on primary microglia for the first time. Here it should be mentioned that the potency of LPS to attract microglia cannot be fully explained and opens a different field of investigation and considerations beyond the present work. Direct treatment of microglia with LPS however, was shown to enhance microglia migration (abd-el-Basset and Fedoroff 1995). Within the brain, microglia are defined as an indispensible player in both beneficial and detrimental inflammatory cascades that determine the final outcome in the context of brain diseases (Hanisch and Kettenmann 2007). Many studies support the idea that glial cells are crucially involved in secondary neuronal damage that follows to the initial

neuronal lesion (Sawada, Kondo et al. 1989; Moss and Bates 2001; Streit 2002). On the other hand, literature underlines as well that microglia exert neuroprotective effects after CNS lesions (Kohl, Dehghani et al. 2003; Simard, Soulet et al. 2006). Recent studies showed a broad range of evidence that LPI enhances proliferation of different cell types, especially demonstrated in cancer cell lines by various groups, summarised recently by Piñeiro et al. (2012). There, it was demonstrated that LPI has a role in migration and orientation of human breast cancer cells by GPR55 activation (Ford, Roelofs et al. 2010) and that LPI, together with GPR55, are involved in an autocrine loop regulating the proliferation of prostate and ovarian cancer cells (Pineiro, Maffucci et al. 2011). Also clinical evidence demonstrates that patients with ovarian cancer or peritoneal cancer had higher accumulated levels of LPI in blood and ascites than healthy controls (Xiao, Chen et al. 2000; Xiao, Schwartz et al. 2001; Xu, Xiao et al. 2001). However, it was recently shown that neutrophils migrate towards LPI and the more stable synthetic cannabinoid GPR55 agonist AM251 (Henstridge, Balenga et al. 2010; Balenga, Aflaki et al. 2011).

Another study showed an effect of LPI/GPR55 mediated Ca^{2+} regulation in endothelial cells (Waldeck-Weiermair, Zoratti et al. 2008; Bondarenko, Waldeck-Weiermair et al. 2010). Primary sensory neurons were observed to release intracellular calcium ($[Ca^{2+}]_i$) and to diminish their M-type potassium currents upon GPR55 activation (Lauckner, Jensen et al. 2008). Ca^{2+} mobilisation from intracellular stores and membrane hyperpolarisation were inhibited upon GPR55 antagonist supplementation (Falasca, Silletta et al. 1995). Further, in rat liver mitochondria, LPI regulated calcium transport, inducing both uptake and release of Ca^{2+} (Dalton, Hughes et al. 1984; Lenzen, Gorlich et al. 1989). Although it is not clarified yet, whether calcium dependent exocytosis is mediated by GRP55 (Ma, Yeo et al. 2010), it is hypothesised that this mechanism might partly be responsible for the here described neuroprotective effect of GPR55 activation by LPI. Ca^{2+} influx was regulated by LPI in

cerebellar granule neurons through store operated Ca^{2+} entry channels at the plasma membrane (Smani, Dominguez-Rodriguez et al. 2007). LPI-induced Ca^{2+} influx can be mediated through channels belonging to the transient receptor potential (TRP) family (Vanden Abeele, Zholos et al. 2006; Andersson, Nash et al. 2007; Monet, Gkika et al. 2009). The used amount of LPI in the present study as well as the cells used, seem to influence the Ca^{2+} mediated signal. Known from literature, LPI can exert various effects also on other membrane channels (Maingret, Patel et al. 2000; Patel, Lazdunski et al. 2001). In particular, TREK and TRAAK K^{+} channels become activated by LPI, which have an important regulatory role on the control of the membrane potential of neurons (Patel, Lazdunski et al. 2001).

However, further evidence is needed to clarify the downstream signaling of GPR55 and its neuroprotective mechanism but also whether it should become a cannabinoid receptor.

Conclusion

Taken together, the activation of the eCBS after neuronal damage by transection of long-range projections apparently provides a strong time-dependent and area confined signal for de novo synthesis of eCB, presumably to prevent or restrict neuronal damage. The present data underlines the importance of eCB in CNS pathologies and helped to identify a site-specific intrinsic regulation of eCB levels in long-range projection damage. The highly dynamic eCBS represents an endogenous protective system and might be involved in dendritic re-organisation in the CNS. The present results should be followed up by in vivo experiments to sustain the temporal regulation and determine optimal treatment possibilities. Other long range projections e.g. denervated neurons in the spinal cord should be considered as a source for eCB and their regulation after transection of long range somato-afferent projections and long range somato-efferent projections needs to be investigated.

Recently, GPR55 is discussed as potential CB_3. In the present study it could be shown that GPR55 mediated neuroprotection after excitotoxic lesion in OHSC. After microglia depletion the GPR55 ligand LPI lost its neuropotective property, suggesting a microglia dependent mechanism. Still, further research is needed to understand the role of GPR55 in neuronal protection and the present experiments should be sustained by *in vivo* studies.

References

abd-el-Basset, E. and S. Fedoroff (1995). "Effect of bacterial wall lipopolysaccharide (LPS) on morphology, motility, and cytoskeletal organization of microglia in cultures." J Neurosci Res **41**(2): 222-237.

Adamchik, Y., M. V. Frantseva, et al. (2000). "Methods to induce primary and secondary traumatic damage in organotypic hippocampal slice cultures." Brain Res Brain Res Protoc **5**(2): 153-158.

Adembri, C., A. Bechi, et al. (2004). "Erythropoietin attenuates post-traumatic injury in organotypic hippocampal slices." J Neurotrauma **21**(8): 1103-1112.

Aguado, T., K. Monory, et al. (2005). "The endocannabinoid system drives neural progenitor proliferation." FASEB J **19**(12): 1704-1706.

Amaral, D. G. (1978). "A Golgi study of cell types in the hilar region of the hippocampus in the rat." J Comp Neurol **182**(4 Pt 2): 851-914.

Amaral, D. G., N. Ishizuka, et al. (1990). "Neurons, numbers and the hippocampal network." Prog Brain Res **83**: 1-11.

Andersson, D. A., M. Nash, et al. (2007). "Modulation of the cold-activated channel TRPM8 by lysophospholipids and polyunsaturated fatty acids." J Neurosci **27**(12): 3347-3355.

Ashton, J. C., D. Friberg, et al. (2006). "Expression of the cannabinoid CB2 receptor in the rat cerebellum: an immunohistochemical study." Neurosci Lett **396**(2): 113-116.

Bab, I. and A. Zimmer (2008). "Cannabinoid receptors and the regulation of bone mass." Br J Pharmacol **153**(2): 182-188.

Baker, D., G. Pryce, et al. (2006). "In silico patent searching reveals a new cannabinoid receptor." Trends Pharmacol Sci **27**(1): 1-4.

Balenga, N. A., E. Aflaki, et al. (2011). "GPR55 regulates cannabinoid 2 receptor-mediated responses in human neutrophils." Cell Res **21**(10): 1452-1469.

Begg, M., P. Pacher, et al. (2005). "Evidence for novel cannabinoid receptors." Pharmacol Ther **106**(2): 133-145.

Beltramo, M., N. Bernardini, et al. (2006). "CB2 receptor-mediated antihyperalgesia: possible direct involvement of neural mechanisms." Eur J Neurosci **23**(6): 1530-1538.

Bishay, P., H. Schmidt, et al. (2010). "R-flurbiprofen reduces neuropathic pain in rodents by restoring endogenous cannabinoids." PLoS One **5**(5): e10628.

Bisogno, T., F. Berrendero, et al. (1999). "Brain regional distribution of endocannabinoids: implications for their biosynthesis and biological function." Biochem Biophys Res Commun **256**(2): 377-380.

Bisogno, T., L. De Petrocellis, et al. (2002). "Fatty acid amide hydrolase, an enzyme with many bioactive substrates. Possible therapeutic implications." Curr Pharm Des **8**(7): 533-547.

Bisogno, T., F. Howell, et al. (2003). "Cloning of the first sn1-DAG lipases points to the spatial and temporal regulation of endocannabinoid signaling in the brain." J Cell Biol **163**(3): 463-468.

Blankman, J. L., G. M. Simon, et al. (2007). "A comprehensive profile of brain enzymes that hydrolyze the endocannabinoid 2-arachidonoylglycerol." Chem Biol **14**(12): 1347-1356.

Blight, A. R. (1985). "Delayed demyelination and macrophage invasion: a candidate for secondary cell damage in spinal cord injury." Cent Nerv Syst Trauma **2**(4): 299-315.

Blondeau, N., I. Lauritzen, et al. (2002). "A potent protective role of lysophospholipids against global cerebral ischemia and glutamate excitotoxicity in neuronal cultures." J Cereb Blood Flow Metab **22**(7): 821-834.

Bondarenko, A., M. Waldeck-Weiermair, et al. (2010). "GPR55-dependent and -independent ion signalling in response to lysophosphatidylinositol in endothelial cells." Br J Pharmacol **161**(2): 308-320.

Bouaboula, M., C. Poinot-Chazel, et al. (1995). "Activation of mitogen-activated protein kinases by stimulation of the central cannabinoid receptor CB1." Biochem J **312 (Pt 2)**: 637-641.

Brewer, G. J., J. R. Torricelli, et al. (1993). "Optimized survival of hippocampal neurons in B27-supplemented Neurobasal, a new serum-free medium combination." J Neurosci Res **35**(5): 567-576.

Brown, A. J. (2007). "Novel cannabinoid receptors." Br J Pharmacol **152**(5): 567-575.
Brusco, A., P. Tagliaferro, et al. (2008). "Postsynaptic localization of CB2 cannabinoid receptors in the rat hippocampus." Synapse **62**(12): 944-949.
Cabral, G. A., E. S. Raborn, et al. (2008). "CB2 receptors in the brain: role in central immune function." Br J Pharmacol **153**(2): 240-251.
Carlisle, S. J., F. Marciano-Cabral, et al. (2002). "Differential expression of the CB2 cannabinoid receptor by rodent macrophages and macrophage-like cells in relation to cell activation." Int Immunopharmacol **2**(1): 69-82.
Carrier, E. J., C. S. Kearn, et al. (2004). "Cultured rat microglial cells synthesize the endocannabinoid 2-arachidonylglycerol, which increases proliferation via a CB2 receptor-dependent mechanism." Mol Pharmacol **65**(4): 999-1007.
Chan, L., J. Doctor, et al. (2001). "Discharge disposition from acute care after traumatic brain injury: the effect of insurance type." Arch Phys Med Rehabil **82**(9): 1151-1154.
Chanda, P. K., Y. Gao, et al. (2010). "Monoacylglycerol lipase activity is a critical modulator of the tone and integrity of the endocannabinoid system." Mol Pharmacol **78**(6): 996-1003.
Chicca, A., J. Marazzi, et al. (2012). "Evidence for bidirectional endocannabinoid transport across cell membranes." J Biol Chem **287**(41): 34660-34682.
Choi, D. W., J. Y. Koh, et al. (1988). "Pharmacology of glutamate neurotoxicity in cortical cell culture: attenuation by NMDA antagonists." J Neurosci **8**(1): 185-196.
Clague, M. J. and S. Urbe (2010). "Ubiquitin: same molecule, different degradation pathways." Cell **143**(5): 682-685.
Coffey, P. J., V. H. Perry, et al. (1990). "An investigation into the early stages of the inflammatory response following ibotenic acid-induced neuronal degeneration." Neuroscience **35**(1): 121-132.
Conti, S., B. Costa, et al. (2002). "Antiinflammatory action of endocannabinoid palmitoylethanolamide and the synthetic cannabinoid nabilone in a model of acute inflammation in the rat." Br J Pharmacol **135**(1): 181-187.
Coulter, D. A., C. Yue, et al. (2011). "Hippocampal microcircuit dynamics probed using optical imaging approaches." J Physiol **589**(Pt 8): 1893-1903.
Cravatt, B. F., D. K. Giang, et al. (1996). "Molecular characterization of an enzyme that degrades neuromodulatory fatty-acid amides." Nature **384**(6604): 83-87.
Dalton, S., B. P. Hughes, et al. (1984). "Effects of lysophospholipids on Ca2+ transport in rat liver mitochondria incubated at physiological Ca2+ concentrations in the presence of Mg2+, phosphate and ATP at 37 degrees C." Biochem J **224**(2): 423-430.
De Petrocellis, L., C. J. Chu, et al. (2004). "Actions of two naturally occurring saturated N-acyldopamines on transient receptor potential vanilloid 1 (TRPV1) channels." Br J Pharmacol **143**(2): 251-256.
De Petrocellis, L., J. B. Davis, et al. (2001). "Palmitoylethanolamide enhances anandamide stimulation of human vanilloid VR1 receptors." FEBS Lett **506**(3): 253-256.
Degn, M., K. L. Lambertsen, et al. (2007). "Changes in brain levels of N-acylethanolamines and 2-arachidonoylglycerol in focal cerebral ischemia in mice." J Neurochem **103**(5): 1907-1916.
Deller, T. (1997). "The anatomy of the rat fascia dentata--new vistas." Ann Anat **179**(6): 501-504.
Devane, W. A., L. Hanus, et al. (1992). "Isolation and structure of a brain constituent that binds to the cannabinoid receptor." Science **258**(5090): 1946-1949.
Di Marzo, V., A. Fontana, et al. (1994). "Formation and inactivation of endogenous cannabinoid anandamide in central neurons." Nature **372**(6507): 686-691.
Diekmann, S., T. G. Ohm, et al. (1996). "Long-lasting transneuronal changes in rat dentate granule cell dendrites after entorhinal cortex lesion. A combined intracellular injection and electron microscopy study." Brain Pathol **6**(3): 205-214; discussion 214-205.
Dinh, T. P., D. Carpenter, et al. (2002). "Brain monoglyceride lipase participating in endocannabinoid inactivation." Proc Natl Acad Sci U S A **99**(16): 10819-10824.

Dittel, B. N. (2008). "Direct suppression of autoreactive lymphocytes in the central nervous system via the CB2 receptor." Br J Pharmacol **153**(2): 271-276.
Dommergues, M. A., F. Plaisant, et al. (2003). "Early microglial activation following neonatal excitotoxic brain damage in mice: a potential target for neuroprotection." Neuroscience **121**(3): 619-628.
Dumont, R. J., D. O. Okonkwo, et al. (2001). "Acute spinal cord injury, part I: pathophysiologic mechanisms." Clin Neuropharmacol **24**(5): 254-264.
Eljaschewitsch, E., A. Witting, et al. (2006). "The endocannabinoid anandamide protects neurons during CNS inflammation by induction of MKP-1 in microglial cells." Neuron **49**(1): 67-79.
Facchinetti, F., E. Del Giudice, et al. (2003). "Cannabinoids ablate release of TNFalpha in rat microglial cells stimulated with lypopolysaccharide." Glia **41**(2): 161-168.
Faden, A. I. and B. Stoica (2007). "Neuroprotection: challenges and opportunities." Arch Neurol **64**(6): 794-800.
Falasca, M. and D. Corda (1994). "Elevated levels and mitogenic activity of lysophosphatidylinositol in k-ras-transformed epithelial cells." Eur J Biochem **221**(1): 383-389.
Falasca, M., M. G. Silletta, et al. (1995). "Signalling pathways involved in the mitogenic action of lysophosphatidylinositol." Oncogene **10**(11): 2113-2124.
Fernandez-Ruiz, J., M. R. Pazos, et al. (2008). "Role of CB2 receptors in neuroprotective effects of cannabinoids." Mol Cell Endocrinol **286**(1-2 Suppl 1): S91-96.
Fiskerstrand, T., D. H'Mida-Ben Brahim, et al. (2010). "Mutations in ABHD12 cause the neurodegenerative disease PHARC: An inborn error of endocannabinoid metabolism." Am J Hum Genet **87**(3): 410-417.
Ford, L. A., A. J. Roelofs, et al. (2010). "A role for L-alpha-lysophosphatidylinositol and GPR55 in the modulation of migration, orientation and polarization of human breast cancer cells." Br J Pharmacol **160**(3): 762-771.
Forster, E., S. Zhao, et al. (2006). "Laminating the hippocampus." Nat Rev Neurosci **7**(4): 259-267.
Fowler, C. J. (2012). "Anandamide uptake explained?" Trends Pharmacol Sci **33**(4): 181-185.
Fowler, C. J., M. L. Rojo, et al. (2010). "Modulation of the endocannabinoid system: neuroprotection or neurotoxicity?" Exp Neurol **224**(1): 37-47.
Frankhauser, M. (2002). "[Haskish as medication; on the significance of cannabis sativa in western medicine]." Veroff Schweiz Ges Gesch Pharm **23**: 1-329.
Franklin, A., S. Parmentier-Batteur, et al. (2003). "Palmitoylethanolamide increases after focal cerebral ischemia and potentiates microglial cell motility." J Neurosci **23**(21): 7767-7775.
Frotscher, M., B. Heimrich, et al. (1997). "Sprouting in the hippocampus is layer-specific." Trends Neurosci **20**(5): 218-223.
Fu, J., S. Gaetani, et al. (2003). "Oleylethanolamide regulates feeding and body weight through activation of the nuclear receptor PPAR-alpha." Nature **425**(6953): 90-93.
Gahwiler, B. H., M. Capogna, et al. (1997). "Organotypic slice cultures: a technique has come of age." Trends Neurosci **20**(10): 471-477.
Galan-Rodriguez, B., J. Suarez, et al. (2009). "Oleoylethanolamide exerts partial and dose-dependent neuroprotection of substantia nigra dopamine neurons." Neuropharmacology **56**(3): 653-664.
Galiegue, S., S. Mary, et al. (1995). "Expression of central and peripheral cannabinoid receptors in human immune tissues and leukocyte subpopulations." Eur J Biochem **232**(1): 54-61.
Gallily, R., A. Breuer, et al. (2000). "2-Arachidonylglycerol, an endogenous cannabinoid, inhibits tumor necrosis factor-alpha production in murine macrophages, and in mice." Eur J Pharmacol **406**(1): R5-7.
Gao, Y., D. V. Vasilyev, et al. (2010). "Loss of retrograde endocannabinoid signaling and reduced adult neurogenesis in diacylglycerol lipase knock-out mice." J Neurosci **30**(6): 2017-2024.
Garcia-Ovejero, D., A. Arevalo-Martin, et al. (2009). "The endocannabinoid system is modulated in response to spinal cord injury in rats." Neurobiol Dis **33**(1): 57-71.

Ghafouri, N., G. Tiger, et al. (2004). "Inhibition of monoacylglycerol lipase and fatty acid amide hydrolase by analogues of 2-arachidonoylglycerol." Br J Pharmacol **143**(6): 774-784.
Giuffrida, A., L. H. Parsons, et al. (1999). "Dopamine activation of endogenous cannabinoid signaling in dorsal striatum." Nat Neurosci **2**(4): 358-363.
Gomez, O., A. Arevalo-Martin, et al. (2010). "The constitutive production of the endocannabinoid 2-arachidonoylglycerol participates in oligodendrocyte differentiation." Glia **58**(16): 1913-1927.
Goncalves, M. B., P. Suetterlin, et al. (2008). "A diacylglycerol lipase-CB2 cannabinoid pathway regulates adult subventricular zone neurogenesis in an age-dependent manner." Mol Cell Neurosci **38**(4): 526-536.
Gong, J. P., E. S. Onaivi, et al. (2006). "Cannabinoid CB2 receptors: immunohistochemical localization in rat brain." Brain Res **1071**(1): 10-23.
Gopez, J. J., H. Yue, et al. (2005). "Cyclooxygenase-2-specific inhibitor improves functional outcomes, provides neuroprotection, and reduces inflammation in a rat model of traumatic brain injury." Neurosurgery **56**(3): 590-604.
Grabiec, U., M. Koch, et al. (2011). "The endocannabinoid N-arachidonoyldopamine (NADA) exerts neuroprotective effects after excitotoxic neuronal damage via cannabinoid receptor 1 (CB(1))." Neuropharmacology.
Hailer, N. P., F. Wirjatijasa, et al. (2001). "Astrocytic factors protect neuronal integrity and reduce microglial activation in an in vitro model of N-methyl-D-aspartate-induced excitotoxic injury in organotypic hippocampal slice cultures." Eur J Neurosci **14**(2): 315-326.
Hanisch, U. K. and H. Kettenmann (2007). "Microglia: active sensor and versatile effector cells in the normal and pathologic brain." Nat Neurosci **10**(11): 1387-1394.
Hansen, H. H., P. C. Schmid, et al. (2001). "Anandamide, but not 2-arachidonoylglycerol, accumulates during in vivo neurodegeneration." J Neurochem **78**(6): 1415-1427.
Hansen, H. S. (2010). "Palmitoylethanolamide and other anandamide congeners. Proposed role in the diseased brain." Exp Neurol **224**(1): 48-55.
Harkany, T., M. Guzman, et al. (2007). "The emerging functions of endocannabinoid signaling during CNS development." Trends Pharmacol Sci **28**(2): 83-92.
Henstridge, C. M., N. A. Balenga, et al. (2010). "GPR55 ligands promote receptor coupling to multiple signalling pathways." Br J Pharmacol **160**(3): 604-614.
Herkenham, M., A. B. Lynn, et al. (1991). "Characterization and localization of cannabinoid receptors in rat brain: a quantitative in vitro autoradiographic study." J Neurosci **11**(2): 563-583.
Hill, M. N., J. S. Kambo, et al. (2006). "Endocannabinoids modulate stress-induced suppression of hippocampal cell proliferation and activation of defensive behaviours." Eur J Neurosci **24**(7): 1845-1849.
Hillard, C. J. (2000). "Biochemistry and pharmacology of the endocannabinoids arachidonylethanolamide and 2-arachidonylglycerol." Prostaglandins Other Lipid Mediat **61**(1-2): 3-18.
Hillard, C. J. (2000). "Endocannabinoids and vascular function." J Pharmacol Exp Ther **294**(1): 27-32.
Hohmann, A. G. (2002). "Spinal and peripheral mechanisms of cannabinoid antinociception: behavioral, neurophysiological and neuroanatomical perspectives." Chem Phys Lipids **121**(1-2): 173-190.
Holopainen, I. E. (2005). "Organotypic hippocampal slice cultures: a model system to study basic cellular and molecular mechanisms of neuronal cell death, neuroprotection, and synaptic plasticity." Neurochem Res **30**(12): 1521-1528.
Holopainen, I. E., H. B. Lauren, et al. (2001). "Changes in neurofilament protein-immunoreactivity after kainic acid treatment of organotypic hippocampal slice cultures." J Neurosci Res **66**(4): 620-629.
Howlett, A. C. (1998). "The CB1 cannabinoid receptor in the brain." Neurobiol Dis **5**(6 Pt B): 405-416.
Howlett, A. C. (2002). "The cannabinoid receptors." Prostaglandins Other Lipid Mediat **68-69**: 619-631.
Howlett, A. C. (2005). "Cannabinoid receptor signaling." Handb Exp Pharmacol(168): 53-79.

Ide, C. F., J. L. Scripter, et al. (1996). "Cellular and molecular correlates to plasticity during recovery from injury in the developing mammalian brain." Prog Brain Res **108**: 365-377.
Jarai, Z., J. A. Wagner, et al. (1999). "Cannabinoid-induced mesenteric vasodilation through an endothelial site distinct from CB1 or CB2 receptors." Proc Natl Acad Sci U S A **96**(24): 14136-14141.
Jarbe, T. U., C. Li, et al. (2010). "Discriminative stimulus functions of methanandamide and delta(9)-THC in rats: tests with aminoalkylindoles (WIN55,212-2 and AM678) and ethanol." Psychopharmacology (Berl) **208**(1): 87-98.
Jiang, W., Y. Zhang, et al. (2005). "Cannabinoids promote embryonic and adult hippocampus neurogenesis and produce anxiolytic- and antidepressant-like effects." J Clin Invest **115**(11): 3104-3116.
Jin, K. L., X. O. Mao, et al. (2000). "CB1 cannabinoid receptor induction in experimental stroke." Ann Neurol **48**(2): 257-261.
Johns, D. G., D. J. Behm, et al. (2007). "The novel endocannabinoid receptor GPR55 is activated by atypical cannabinoids but does not mediate their vasodilator effects." Br J Pharmacol **152**(5): 825-831.
Jung, J., S. W. Hwang, et al. (1999). "Capsaicin binds to the intracellular domain of the capsaicin-activated ion channel." J Neurosci **19**(2): 529-538.
Kargl, J., N. Balenga, et al. (2012). "The Cannabinoid Receptor CB1 Modulates the Signaling Properties of the Lysophosphatidylinositol Receptor GPR55." J Biol Chem **287**(53): 44234-44248.
Karlsson, M., K. Reue, et al. (2001). "Exon-intron organization and chromosomal localization of the mouse monoglyceride lipase gene." Gene **272**(1-2): 11-18.
Kathuria, S., S. Gaetani, et al. (2003). "Modulation of anxiety through blockade of anandamide hydrolysis." Nat Med **9**(1): 76-81.
Katona, I. and T. F. Freund (2008). "Endocannabinoid signaling as a synaptic circuit breaker in neurological disease." Nat Med **14**(9): 923-930.
Katona, I., B. Sperlagh, et al. (1999). "Presynaptically located CB1 cannabinoid receptors regulate GABA release from axon terminals of specific hippocampal interneurons." J Neurosci **19**(11): 4544-4558.
Katona, I., G. M. Urban, et al. (2006). "Molecular composition of the endocannabinoid system at glutamatergic synapses." Journal of Neuroscience **26**(21): 5628-5637.
Katona, I., G. M. Urban, et al. (2006). "Molecular composition of the endocannabinoid system at glutamatergic synapses." J Neurosci **26**(21): 5628-5637.
Kishimoto, S., M. Gokoh, et al. (2003). "2-arachidonoylglycerol induces the migration of HL-60 cells differentiated into macrophage-like cells and human peripheral blood monocytes through the cannabinoid CB2 receptor-dependent mechanism." J Biol Chem **278**(27): 24469-24475.
Klein, T. W. (2005). "Cannabinoid-based drugs as anti-inflammatory therapeutics." Nat Rev Immunol **5**(5): 400-411.
Koch, M., S. Kreutz, et al. (2011). "Palmitoylethanolamide protects dentate gyrus granule cells via peroxisome proliferator-activated receptor-alpha." Neurotox Res **19**(2): 330-340.
Koch, M., S. Kreutz, et al. (2011). "The cannabinoid WIN 55,212-2-mediated protection of dentate gyrus granule cells is driven by CB1 receptors and modulated by TRPA1 and Ca(v) 2.2 channels." Hippocampus **21**(5): 554-564.
Kohl, A., F. Dehghani, et al. (2003). "The bisphosphonate clodronate depletes microglial cells in excitotoxically injured organotypic hippocampal slice cultures." Exp Neurol **181**(1): 1-11.
Kovac, A. D., E. Kwidzinski, et al. (2004). "Entorhinal cortex lesion in the mouse induces transsynaptic death of perforant path target neurons." Brain Pathol **14**(3): 249-257.
Kozak, K. R., S. W. Rowlinson, et al. (2000). "Oxygenation of the endocannabinoid, 2-arachidonylglycerol, to glyceryl prostaglandins by cyclooxygenase-2." J Biol Chem **275**(43): 33744-33749.

Kreutz, S., M. Koch, et al. (2009). "2-Arachidonoylglycerol elicits neuroprotective effects on excitotoxically lesioned dentate gyrus granule cells via abnormal-cannabidiol-sensitive receptors on microglial cells." Glia **57**(3): 286-294.
Kristensen, B. W., J. Noraberg, et al. (2001). "Comparison of excitotoxic profiles of ATPA, AMPA, KA and NMDA in organotypic hippocampal slice cultures." Brain Res **917**(1): 21-44.
Kunkler, P. E. and R. P. Kraig (1997). "Reactive astrocytosis from excitotoxic injury in hippocampal organ culture parallels that seen in vivo." J Cereb Blood Flow Metab **17**(1): 26-43.
Kurihara, R., Y. Tohyama, et al. (2006). "Effects of peripheral cannabinoid receptor ligands on motility and polarization in neutrophil-like HL60 cells and human neutrophils." J Biol Chem **281**(18): 12908-12918.
Lauckner, J. E., J. B. Jensen, et al. (2008). "GPR55 is a cannabinoid receptor that increases intracellular calcium and inhibits M current." Proc Natl Acad Sci U S A **105**(7): 2699-2704.
Lenzen, S., J. K. Gorlich, et al. (1989). "Regulation of transmembrane ion transport by reaction products of phospholipase A2. I. Effects of lysophospholipids on mitochondrial Ca2+ transport." Biochim Biophys Acta **982**(1): 140-146.
Leung, D., A. Saghatelian, et al. (2006). "Inactivation of N-acyl phosphatidylethanolamine phospholipase D reveals multiple mechanisms for the biosynthesis of endocannabinoids." Biochemistry **45**(15): 4720-4726.
Lever, I. J., M. Robinson, et al. (2009). "Localization of the endocannabinoid-degrading enzyme fatty acid amide hydrolase in rat dorsal root ganglion cells and its regulation after peripheral nerve injury." J Neurosci **29**(12): 3766-3780.
Lichtman, A. H., E. G. Hawkins, et al. (2002). "Pharmacological activity of fatty acid amides is regulated, but not mediated, by fatty acid amide hydrolase in vivo." J Pharmacol Exp Ther **302**(1): 73-79.
Liu, J., B. Gao, et al. (2000). "Functional CB1 cannabinoid receptors in human vascular endothelial cells." Biochem J **346 Pt 3**: 835-840.
Lo Verme, J., J. Fu, et al. (2005). "The nuclear receptor peroxisome proliferator-activated receptor-alpha mediates the anti-inflammatory actions of palmitoylethanolamide." Mol Pharmacol **67**(1): 15-19.
Lothman, E. W., E. H. Bertram, 3rd, et al. (1991). "Functional anatomy of hippocampal seizures." Prog Neurobiol **37**(1): 1-82.
Ludanyi, A., S. S. Hu, et al. (2011). "Complementary synaptic distribution of enzymes responsible for synthesis and inactivation of the endocannabinoid 2-arachidonoylglycerol in the human hippocampus." Neuroscience **174**: 50-63.
Lutz, B. (2002). "Molecular biology of cannabinoid receptors." Prostaglandins Leukot Essent Fatty Acids **66**(2-3): 123-142.
Ma, M. T., J. F. Yeo, et al. (2010). "Differential effects of lysophospholipids on exocytosis in rat PC12 cells." J Neural Transm **117**(3): 301-308.
Maccarrone, M., P. Gubellini, et al. (2003). "Levodopa treatment reverses endocannabinoid system abnormalities in experimental parkinsonism." J Neurochem **85**(4): 1018-1025.
Maccarrone, M., S. Piccirilli, et al. (2004). "Enhanced anandamide degradation is associated with neuronal apoptosis induced by the HIV-1 coat glycoprotein gp120 in the rat neocortex." J Neurochem **89**(5): 1293-1300.
Mackie, K. (2006). "Cannabinoid receptors as therapeutic targets." Annu Rev Pharmacol Toxicol **46**: 101-122.
Mackie, K. and N. Stella (2006). "Cannabinoid receptors and endocannabinoids: evidence for new players." AAPS J **8**(2): E298-306.
Maestroni, G. J. (2004). "The endogenous cannabinoid 2-arachidonoyl glycerol as in vivo chemoattractant for dendritic cells and adjuvant for Th1 response to a soluble protein." FASEB J **18**(15): 1914-1916.
Maingret, F., A. J. Patel, et al. (2000). "Lysophospholipids open the two-pore domain mechano-gated K(+) channels TREK-1 and TRAAK." J Biol Chem **275**(14): 10128-10133.

Maresz, K., G. Pryce, et al. (2007). "Direct suppression of CNS autoimmune inflammation via the cannabinoid receptor CB1 on neurons and CB2 on autoreactive T cells." Nat Med **13**(4): 492-497.
Marsicano, G., S. Goodenough, et al. (2003). "CB1 cannabinoid receptors and on-demand defense against excitotoxicity." Science **302**(5642): 84-88.
Marsicano, G., B. Moosmann, et al. (2002). "Neuroprotective properties of cannabinoids against oxidative stress: role of the cannabinoid receptor CB1." J Neurochem **80**(3): 448-456.
Matsuda, L. A., S. J. Lolait, et al. (1990). "Structure of a cannabinoid receptor and functional expression of the cloned cDNA." Nature **346**(6284): 561-564.
McHugh, D., J. Page, et al. (2012). "Delta(9) -Tetrahydrocannabinol and N-arachidonyl glycine are full agonists at GPR18 receptors and induce migration in human endometrial HEC-1B cells." Br J Pharmacol **165**(8): 2414-2424.
McPartland, J. M., R. W. Norris, et al. (2007). "Coevolution between cannabinoid receptors and endocannabinoid ligands." Gene **397**(1-2): 126-135.
Mechoulam, R., S. Ben-Shabat, et al. (1995). "Identification of an endogenous 2-monoglyceride, present in canine gut, that binds to cannabinoid receptors." Biochem Pharmacol **50**(1): 83-90.
Milton, N. G. (2002). "Anandamide and noladin ether prevent neurotoxicity of the human amyloid-beta peptide." Neurosci Lett **332**(2): 127-130.
Monet, M., D. Gkika, et al. (2009). "Lysophospholipids stimulate prostate cancer cell migration via TRPV2 channel activation." Biochim Biophys Acta **1793**(3): 528-539.
Morozov, Y. M. and T. F. Freund (2003). "Post-natal development of type 1 cannabinoid receptor immunoreactivity in the rat hippocampus." Eur J Neurosci **18**(5): 1213-1222.
Moss, D. W. and T. E. Bates (2001). "Activation of murine microglial cell lines by lipopolysaccharide and interferon-gamma causes NO-mediated decreases in mitochondrial and cellular function." Eur J Neurosci **13**(3): 529-538.
Munro, S., K. L. Thomas, et al. (1993). "Molecular characterization of a peripheral receptor for cannabinoids." Nature **365**(6441): 61-65.
Navarrete, M. and A. Araque (2008). "Endocannabinoids mediate neuron-astrocyte communication." Neuron **57**(6): 883-893.
Nunez, E., C. Benito, et al. (2004). "Cannabinoid CB2 receptors are expressed by perivascular microglial cells in the human brain: an immunohistochemical study." Synapse **53**(4): 208-213.
Nunez, E., C. Benito, et al. (2008). "Glial expression of cannabinoid CB(2) receptors and fatty acid amide hydrolase are beta amyloid-linked events in Down's syndrome." Neuroscience **151**(1): 104-110.
Nyilas, R., B. Dudok, et al. (2008). "Enzymatic machinery for endocannabinoid biosynthesis associated with calcium stores in glutamatergic axon terminals." J Neurosci **28**(5): 1058-1063.
Obara, Y., S. Ueno, et al. (2011). "Lysophosphatidylinositol causes neurite retraction via GPR55, G13 and RhoA in PC12 cells." PLoS One **6**(8): e24284.
Oka, S., K. Nakajima, et al. (2007). "Identification of GPR55 as a lysophosphatidylinositol receptor." Biochem Biophys Res Commun **362**(4): 928-934.
Okamoto, Y., J. Morishita, et al. (2004). "Molecular characterization of a phospholipase D generating anandamide and its congeners." J Biol Chem **279**(7): 5298-5305.
Onaivi, E. S. (2009). "Cannabinoid receptors in brain: pharmacogenetics, neuropharmacology, neurotoxicology, and potential therapeutic applications." Int Rev Neurobiol **88**: 335-369.
Pacher, P., S. Batkai, et al. (2006). "The endocannabinoid system as an emerging target of pharmacotherapy." Pharmacol Rev **58**(3): 389-462.
Pagotto, U., G. Marsicano, et al. (2006). "The emerging role of the endocannabinoid system in endocrine regulation and energy balance." Endocr Rev **27**(1): 73-100.
Pan, B., W. Wang, et al. (2011). "Alterations of endocannabinoid signaling, synaptic plasticity, learning, and memory in monoacylglycerol lipase knock-out mice." J Neurosci **31**(38): 13420-13430.

Panikashvili, D., R. Mechoulam, et al. (2005). "CB1 cannabinoid receptors are involved in neuroprotection via NF-kappa B inhibition." J Cereb Blood Flow Metab **25**(4): 477-484.
Panikashvili, D., N. A. Shein, et al. (2006). "The endocannabinoid 2-AG protects the blood-brain barrier after closed head injury and inhibits mRNA expression of proinflammatory cytokines." Neurobiol Dis **22**(2): 257-264.
Panikashvili, D., C. Simeonidou, et al. (2001). "An endogenous cannabinoid (2-AG) is neuroprotective after brain injury." Nature **413**(6855): 527-531.
Patel, A. J., M. Lazdunski, et al. (2001). "Lipid and mechano-gated 2P domain K(+) channels." Curr Opin Cell Biol **13**(4): 422-428.
Pertwee, R. G. (1997). "Pharmacology of cannabinoid CB1 and CB2 receptors." Pharmacol Ther **74**(2): 129-180.
Pertwee, R. G. (2008). "Ligands that target cannabinoid receptors in the brain: from THC to anandamide and beyond." Addict Biol **13**(2): 147-159.
Pertwee, R. G. (2010). "Receptors and channels targeted by synthetic cannabinoid receptor agonists and antagonists." Curr Med Chem **17**(14): 1360-1381.
Pertwee, R. G., A. C. Howlett, et al. (2010). "International Union of Basic and Clinical Pharmacology. LXXIX. Cannabinoid receptors and their ligands: beyond CB and CB." Pharmacol Rev **62**(4): 588-631.
Pertwee, R. G. and R. A. Ross (2002). "Cannabinoid receptors and their ligands." Prostaglandins Leukot Essent Fatty Acids **66**(2-3): 101-121.
Peterfi, Z., G. M. Urban, et al. (2012). "Endocannabinoid-mediated long-term depression of afferent excitatory synapses in hippocampal pyramidal cells and GABAergic interneurons." J Neurosci **32**(41): 14448-14463.
Petitet, F., M. Donlan, et al. (2006). "GPR55 as a new cannabinoid receptor: still a long way to prove it." Chem Biol Drug Des **67**(3): 252-253.
Pietr, M., E. Kozela, et al. (2009). "Differential changes in GPR55 during microglial cell activation." FEBS Lett **583**(12): 2071-2076.
Pineiro, R. and M. Falasca (2012). "Lysophosphatidylinositol signalling: New wine from an old bottle." Biochim Biophys Acta **1821**(4): 694-705.
Pineiro, R., T. Maffucci, et al. (2011). "The putative cannabinoid receptor GPR55 defines a novel autocrine loop in cancer cell proliferation." Oncogene **30**(2): 142-152.
Piomelli, D. (2003). "The molecular logic of endocannabinoid signalling." Nat Rev Neurosci **4**(11): 873-884.
Piomelli, D., M. Beltramo, et al. (1998). "Endogenous cannabinoid signaling." Neurobiol Dis **5**(6 Pt B): 462-473.
Pisani, A., F. Fezza, et al. (2005). "High endogenous cannabinoid levels in the cerebrospinal fluid of untreated Parkinson's disease patients." Ann Neurol **57**(5): 777-779.
Ramirez, B. G., C. Blazquez, et al. (2005). "Prevention of Alzheimer's disease pathology by cannabinoids: neuroprotection mediated by blockade of microglial activation." J Neurosci **25**(8): 1904-1913.
Ramirez, J. J. (2001). "The role of axonal sprouting in functional reorganization after CNS injury: lessons from the hippocampal formation." Restor Neurol Neurosci **19**(3-4): 237-262.
Raso, G. M., E. Esposito, et al. (2011). "Palmitoylethanolamide stimulation induces allopregnanolone synthesis in C6 Cells and primary astrocytes: involvement of peroxisome-proliferator activated receptor-alpha." J Neuroendocrinol **23**(7): 591-600.
Rodriguez De Fonseca, F., M. A. Gorriti, et al. (2001). "Role of the endogenous cannabinoid system as a modulator of dopamine transmission: implications for Parkinson's disease and schizophrenia." Neurotox Res **3**(1): 23-35.
Romero-Zerbo, S. Y., A. Rafacho, et al. (2011). "A role for the putative cannabinoid receptor GPR55 in the islets of Langerhans." J Endocrinol **211**(2): 177-185.
Ross, R. A. (2009). "The enigmatic pharmacology of GPR55." Trends Pharmacol Sci **30**(3): 156-163.

Ryberg, E., N. Larsson, et al. (2007). "The orphan receptor GPR55 is a novel cannabinoid receptor." Br J Pharmacol **152**(7): 1092-1101.
Salio, C., S. Doly, et al. (2002). "Neuronal and astrocytic localization of the cannabinoid receptor-1 in the dorsal horn of the rat spinal cord." Neurosci Lett **329**(1): 13-16.
Savinainen, J. R., T. Jarvinen, et al. (2001). "Despite substantial degradation, 2-arachidonoylglycerol is a potent full efficacy agonist mediating CB(1) receptor-dependent G-protein activation in rat cerebellar membranes." Br J Pharmacol **134**(3): 664-672.
Savinainen, J. R., S. M. Saario, et al. (2012). "The serine hydrolases MAGL, ABHD6 and ABHD12 as guardians of 2-arachidonoylglycerol signalling through cannabinoid receptors." Acta Physiol (Oxf) **204**(2): 267-276.
Sawada, M., N. Kondo, et al. (1989). "Production of tumor necrosis factor-alpha by microglia and astrocytes in culture." Brain Res **491**(2): 394-397.
Sawzdargo, M., T. Nguyen, et al. (1999). "Identification and cloning of three novel human G protein-coupled receptor genes GPR52, PsiGPR53 and GPR55: GPR55 is extensively expressed in human brain." Brain Res Mol Brain Res **64**(2): 193-198.
Schabitz, W. R., A. Giuffrida, et al. (2002). "Release of fatty acid amides in a patient with hemispheric stroke: a microdialysis study." Stroke **33**(8): 2112-2114.
Schafer, D. P., E. K. Lehrman, et al. (2012). "Microglia sculpt postnatal neural circuits in an activity and complement-dependent manner." Neuron **74**(4): 691-705.
Schlosburg, J. E., J. L. Blankman, et al. (2010). "Chronic monoacylglycerol lipase blockade causes functional antagonism of the endocannabinoid system." Nat Neurosci **13**(9): 1113-1119.
Sharir, H. and M. E. Abood (2010). "Pharmacological characterization of GPR55, a putative cannabinoid receptor." Pharmacol Ther **126**(3): 301-313.
Shire, D., B. Calandra, et al. (1996). "Structural features of the central cannabinoid CB1 receptor involved in the binding of the specific CB1 antagonist SR 141716A." J Biol Chem **271**(12): 6941-6946.
Shohami, E., A. Cohen-Yeshurun, et al. (2011). "Endocannabinoids and traumatic brain injury." Br J Pharmacol **163**(7): 1402-1410.
Shohami, E., I. Ginis, et al. (1999). "Dual role of tumor necrosis factor alpha in brain injury." Cytokine Growth Factor Rev **10**(2): 119-130.
Signoretti, S., R. Vagnozzi, et al. (2010). "Biochemical and neurochemical sequelae following mild traumatic brain injury: summary of experimental data and clinical implications." Neurosurg Focus **29**(5): E1.
Simard, A. R., D. Soulet, et al. (2006). "Bone marrow-derived microglia play a critical role in restricting senile plaque formation in Alzheimer's disease." Neuron **49**(4): 489-502.
Simon, G. M. and B. F. Cravatt (2008). "Anandamide biosynthesis catalyzed by the phosphodiesterase GDE1 and detection of glycerophospho-N-acyl ethanolamine precursors in mouse brain." J Biol Chem **283**(14): 9341-9349.
Sinor, A. D., S. M. Irvin, et al. (2000). "Endocannabinoids protect cerebral cortical neurons from in vitro ischemia in rats." Neurosci Lett **278**(3): 157-160.
Smani, T., A. Dominguez-Rodriguez, et al. (2007). "Role of Ca2+-independent phospholipase A2 and store-operated pathway in urocortin-induced vasodilatation of rat coronary artery." Circ Res **101**(11): 1194-1203.
Smart, D., M. J. Gunthorpe, et al. (2000). "The endogenous lipid anandamide is a full agonist at the human vanilloid receptor (hVR1)." Br J Pharmacol **129**(2): 227-230.
Solorzano, C., C. Zhu, et al. (2009). "Selective N-acylethanolamine-hydrolyzing acid amidase inhibition reveals a key role for endogenous palmitoylethanolamide in inflammation." Proc Natl Acad Sci U S A **106**(49): 20966-20971.
Staiger, J. F., K. Zilles, et al. (1996). "Recurrent axon collaterals of corticothalamic projection neurons in rat primary somatosensory cortex contribute to excitatory and inhibitory feedback-loops." Anat Embryol (Berl) **194**(6): 533-543.
Stella, N. (2004). "Cannabinoid signaling in glial cells." Glia **48**(4): 267-277.

Stella, N. (2010). "Cannabinoid and cannabinoid-like receptors in microglia, astrocytes, and astrocytomas." Glia **58**(9): 1017-1030.
Stella, N., P. Schweitzer, et al. (1997). "A second endogenous cannabinoid that modulates long-term potentiation." Nature **388**(6644): 773-778.
Stoppini, L., P. A. Buchs, et al. (1991). "A simple method for organotypic cultures of nervous tissue." J Neurosci Methods **37**(2): 173-182.
Straiker, A., J. Wager-Miller, et al. (2011). "COX-2 and fatty acid amide hydrolase can regulate the time course of depolarization-induced suppression of excitation." Br J Pharmacol **164**(6): 1672-1683.
Straus, D. S. and C. K. Glass (2007). "Anti-inflammatory actions of PPAR ligands: new insights on cellular and molecular mechanisms." Trends Immunol **28**(12): 551-558.
Streit, W. J. (2002). "Microglia as neuroprotective, immunocompetent cells of the CNS." Glia **40**(2): 133-139.
Suardiaz, M., G. Estivill-Torrus, et al. (2007). "Analgesic properties of oleoylethanolamide (OEA) in visceral and inflammatory pain." Pain **133**(1-3): 99-110.
Sugiura, T., Y. Kobayashi, et al. (2002). "Biosynthesis and degradation of anandamide and 2-arachidonoylglycerol and their possible physiological significance." Prostaglandins Leukot Essent Fatty Acids **66**(2-3): 173-192.
Sugiura, T., S. Kondo, et al. (1995). "2-Arachidonoylglycerol: a possible endogenous cannabinoid receptor ligand in brain." Biochem Biophys Res Commun **215**(1): 89-97.
Sun, Y. X., K. Tsuboi, et al. (2004). "Biosynthesis of anandamide and N-palmitoylethanolamine by sequential actions of phospholipase A2 and lysophospholipase D." Biochem J **380**(Pt 3): 749-756.
Sun, Y. X., K. Tsuboi, et al. (2005). "Involvement of N-acylethanolamine-hydrolyzing acid amidase in the degradation of anandamide and other N-acylethanolamines in macrophages." Biochim Biophys Acta **1736**(3): 211-220.
Thabuis, C., D. Tissot-Favre, et al. (2008). "Biological functions and metabolism of oleoylethanolamide." Lipids **43**(10): 887-894.
Tham, C. S., J. Whitaker, et al. (2007). "Inhibition of microglial fatty acid amide hydrolase modulates LPS stimulated release of inflammatory mediators." FEBS Lett **581**(16): 2899-2904.
Topper, R., J. Gehrmann, et al. (1993). "Remote microglial activation in the quinolinic acid model of Huntington's disease." Exp Neurol **123**(2): 271-283.
Tsuboi, K., Y. X. Sun, et al. (2005). "Molecular characterization of N-acylethanolamine-hydrolyzing acid amidase, a novel member of the choloylglycine hydrolase family with structural and functional similarity to acid ceramidase." J Biol Chem **280**(12): 11082-11092.
Uchigashima, M., M. Narushima, et al. (2007). "Subcellular arrangement of molecules for 2-arachidonoyl-glycerol-mediated retrograde signaling and its physiological contribution to synaptic modulation in the striatum." J Neurosci **27**(14): 3663-3676.
Uchigashima, M., M. Yamazaki, et al. (2011). "Molecular and morphological configuration for 2-arachidonoylglycerol-mediated retrograde signaling at mossy cell-granule cell synapses in the dentate gyrus." J Neurosci **31**(21): 7700-7714.
Ueda, N. (2002). "Endocannabinoid hydrolases." Prostaglandins Other Lipid Mediat **68-69**: 521-534.
Ueda, N., Y. Kurahashi, et al. (1995). "Partial purification and characterization of the porcine brain enzyme hydrolyzing and synthesizing anandamide." J Biol Chem **270**(40): 23823-23827.
Ueda, N., K. Tsuboi, et al. (2010). "N-acylethanolamine metabolism with special reference to N-acylethanolamine-hydrolyzing acid amidase (NAAA)." Prog Lipid Res **49**(4): 299-315.
Ueda, N., K. Yamanaka, et al. (2001). "Purification and characterization of an acid amidase selective for N-palmitoylethanolamine, a putative endogenous anti-inflammatory substance." J Biol Chem **276**(38): 35552-35557.
van der Stelt, M. and V. Di Marzo (2005). "Cannabinoid receptors and their role in neuroprotection." Neuromolecular Med **7**(1-2): 37-50.

van der Stelt, M., M. Trevisani, et al. (2005). "Anandamide acts as an intracellular messenger amplifying Ca2+ influx via TRPV1 channels." EMBO J **24**(17): 3026-3037.
Van Sickle, M. D., M. Duncan, et al. (2005). "Identification and functional characterization of brainstem cannabinoid CB2 receptors." Science **310**(5746): 329-332.
Vanden Abeele, F., A. Zholos, et al. (2006). "Ca2+-independent phospholipase A2-dependent gating of TRPM8 by lysophospholipids." J Biol Chem **281**(52): 40174-40182.
Varga, K., J. A. Wagner, et al. (1998). "Platelet- and macrophage-derived endogenous cannabinoids are involved in endotoxin-induced hypotension." FASEB J **12**(11): 1035-1044.
Vuksic, M., D. Del Turco, et al. (2011). "Unilateral entorhinal denervation leads to long-lasting dendritic alterations of mouse hippocampal granule cells." Exp Neurol **230**(2): 176-185.
Waldeck-Weiermair, M., C. Zoratti, et al. (2008). "Integrin clustering enables anandamide-induced Ca2+ signaling in endothelial cells via GPR55 by protection against CB1-receptor-triggered repression." J Cell Sci **121**(Pt 10): 1704-1717.
Walker, D. J., P. Suetterlin, et al. (2010). "Down-regulation of diacylglycerol lipase-alpha during neural stem cell differentiation: identification of elements that regulate transcription." J Neurosci Res **88**(4): 735-745.
Walter, L., T. Dinh, et al. (2004). "ATP induces a rapid and pronounced increase in 2-arachidonoylglycerol production by astrocytes, a response limited by monoacylglycerol lipase." J Neurosci **24**(37): 8068-8074.
Walter, L., A. Franklin, et al. (2002). "Astrocytes in culture produce anandamide and other acylethanolamides." J Biol Chem **277**(23): 20869-20876.
Walter, L., A. Franklin, et al. (2003). "Nonpsychotropic cannabinoid receptors regulate microglial cell migration." J Neurosci **23**(4): 1398-1405.
Wickliffe, K., A. Williamson, et al. (2009). "The multiple layers of ubiquitin-dependent cell cycle control." Chem Rev **109**(4): 1537-1548.
Witting, A., L. Chen, et al. (2006). "Experimental autoimmune encephalomyelitis disrupts endocannabinoid-mediated neuroprotection." Proc Natl Acad Sci U S A **103**(16): 6362-6367.
Witting, A., L. Walter, et al. (2004). "P2X7 receptors control 2-arachidonoylglycerol production by microglial cells." Proc Natl Acad Sci U S A **101**(9): 3214-3219.
Xiao, Y., Y. Chen, et al. (2000). "Evaluation of plasma lysophospholipids for diagnostic significance using electrospray ionization mass spectrometry (ESI-MS) analyses." Ann N Y Acad Sci **905**: 242-259.
Xiao, Y. J., B. Schwartz, et al. (2001). "Electrospray ionization mass spectrometry analysis of lysophospholipids in human ascitic fluids: comparison of the lysophospholipid contents in malignant vs nonmalignant ascitic fluids." Anal Biochem **290**(2): 302-313.
Xu, Y., Y. J. Xiao, et al. (2001). "The role and clinical applications of bioactive lysolipids in ovarian cancer." J Soc Gynecol Investig **8**(1): 1-13.
Yakovlev, A. G. and A. I. Faden (2004). "Mechanisms of neural cell death: implications for development of neuroprotective treatment strategies." NeuroRx **1**(1): 5-16.
Yazaki, M., K. Kashiwagi, et al. (2012). "Rapid degradation of cyclooxygenase-1 and hematopoietic prostaglandin D synthase through ubiquitin-proteasome system in response to intracellular calcium level." Mol Biol Cell **23**(1): 12-21.
Yin, H., Y. Gui, et al. (2010). "Dependence of phospholipase D1 multi-monoubiquitination on its enzymatic activity and palmitoylation." J Biol Chem **285**(18): 13580-13588.
Yoshida, T., M. Fukaya, et al. (2006). "Localization of diacylglycerol lipase-alpha around postsynaptic spine suggests close proximity between production site of an endocannabinoid, 2-arachidonoyl-glycerol, and presynaptic cannabinoid CB1 receptor." J Neurosci **26**(18): 4740-4751.
Zhang, H., D. A. Hilton, et al. (2011). "Cannabinoid Receptor and N-acyl Phosphatidylethanolamine Phospholipase D-Evidence for Altered Expression in Multiple Sclerosis." Brain Pathol.

Zhao, L. Y., K. Tsuboi, et al. (2007). "Proteolytic activation and glycosylation of N-acylethanolamine-hydrolyzing acid amidase, a lysosomal enzyme involved in the endocannabinoid metabolism." Biochim Biophys Acta **1771**(11): 1397-1405.

Zhao, Y., Z. Yuan, et al. (2010). "Activation of cannabinoid CB2 receptor ameliorates atherosclerosis associated with suppression of adhesion molecules." J Cardiovasc Pharmacol **55**(3): 292-298.

Zhu, C., C. Solorzano, et al. (2011). "Proinflammatory stimuli control N-acylphosphatidylethanolamine-specific phospholipase D expression in macrophages." Mol Pharmacol **79**(4): 786-792.

Ziebell, J. M. and M. C. Morganti-Kossmann (2010). "Involvement of pro- and anti-inflammatory cytokines and chemokines in the pathophysiology of traumatic brain injury." Neurotherapeutics **7**(1): 22-30.

Zygmunt, P. M., J. Petersson, et al. (1999). "Vanilloid receptors on sensory nerves mediate the vasodilator action of anandamide." Nature **400**(6743): 452-457.